1. Report No. FHWA/TX-16/0-6814-1	2. Government Accession No.	3. Recipient's Catalog No.
4. Title and Subtitle PERFORMANCE EVALUATION AND SPECIFICATION OF TRACKLESS TACK		5. Report Date Published: September 2016 6. Performing Organization Code
7. Author(s) Bryan Wilson, Ah Young Seo, and Maryam Sakhaeifar		8. Performing Organization Report No. Report 0-6814-1
9. Performing Organization Name and Address Texas A&M Transportation Institute College Station, Texas 77843-3135		10. Work Unit No. (TRAIS) 11. Contract or Grant No. Project 0-6814
12. Sponsoring Agency Name and Address Texas Department of Transportation Research and Technology Implementation Office 125 E. 11th Street Austin, Texas 78701-2483		13. Type of Report and Period Covered Technical Report: May 2014–April 2016 14. Sponsoring Agency Code

15. Supplementary Notes

Project performed in cooperation with the Texas Department of Transportation and the Federal Highway Administration.

Project Title: Performance Evaluation, Specifications and Implementation of Non-Tracking Tack Coat

URL: http://tti.tamu.edu/documents/0-6814-1.pdf

16. Abstract

Several trackless tack products have come to market in Texas; however, there are currently no specifications to ensure the products have trackless properties and adequate bond strength. The objectives of this project were to (1) evaluate the tracking resistance of different trackless tacks, (2) evaluate bond strength and other construction parameters of different trackless tacks, (3) construct test sections in the field to evaluate performance, and (4) develop test procedures and specifications for trackless tack.

For tracking resistance, a track-free time test and a dynamic shear rheometer (DSR) tackiness test both distinguished between trackless tack and conventional tack. The DSR test further distinguished among stiff-residue and soft-residue trackless tacks. For bond strength of laboratory samples, all samples had acceptable bonding, but stiff-residue trackless tack had the highest bond energy, followed by soft-residue trackless tack, conventional tack, and then no tack. Higher ambient and hot mix asphalt (HMA) compaction temperatures improved bonding. Bonded trackless tack samples were resistant to fatigue cracking and cold temperature delamination. Bond strengths from field samples were considerably lower (15–95 psi) than for lab-molded samples (100–200 psi) and varied among different overlay projects. This was likely due to different project conditions (e.g., pavement surfaces, HMA overlay designs, compaction temperatures). In most cases tack rate did not affect the bond strength.

The researchers recommend adopting the DSR tackiness test and track-free time test to qualify trackless tack materials. The researchers also recommend adopting the shear bond strength test. Draft test methods and a trackless tack material specification are provided.

17. Key Words	18. Distribution Statement
Trackless Tack Coat, Tracking Resistance, Cracking Resistance, Rheology, Bond Strength, Bond Energy, DSR Frequency Sweep Test, Pull-off Test, Interface Shear Test	No restrictions. This document is available to the public through NTIS: National Technical Information Service Alexandria, Virginia 22312 http://www.ntis.gov

19. Security Classif. (of this report)	20. Security Classif. (of this page)	21. No. of Pages	22. Price
Unclassified	Unclassified	142	

PERFORMANCE EVALUATION AND SPECIFICATION OF TRACKLESS TACK

by

Bryan Wilson
Associate Research Scientist
Texas A&M Transportation Institute

Ah Young Seo
Graduate Research Assistant
Texas A&M University

and

Maryam Sakhaeifar, PhD
Assistant Professor
Texas A&M University

Report 0-6814-1
Project 0-6814
Project Title: Performance Evaluation, Specifications and Implementation of Non-Tracking Tack Coat

Performed in cooperation with the
Texas Department of Transportation
and the
Federal Highway Administration

Published: September 2016

TEXAS A&M TRANSPORTATION INSTITUTE

College Station, Texas 77843-3135

DISCLAIMER

This research was performed in cooperation with the Texas Department of Transportation (TxDOT) and the Federal Highway Administration (FHWA). The contents of this report reflect the views of the authors, who are responsible for the facts and the accuracy of the data presented herein. The contents do not necessarily reflect the official view or policies of the FHWA or TxDOT. This report does not constitute a standard, specification, or regulation. It is not intended for construction, bidding, or permit purposes. The researcher in charge of the project was Bryan Wilson. The United States Government and the State of Texas do not endorse products or manufacturers. Trade or manufacturers' names appear herein solely because they are considered essential to the object of this report.

ACKNOWLEDGMENTS

This project was conducted for TxDOT, and the authors thank TxDOT and FHWA for their support in funding this research. We acknowledge the continuing support of the members of the Project Monitoring Committee, past and present, including Dar Hao Chen, Jerry Peterson, Lance Simmons, and Stevan Perez. We also appreciate the help of Darrin Jensen as the project manager.

Field evaluations were assisted by Mike Arellano (TxDOT-Austin), Arif Chowdhury (TTI), Rick Canatella (TTI), Tony Barbosa (TTI), APAC-Wheeler, and Foremost Paving, Inc. Lubinda Walubita (TTI) assisted with laboratory testing. Test materials and technical advice were provided by the following asphalt emulsion vendors: Blacklidge Emulsions (Grover Allen), Calumet Specialty Products Partners (Jerry Bach), Asphalt Products Unlimited (Jerry Bach), Ergon Asphalt & Emulsions (Tom Flowers and Cordin Daranga), and Western Emulsions (Randy Woods and Rusty Smallwood). The help of several Texas A&M students was invaluable, namely Mayur Yelpale, Sanket Shah, Sridhar Avva, Mallikarjun Nakkala, and Hyungsup Cho.

TABLE OF CONTENTS

Page

LIST OF FIGURES

Page

LIST OF TABLES

Page

CHAPTER 1
INTRODUCTION

PROBLEM STATEMENT

Correct tack application is important in the bonding quality of pavement layers. Insufficient tack rate and uniformity cause inadequate and inconsistent bonding, which can lead to pavement failure (*1*). Bonding failures can be manifested as slippage cracking, fatigue cracking, and delamination (*2*). During construction, conventional tack tends to track under paving equipment tires, which can lead to the loss of tack in the wheel path, where it is most required.

Trackless tack is resistant to tracking and pick-up under construction traffic. This material hardens after application and adheres minimally to tires. Later, when the hot mix asphalt (HMA) overlay is applied over the tack, the heated tack is reactivated and bonds the new overlay to the existing surface. In Texas, a wide variety of trackless tack products has come to market, but there are currently no specification or test procedures for trackless tack.

SCOPE AND OBJECTIVE

The objectives of this study are to:

1. Evaluate the tracking resistance of different trackless tacks.
2. Evaluate bond strength of different trackless tacks and other construction parameters (e.g., surface type, temperature, compaction effort).
3. Construct test sections to validate the laboratory findings.
4. Develop test procedures and specifications for trackless tack.

The scope of this research was to:

1. Conduct a literature review of tack tracking/bonding issues and associated tests.
2. Characterize different trackless tacks and traditional tacks.
3. Identify the best test procedure to measure tackiness/tracking resistance in the lab.
4. Identify the best test procedure to measure bond strength in the lab and verify results in the field.
5. Demonstrate trackless tack specifications in field projects.
6. Develop specifications, write a comprehensive report of methods and findings, and share information via webinar to division and district personnel.

DELIVERABLES

In addition to this report, the deliverables for this project were:

- Draft specification for trackless tack.
- Draft test method for the dynamic shear rheometer (DSR) tackiness test.
- Draft test method for the track-free time test.
- Draft test method for the shear bond strength test.
- Webinar presentation on the draft specification and methods.

OUTLINE

This report contains seven chapters:

- Chapter 1 describes the problem statement, objective and scope, and deliverables.
- Chapter 2 gives background information for tack coats, trackless tack, and bonded pavement layers.
- Chapter 3 summarizes the material characterization of the tack materials.
- Chapter 4 presents an evaluation of tracking resistance.
- Chapter 5 presents an evaluation of bonded pavement layer performance in the laboratory.
- Chapter 6 discusses the field implementation and testing.
- Chapter 7 summarizes the research and findings, and offers recommendations.

CHAPTER 2
BACKGROUND

This chapter gives background information on the following topics:

- Performance of bonded pavements.
- Tack coat materials.
- Tack tracking theory.
- Tracking resistance tests.
- Bond strength tests.

PERFORMANCE OF BONDED PAVEMENTS

The effectiveness of a HMA overlay is largely dependent on the quality of its bond to the underlying layer. A good bond will evenly disperse traffic loads from one layer into the next, while a poor bond will concentrate stresses within the relatively thin upper layer. This condition will expedite premature distress such as fatigue cracking, slippage cracking, and delamination. All of these problems are then exacerbated by moisture accumulating at the debonded interface.

Debonding at the overlay–substrate interface can lead to a more dramatic loss of the pavement life, compared to interface failure between two base layers. The bonding quality may be dependent on construction practices and material properties. Also, thickness and dynamic stiffness modulus of layers are essential factors affecting the pavement life (*3*).

Various studies have focused on factors that influence interlayer bond strength. Most of that research considered parameters such as tack coat type, curing time, temperature, and mix type. Briefly, researchers concluded that the curing time of tack coat had a significant impact on interface strength (*4*), and that surface milling provided a higher shear strength (*1*,*4*,*5*), while higher test temperatures lowered the bond performance (*1*,*5*,*6*). However, the effect of tack coat type and application rate varied depending on the mix type (*5*). The interface shear resistance was improved as the mix type became coarser (*6*), and bond strength was sensitive to the normal pressure (*5*). An increase in viscosity and softening point was also observed with an increase in tensile bond strength (*1*).

Since an open-graded friction course overlay has an open gradation, it has less physical contact to the substrate than a conventional mixture and, therefore, can be vulnerable to debonding. For this reason, engineers often recommend applying a heavier tack coat to strengthen the bond interface (*7*).

TACK COAT MATERIALS

Tack coat is the basic approach to ensure bonding, though common construction practices prevent traditional tack coats from being fully effective. Even if the tack is applied correctly to

the surface, the material is often picked up and contaminated by construction traffic. Worse yet, the tack is usually lost in the wheel path, where it is needed the most.

Trackless tacks were recently introduced to the Texas paving industry. They harden shortly after application, lose their tackiness, and, therefore, do not stick to tires but remain intact and uncontaminated. Subsequently, when HMA is applied and compacted over trackless tack, the tack heats up, reactivates, and bonds the new overlay with the existing surface. These products are very new, and while performance seems acceptable to date, the short- and long-term benefits of trackless tack are not well documented. Some in the industry suggest the stiff trackless tacks can lead to long-term problems such as fatigue cracking.

Several studies (*1,8,9*) showed that the bonding strength of trackless tack coat materials was higher than that of conventional ones. However, McGhee et al. (*10*) produced the opposite result, albeit with a limited test scope. One study suggested that high brittleness of trackless tack residue contributed to a lower cracking resistance (*9*).

TACK TRACKING THEORY

Tack tracking is a complex interaction of adhesion and cohesion failures of the tack coat with the original paving surface, vehicle tire, and the untacked pavement. Adhesion is the bonding force between two different materials (tack and the pavement, or tack and the tire) and cohesion is the internal bonding force within a homogenous material (internal tack bond).

The process of tack tracking can be illustrated by a sequence of adhesion and cohesion bonds/failures as follows:

1. A tire makes contact with and **adheres** to the tack coat surface.
2. When the tire rolls forward, the tack coat fails in **cohesion**.
3. Wet tack on tire then **adheres** (tracks) onto another surface.

In the case of trackless tack, the sequence of adhesion/cohesion bond/failures is as follows:

1. The tire **adheres minimally** to the tack surface.
2. When the tire rolls forward, the tack coat **cohesive** force and **adhesive** force with the pavement are *greater* than the minimal tire-tack **adhesive** force.
3. Tack remains on the pavement.

Tack tracking potential can be defined by a few strength ratios as shown in Table 2-1.

Table 2-1. Tracking and Trackless Condition Ratios.

Tracking Condition
$\frac{\sigma A_{Tire-Tack}}{\sigma C_{Tack}}$ and/or $\frac{\sigma A_{Tire-Tack}}{\sigma A_{Tack-Pavement}} > 1$
Trackless Condition
$\frac{\sigma A_{Tire-Tack}}{\sigma C_{Tack}}$ and $\frac{\sigma A_{Tire-Tack}}{\sigma A_{Tack-Pavement}} < 1$

Notes: σA= Adhesive Strength;
σC = Cohesive Strength

TRACKING RESISTANCE TESTS

A number of tests are used to characterize tack coats, mostly looking at material properties (e.g., viscosity, elasticity, softening point) and emulsion mix properties (e.g., storage stability, settlement, gradation). However, there are no standardized tests to address tracking resistance. The current subjective touch test and the in-the-field shoe test leave a lot to be desired. The researchers have identified three experimental tests that attempt to quantify this property.

Track-Free Time Test

The modified no-pick-up time test (called the track-free time test in this study) was used by researchers at the Virginia Center for Transportation Innovation and Research (VCTIR) to test tracking resistance (*8*). The device is presented in Figure 2-1 and the test protocol can be found through ASTM D 711 (Standard Test Method for No-Pick-Up Time of Traffic Paint). The stainless steel roller is 11.9 lb, and fitted with rounded gaskets. The rolling speed across the tack sample and tracking paper is controlled by allowing the device to freely roll down a ramp. In the ASTM method, the existence of tracking is simply observed and not quantified.

In the VCTIR study, two curing conditions were evaluated: room temperature curing and oven dried constant mass curing. The results showed that the trackless materials had superior tracking resistance under room temperature and oven dried conditions compared to conventional tack.

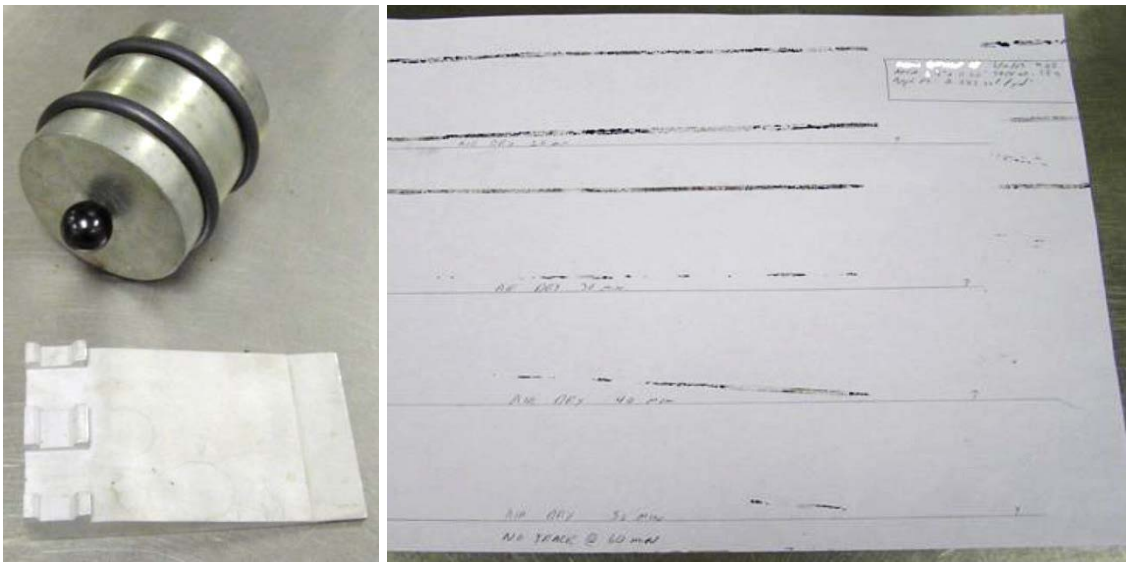

Figure 2-1. Tracking Test Used by VCTIR.

BASF Roller

The roller tracking test in Figure 2-2, was developed by the chemical company BASF. The test rolls a 10-lb steel wheel with rubber square-cut O-rings across a tack sample at predetermined curing time intervals. The length of tack tracked onto a white piece of cardstock is measured and recorded. The Texas A&M Transportation Institute (TTI) experimented with this device in project 0-6742, Performance Tests for Thin Overlays. The simple test successfully distinguished between different tack types. The researchers could not find any publications presenting the results from this test device.

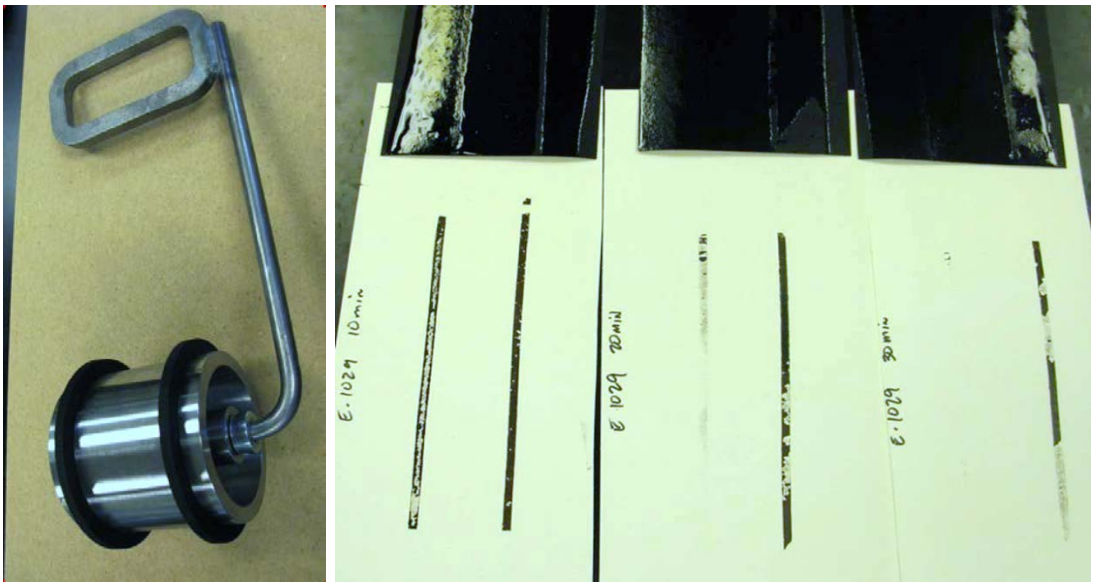

Figure 2-2. BASF Roller Tracking Test.

DSR Tackiness

The third test the researchers identified is a modified application of the dynamic shear rheometer test. The DSR is normally used to measure viscoelastic properties of binder at different temperatures and loading frequencies and is an integral part of the Superpave design method. Researchers with Akzo Nobel and Blacklidge Emulsion's Technical Center have worked on a method for testing the tackiness of tack coat materials. They placed an open-faced sample in the DSR, lowered the top plate until it contacted the sample surface, and then removed the top plate. The normal force was recorded and plotted, and the shape of the plot then indicated the material's tackiness properties (Figure 2-3). Some advantages of this method are that temperature, strain rate, and film thickness can be controlled in the DSR setup (*11*).

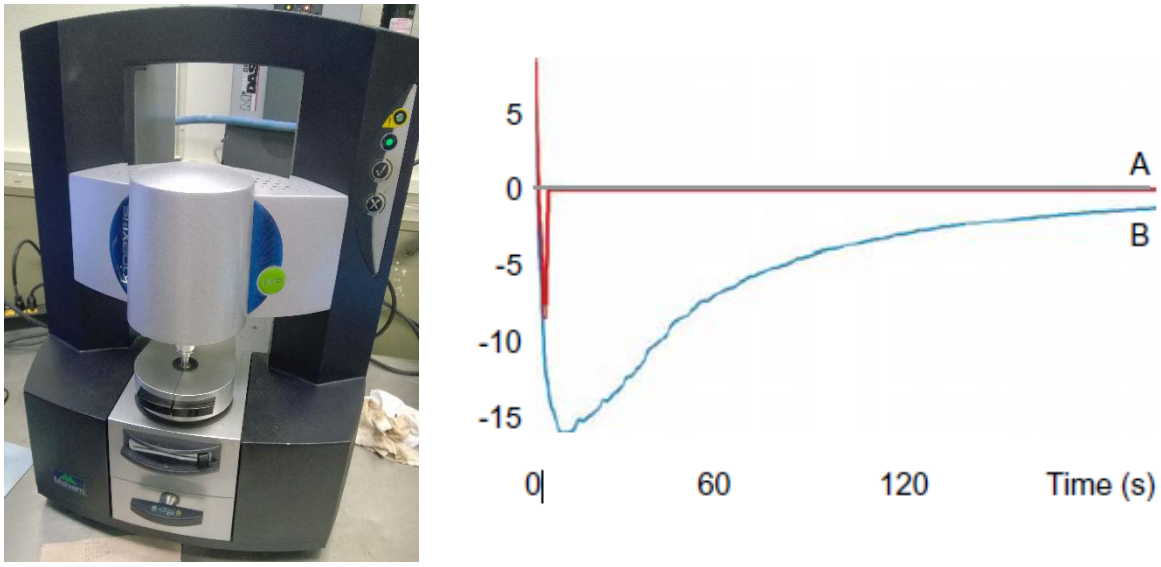

Figure 2-3. DSR and Normal Force Plot from Tackiness Testing.

BONDED PAVEMENT LAYER TESTS

Tracking resistance is not the only important property of trackless tacks. These products should, primarily, have acceptable bonding properties. To date, the bonding performance of trackless tacks seems acceptable (*8*), but the quantified short- and long-term performance of trackless tack is not well documented. A wide array of bond strength tests are available that are well documented in NCHRP 712 (*Optimization of Tack Coat for HMA Placements*) (*1*). Many of these tests offer to assess the maximum bond strength by testing laboratory or field compacted samples in shear, tension, or torque; however, the most common mode tested is shear as this is a failure mechanism in the field.

Other aspects of bonded pavement layer performance the possibility of cold weather debonding and the total stiffness. One concern is that the hard nature of trackless tack makes it brittle and liable to crack. Some worry about the layer interface delaminating or causing fatigue cracking. Possible tests to evaluate this issue are the Texas overlay tester and the beam fatigue test.

This subsection will address the following types of tests:

- Shear.
- Tension.
- Cracking resistance.

Shear

A direct shear bond strength test was developed at the National Center for Asphalt Technology (NCAT) (*4*,*5*). For this test, a bonded specimen is placed horizontally in the device (Figure 2-4) and a normal confining load can be applied. One side of the device holds the sample in place while the other is free to slide vertically. A load is applied to the free-sliding side in a loading frame and the maximum load is recorded. NCAT suggested that the device can be used successfully to assess bond strength and that a minimum strength of 100 psi is recommended (*5*). Devices with a similar setup include the Louisiana Interlayer Shear Strength Tester (*1*), the layer-parallel direct shear test (*12*), and an unnamed shear test from the Virginia Transportation Research Council (*10*).

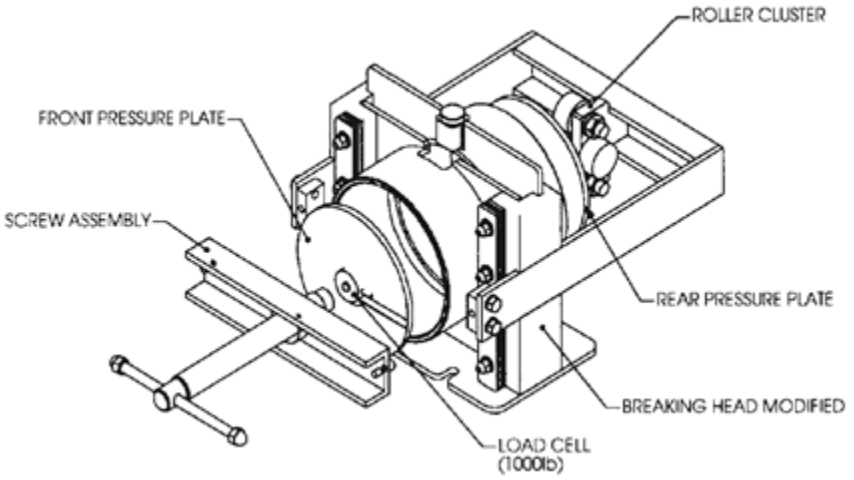

Figure 2-4. NCAT Shear Strength Apparatus (*5*).

Tension

One commonly used direct tension test is the Switzerland pull-off test. A bonded specimen is cored through the upper layer and partway through the bottom layer. A disk is glued to the top surface and is pulled in tension with a pull-off tester (Figure 2-5) until failure. The sample is then evaluated to see if failure occurred at the bond, in the upper or lower layers, or at the glue interface. One drawback with the test is that if failure occurs in either layer, no exact determination on the bond strength can be made except the fact that it is stronger than the interlayer tensile strength. Also, the ratio between HMA lift thickness and maximum aggregate size will often break the rule of thumb for a 3:1 ratio requirement. TTI has used this test in a

number of studies (*13*) and has assisted the TxDOT construction division with an in-house trackless study.

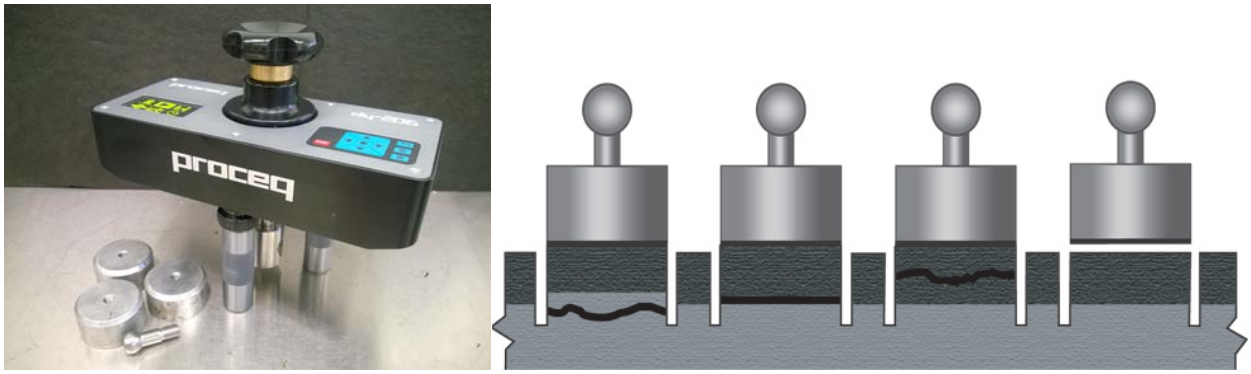

Figure 2-5. Switzerland Pull-Off Tester and Failure Modes.

Cracking Resistance

Another approach for investigating bond strength is to evaluate the cracking resistance. This can be done with an overlay test or the flexural bending beam fatigue test (FBBFT). The overlay tester was originally designed by Germann and Lytton (*14*) and later modified by Zhou and Scullion (*15*) for characterizing the reflective cracking resistance of HMA overlays. The tester contains two aluminum plates; one plate is controlled to move in a horizontal direction, and the other one is fixed An HMA sample is glued to the two plates and a cyclic load is applied at a specified rate in a displacement-controlled mode. The test is run until failure, defined by a 93 percent drop in the peak load. The benefits of this test are an easy sample fabrication process using the Superpave Gyratory Compactor and relatively short testing time (*16*).

The flexural bending beam fatigue test is specified in the American Association of State Highway and Transportation Officials' TP8-94 Standard Test Method for Determination of the Fatigue Life of Compacted HMA Subjected to Repeated Flexural Bending. As exemplified in Figure 2-6, the FBBFT consists of applying a repeated constant vertical strain to a beam specimen in flexural tension mode until failure or up to a specified number of load cycles.

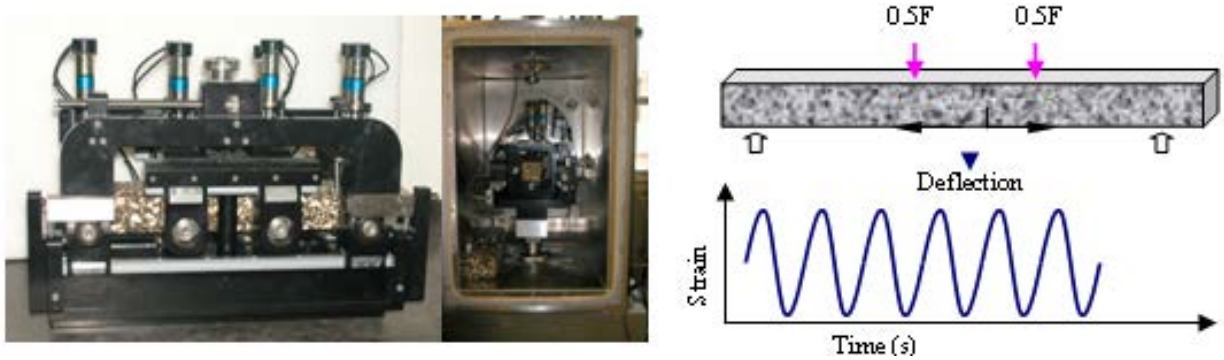

Figure 2-6. Flexural Bending Beam Fatigue Test and Load Configuration.

The desired output from this test is the change in flexural stiffness of the composite beam specimen over loading cycles. If the bond is working as it should, the composite stiffness and the load cycles at failure should be significantly higher than the two layers unbonded. Figure 2-7 shows that flexural stiffness has a decaying tendency as a function of the number of load cycles. At any given load cycle, the HMA flexural stiffness (*S*) is typically computed by dividing the maximum measured tensile stress per given load cycle by the maximum measured tensile strain per load cycle based on AASHTO TP8-94 procedure. The undamaged HMA flexural stiffness (initial peak stiffness) is often calculated at the 50th load cycle. The failure life in the strain-controlled mode is traditionally defined as the stiffness reduction of 50 percent.

Figure 2-7 allows other important observations such as the rate of decay in flexural stiffness, the flexural stiffness at initial/final state, and load cycles measured at failure. These data could also be used as indicative parameters to evaluate and differentiate the bonding strengths and fatigue crack life of different tack coats and trackless tack coats within the composite beam specimens.

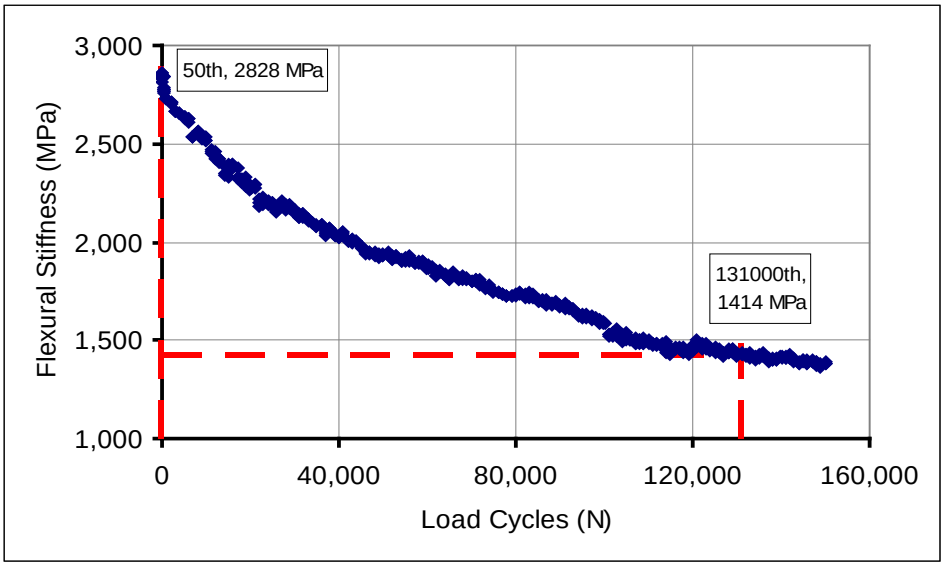

Figure 2-7. Example Plot of the FBBFT Flexural Stiffness versus Load Cycles.

CHAPTER 3
MATERIAL CHARACTERIZATION

This chapter reports the material characterization of trackless tacks and a standard tack.

MATERIALS

The researchers contacted asphalt emulsion suppliers and requested samples of the tack materials listed in Table 3-1.

Table 3-1. Tack Materials.

Tack Index	Material Type
Control	Conventional emulsion (cationic)
A	Trackless emulsion (cationic)
B	Trackless emulsion (cationic)
C	Trackless emulsion (anionic)
D	Trackless emulsion (anionic)
E	Trackless emulsion (anionic)
F	Trackless hot-applied

Most of the tests in this task were performed on binder residues. The residue was collected using the 6-hour evaporative technique specified in AASHTO PP72 Method B. The emulsion was first stirred and then spread over a silicon mat to a thickness of 0.015 inches with a thin film applicator (Figure 3-1a). The mat was transferred to a flat tray, tested for correct film thickness with a wet film thickness gauge, and placed in an oven at 60ºC for 6 hours (Figure 3-1b). The leftover emulsion residue after evaporation was peeled from the mat and stored for testing.

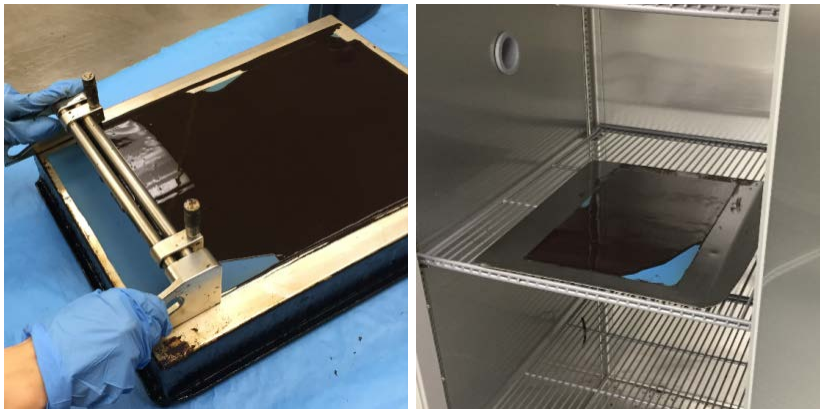

(a) **(b)**

Figure 3-1. Sample Preparation for Emulsion Recovery: (a) Thin-Film Application and (b) Evaporation of Water in Oven.

CHARACTERIZATION METHODS

Different properties of the tack emulsions and residues were collected as summarized in Table 3-2. Properties from standard test types were requested from the suppliers. The viscoelastic properties of samples were measured through three different tests at TTI. These tests include (1) frequency sweep test, (2) multiple-stress creep-recovery test (MSCR), and (3) linear amplitude sweep (LAS) test. Summarized test procedures are given in this chapter and more detailed description of the test methods and parameters are included in Appendix A.

Table 3-2. Properties of Residual Binders and Emulsions.

Material Type	Property	Test Type	Test Procedures
Residue	Viscosity	Standard	AASHTO T 316
	Penetration	Standard	AASHTO T 49
	Softening point	Standard	AASHTO T 53
	Complex shear modulus ($\|G^*\|$) Phase angle ($\boldsymbol{\delta}$)	Standard/ Advanced	AASHTO T 315
	Percent recovery Non-recoverable creep (J_{nr})	Advanced	MSCR test: ASTM (D7405)
	Failure strain @ max stress Cycles to failure ($\boldsymbol{N_f}$)	Advanced	Linear Amplitude Sweep: AASHTO TP 101
Emulsion	Residue content (%)	Standard	Tex-543-C
	Saybolt viscosity	Standard	D 562

In both the frequency sweep and MSCR tests, unaged residual binders were used. Aged binders were used in the LAS test to address fatigue characteristics. Aging was done through the pressure-aging vessel (PAV) process following AASHTO R 28 test protocol to simulate long-term aging during in-service life of asphalt pavements. The short-term aging procedure through rolling thin-film oven (RTFO) was not considered in this study. The RTFO process is used to simulate the aging of asphalt in the batching process, and, therefore, is not suitable for emulsion applications (*17*).

DSR Frequency Sweep

The frequency sweep test was conducted to identify the undamaged rheological properties of asphalt binder by applying constant loading with low amplitude. The test was run over a wide range of loading frequencies at multiple temperatures using DSR. In this test, the absolute value of complex shear modulus ($|G^*|$) and phase angle (δ) of the asphalt binder are measured. The range of loading frequencies was considered from 1 to 100 rad/sec and the test temperature was stabilized in a forced air chamber. The 25 mm parallel plates with a 1.0 mm gap were used at high temperatures (46, 58, and 70°C), and 8 mm parallel plates with a 2.0 mm gap were used at low and intermediate temperatures (6, 10, 22, and 34°C). The master curves were created for

tack residues using DSR frequency sweep data. The reference temperature considered for construction of all master curves was 34°C.

Multiple-Stress Creep-Recovery

The MSCR test is the latest method to improve the current performance grade (PG) specification. This method is suggested to replace the existing dynamic shear test because of a better correlation with field performance, particularly with rutting (*18,19*). Furthermore, the MSCR recovery can indicate the fatigue resistance of asphalt binder when elastic response is evaluated (*20,21*). This study, therefore, used the MSCR test to address the resistance to fatigue cracking in addition to rutting.

Figure 3-2 shows the stress input and strain output of a sample based on ASTM D7405 specification. In this test, a 1-second creep load is applied to the sample, which results in a gradual increase in strain. After each loading cycle, the sample is allowed to rest for 9 seconds. Each portion of recoverable and non-recoverable strain is recorded. The MSCR test procedure used here includes two different sets: first, a low stress level of 0.1 kPa is applied for 10 cycles; and second, a high stress level of 3.2 kPa is loaded for 10 cycles. As the loading cycles increase, the non-recoverable strain is accumulated representing the potential of permanent deformation in pavement. The samples are tested with the 25 mm plate geometry and 1 mm gap setting in DSR. The test was conducted at 60°C, which was the same as the curing temperature.

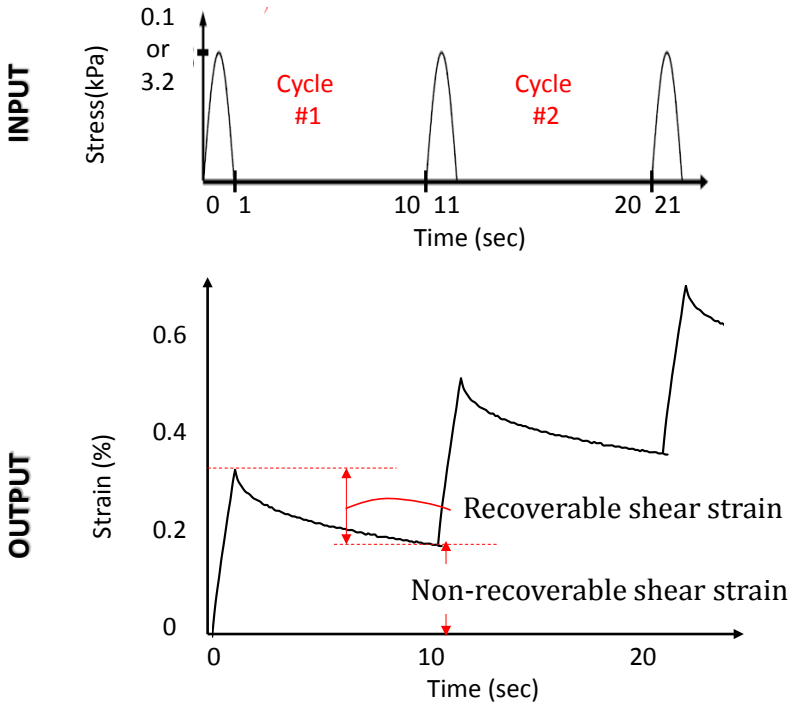

Figure 3-2. Input and Output of MSCR Test.

Linear Amplitude Sweep

The linear amplitude sweep test is an advanced method for characterizing the fatigue resistance of asphalt binder. This test was developed to compensate for the limitation of existing PG specification. Since properties of binder in the existing specification are within a linear viscoelastic range, the specification is deficient to predict the actual fatigue life (*22*). Moreover, the existing PG fatigue parameter is measured at only a few loading cycles and one strain level so that the impact of traffic and pavement structure on fatigue resistance is neglected (*23*).

The LAS test procedure involves a frequency sweep test and an amplitude sweep test. First, the frequency sweep test investigates the rheological properties of undamaged material. This test is conducted at constant strain amplitude over various loading frequencies. The strain level is 0.1 percent, and 12 loading frequencies are applied: 0.2, 0.4, 0.6, 0.8, 1.0, 2.0, 4.0, 6.0, 8.0, 10, 20, and 30 Hz. The amplitude sweep identifies the characteristic of fatigue damage. It is performed using oscillatory loading in a strain-controlled mode at a constant frequency of 10 Hz, and is accelerated by applying a linearly increasing load. The loading step consists of 100 cycles increasing at 0.1 percent strain from 0.1 to 30 percent applied strain.

Two tests in the LAS test procedure are run using the DSR with 8 mm parallel plates with a 2 mm gap at intermediate temperature. The intermediate temperature is determined as where the fatigue parameter ($|G^*| \cdot sin\delta$) reaches the current PG specification limit of 5.0 GPa at the rate of 10 rad/sec (*24*). Table 3-3 lists the selected intermediate temperatures for the test condition of PAV-aged binders. The intermediate temperatures of the soft-residue group were lower than those of the stiff-residue group.

Table 3-3. Test Temperatures of LAS Test.

Tack Type	Test Temperature (°C)
Control	15.1
A	14.6
B	19.3
C	25.4
D	33.4
E	37.1
F	32.1

CHARACTERIZATION RESULTS

DSR Frequency Sweep

The shift factor coefficients and model parameters for the master curve modulus data are presented in Appendix B. These parameters can be used to predict the properties at various testing conditions.

Figure 3-3 shows the master curves of all tack residues together. As frequency decreases, the difference in stiffness among different products becomes more significant. The control tack is the softest and most viscous of all the materials, followed by Tacks A and B. The residues of Tacks A and B exhibit similar stiffness values throughout a wide frequency range. Tack C belongs to the middle ranked group with respect to its stiffness and has similar viscosity to Tacks A and B at low frequency or high temperature. Tacks D, E, and F contain the hardened binders. Tack F exhibits the same rheological properties as Tack D, and the slopes of the Tacks D and F stiffness curves seem to be slightly flatter than the slope of Tack E. In phase angles master curves, the difference between Tack D/Tack F and Tack E is significant. Tack E is more viscous at low and intermediate frequencies than other stiff materials. However, three stiff residues do not exhibit reverse slope in phase angle master curves at low frequency range.

Based on the complex shear modulus master curve, the materials used in this study are classified into two major groups: soft residue and stiff residue (see Figure 3-3) where the control tack and Tacks A, B, and C belong to the soft-residue group and Tacks D, E, and F belong to the stiff-residue group. These groupings will be used to investigate the performance characteristics of different tack products.

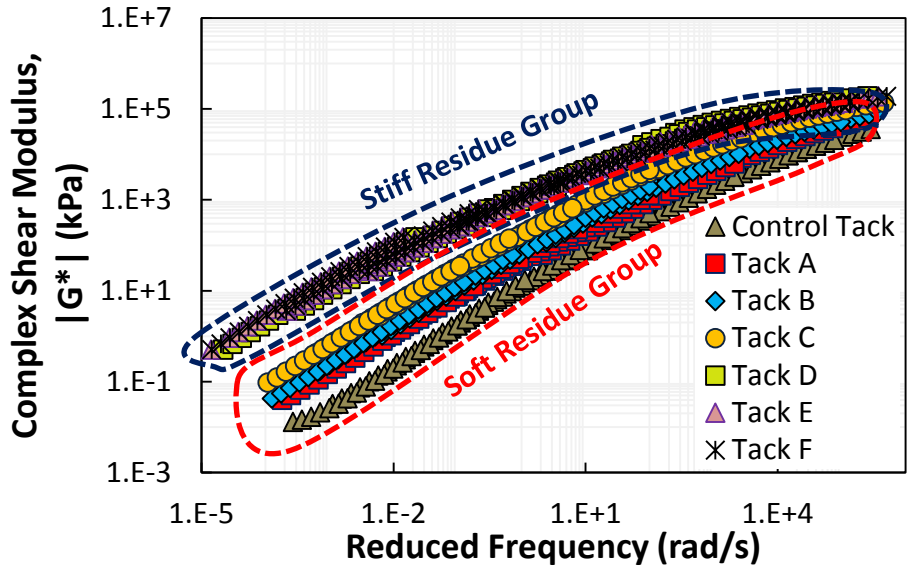

(a)

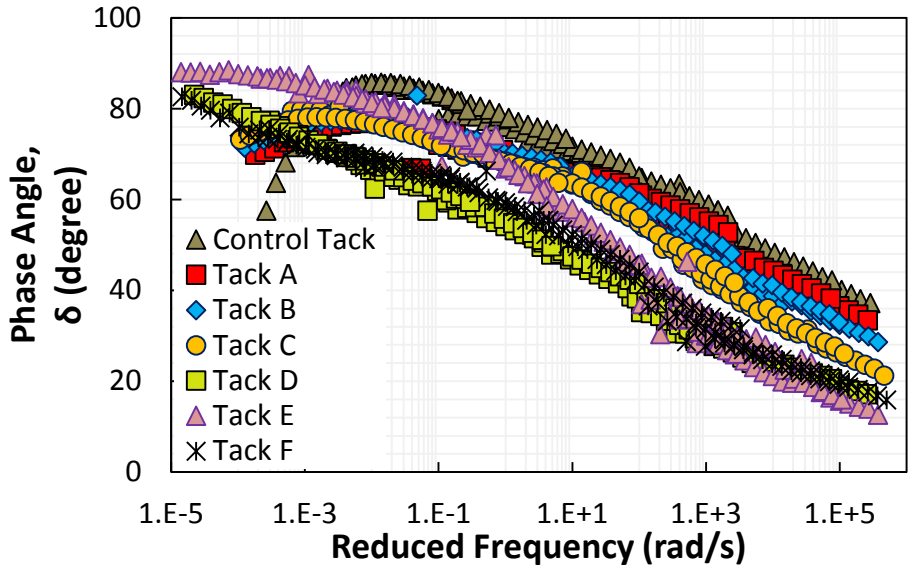

(b)

Figure 3-3. Master Curve for Trackless Tack Coat Materials: (a) Complex Shear Modulus and (b) Phase Angle.

Multiple-Stress Creep-Recovery

The average percent recovery represents the amount of recovery in strain after the unloading process. A high percent recovery represents a higher level of elasticity contribution, thereby resulting in better performance against rutting and fatigue cracking (*21*).

Figure 3-4 presents the percent recovery at different stress levels. The percent recovery decreased with an increase in stress level. The control tack exhibited the lowest level of recovery; this material had no recovery at the high stress level. For the soft-residue group (control tack and Tacks A, B, and C), considerable change in percent recovery was observed at higher stress condition, indicating that the residues in the soft-residue group had high sensitivity to stress level. On the contrary, the percent recovery of the stiff-residue group did not decrease significantly at higher stress levels. Within the stiff-residue group (Tacks D, E, and F), Tack E yielded the lowest elastic recovery. The tack with the highest level of recovery was Tack A at low stress level and Tack F at high stress level.

Figure 3-5 shows the non-recoverable creep compliance of the residues of the soft- and stiff-residue groups at different stress levels. The J_{nr} increased as stress level increased while different tack types had different sensitivity to stress level. The J_{nr} of the stiff-residue group was significantly lower than that of the soft-residue group. Also, the stiff-residue group was less sensitive to stress level than the soft-residue group. Among the stiff residues, Tack D had the lowest value of J_{nr}, followed by Tacks F and E. The control tack exhibited the highest J_{nr} at two stress levels, followed by Tacks A, B, and C.

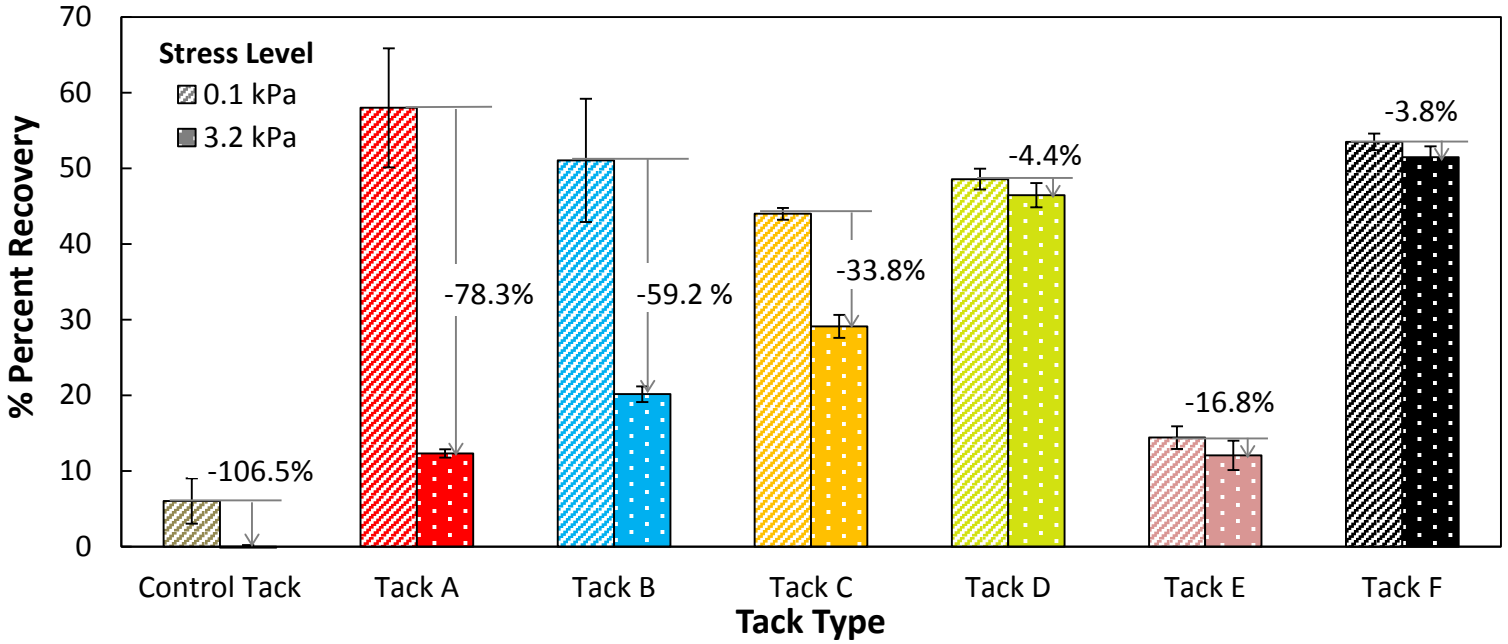

Figure 3-4. Percent Recovery of Emulsion Residues.

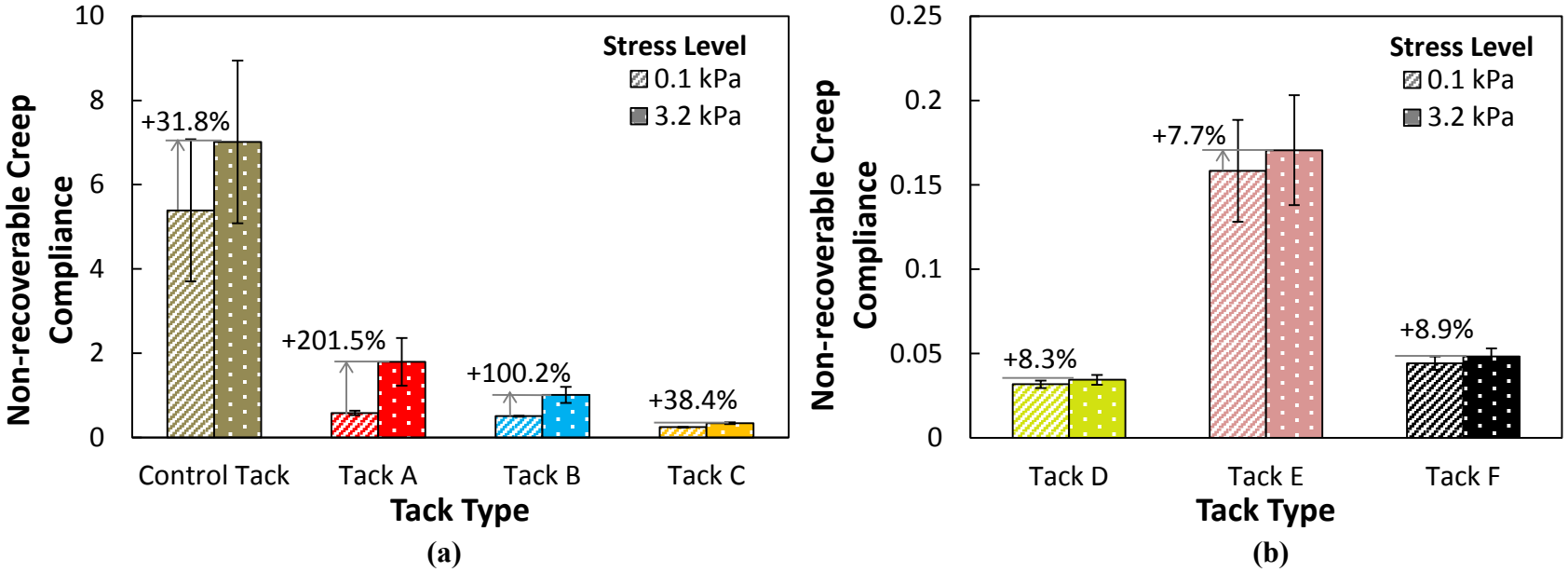

Figure 3-5. Non-Recoverable Creep Compliance of Emulsion Residues: (a) Soft-Residue Group and (b) Stiff-Residue Group.

Linear Amplitude Sweep

Based on the LAS procedure, the response of shear stress and strain and the calibrated fatigue parameters are shown in Appendix B. Using the fatigue parameters, the number of cycles to failure at any level of shear strain can be predicted. Figure 3-6 shows the predicted number of cycles to failure at 2.5 percent strain. Tack F exhibited the longest fatigue life, followed by the control tack. Of all materials, Tack E had the lowest resistance to fatigue cracking at the selected intermediate temperature.

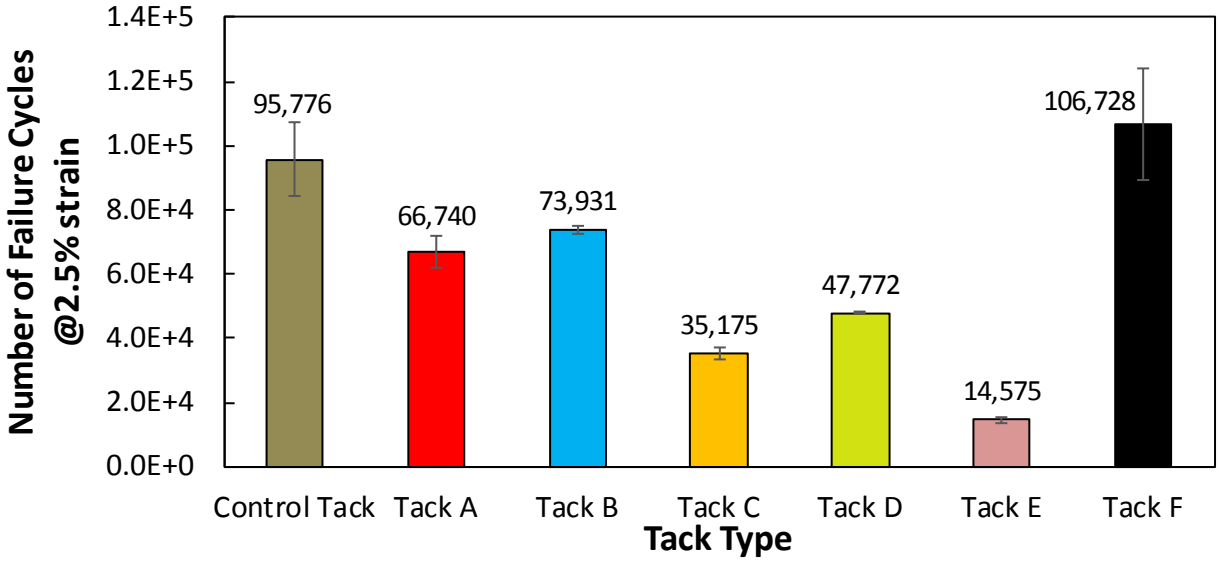

Figure 3-6. Number of Cycles to Fatigue Failure at 2.5 Percent Strain.

Standard Properties

Table 3-4 reports the values that were provided by the manufacturers. Data for other materials were not made available. These data have not been verified by a third party.

Table 3-4. Standard Tack Properties.

Tack Type	Penetration (25°C, 100 g, 5 sec)	Softening Point, °C	Residue, % (distillation)	Saybolt Viscosity, sec (25°C)
Control Tack	–	–	–	–
A	–	–	–	–
B	48	–	61	30
C	5	68	68	31.7
D	–	–	–	–
E	9	68	57	31.3
F	–	–	–	–

SUMMARY

The purpose of this task was to characterize trackless tacks and a traditional tack. For this purpose, six trackless tacks and one conventional tack were evaluated. The residues were collected after 6 hours of heating using a low-temperature evaporative method. The properties and performance of the tacks and tack residues were obtained through three advanced test methods including (1) DSR Frequency Sweep, (2) MSCR, and (3) LAS.

The key findings of this task include the following:

- According to the DSR frequency sweep test, the control tack is the softest tack, followed by Tacks A, B, and C, respectively. These materials are classified as part of the soft-residue group. Tacks D, E, and F belong to a stiff-residue group.
- The MSCR test revealed that the percent recovery decreases with increase in stress level for all material types. For the soft-residue group, considerable changes in percent recovery and non-recoverable creep compliance were observed at high stress level conditions. However, the percent recovery and non-recoverable creep compliance of the stiff-residue group did not decrease significantly under this condition.
- The LAS test showed that Tack F has the most resistance to fatigue cracking and Tack E has the lowest resistance to fatigue cracking at the corresponding intermediate temperatures.

CHAPTER 4
TRACKING RESISTANCE TESTING

This chapter reports the development of test procedures to measure tracking resistance of tack materials. These tests are called the track-free time test and the dynamic shear rheometer tackiness test. These methods were evaluated on different tack materials, at three different temperatures, and were used on tack throughout curing and on tack residue.

MATERIALS

The researchers contacted asphalt emulsion suppliers and requested samples of the tack materials listed in Table 4-1.

Table 4-1. Tack Materials.

Tack Index	Material Type	Residue Category*
Control	Conventional emulsion (cationic)	Soft
A	Trackless emulsion (cationic)	Soft
B	Trackless emulsion (cationic)	Soft
C	Trackless emulsion (anionic)	Soft
D	Trackless emulsion (anionic)	Stiff
E	Trackless emulsion (anionic)	Stiff
F	Trackless hot-applied	Stiff

* Chapter 3 material characterization result

All emulsion tacks were mixed before sample preparation to mitigate internal separation. Emulsions were replaced with the same products after 45 days of use. For sample preparation, the emulsions were first stirred and then spread on a desired surface to a thickness of 0.38 mm (15 mils) with a thin film applicator.

TEST PROCEDURES

Track-Free Time Test

The track-free time test is based on research at the Virginia Center for Transportation Innovation and Research (*8*) and ASTM D711 Standard Test Method for No-Pick-Up Time of Traffic Paint. The outcome of this test is track-free time: the time at which a tack will no longer pick up or track.

Tack coat samples were prepared by spreading room-temperature tack to 0.38 mm (15 mils) thick and 7.6 cm (3 in.) wide with a thin film applicator over asphalt paper. The asphalt paper was previously glued to a wooden board to aid in handling and provided a ridged surface for tack

application. The film thickness was confirmed with a thin film thickness gauge. The samples were cured at different temperatures with no measureable air movement: 25°C (room temperature), 40°C, and 60°C.

Throughout curing, a 5.4 kg (11.9-lb) roller, equipped with rubber rings, was rolled over the sample and across the white poster board paper, where a visible tack track was observed (Figure 4-1). This was repeated until either 60 minutes or when there was no visible tack tracking on the paper. Triplicate samples were prepared and tested for each tack type and temperature.

The end of tracking was defined as the time at which no tracking was observed. Other end-of-test definitions were considered that could quantify the amount of tracking throughout the test, but these methods were overly cumbersome with negligible improvements in test repeatability.

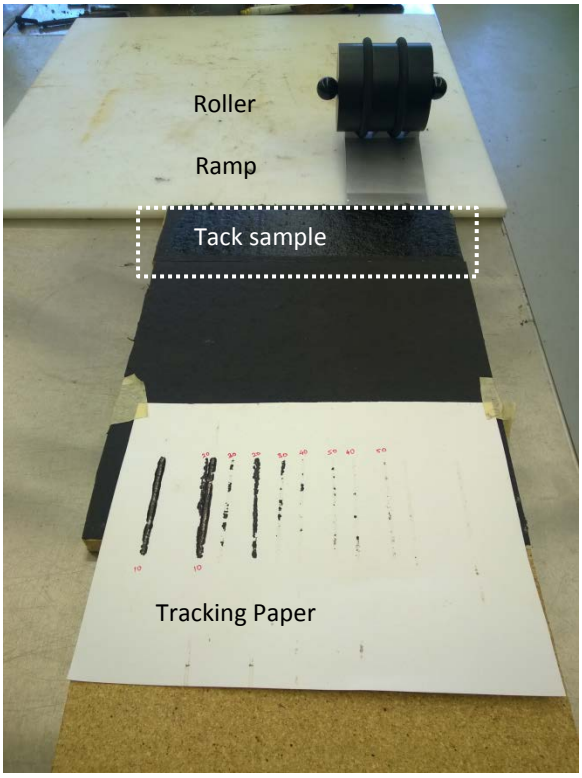

Figure 4-1. Track-Free Time Test.

DSR Tackiness Test

The test procedures adopted here are based on the work done by Gorsuch et al. (*11*). Samples were tested using a Kinexus rotational rheometer manufactured by Malvern. The research team performed tests on the residual binder to measure the tackiness of cured tack (Figure 4-2a). The test was also conducted on the emulsion throughout the curing process (Figure 4-2b); however, researchers focused on the residual testing since emulsion testing made the result less reliable and the test procedure more difficult to perform.

(a) **(b)**

Figure 4-2. Tack Sample in the DSR on (a) Residue Testing and (b) Emulsion Testing.

The tack residue was prepared using the low temperature evaporative technique specified in AASHTO PP72 Method B, as described in Chapter 3. The residue was poured in a 25 mm DSR mold and cooled in a refrigerator. After the thickness of residue was made into 1 mm at cool temperature, the sample was placed on the 25 mm DSR bottom plate. An 8 mm DSR tip was used for this test. The residue was preheated at over 60°C for 10 minutes to prevent debonding at the interface between the sample and bottom plate. Then, the temperature in the testing machine was stabilized to a specified temperature for 15 minutes. The sample on the bottom plate was loaded at 10.5 N with a touch speed of 1.0 mm/sec held for 10 seconds. Then, the tip was detached from the sample at the same 1.0 mm/sec speed. The normal force versus time was recorded during the test. Two samples at each temperature were tested.

The tack energy was calculated using Equation (1), and the results are illustrated in Figure 4-3. This energy is also referred to as adhesive failure energy, defined by Gent and Kinloch (*25)* and Andrews and Kinloch (*26)*:

$$G = \frac{r}{A}\int F(t)dt \tag{1}$$

where,

G = tack energy (J/m^2).
r = pull-off speed rate (m/s).
A = contact area (m^2).
F = normal force (N).

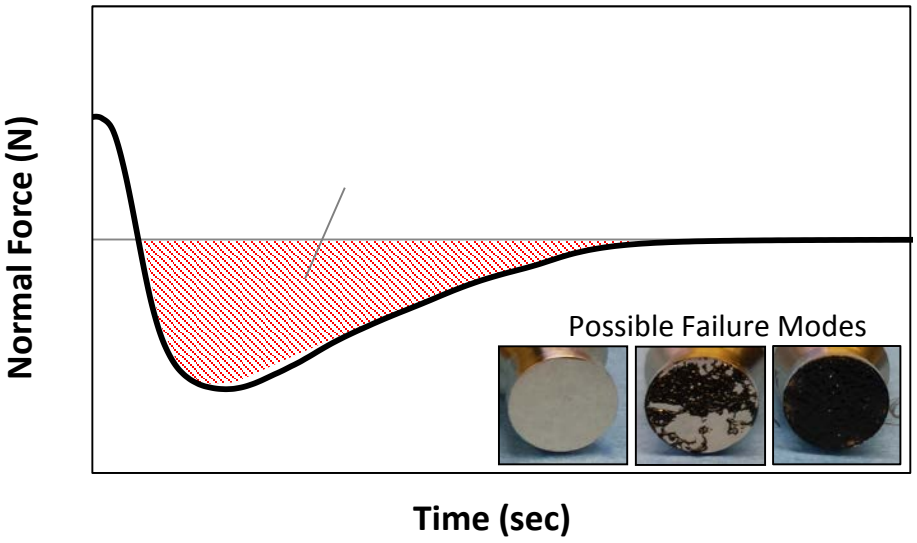

Figure 4-3. Calculating Tack Energy from DSR Tackiness Test.

The contact area is changed after the peak load is applied; however, it would be difficult to capture the instant change in the contact area. Therefore, the initial contact area was used for the calculation of apparent tack energy in this study. The change in tackiness at various curing times or different temperatures was estimated by comparing the differences in area under the curve. In addition, the failure modes were determined by checking the amount of material remaining on the DSR tip. Failure modes were classified as adhesive (clean tip), cohesive (completely dirty tip), and both (partially dirty tip).

TEST RESULTS

Track-Free Time Test

Figure 4-4 shows the track-free time of tacks at different curing temperature. Tack D was evaluated in this test. For reference, the material is most similar to Tack E. At all three temperatures, the control tack had the highest track-free times, and the track-free times of Tack F were almost zero. The control tack at 60°C never reached no-tracking, and the tackiness was enough to tear the roofing paper substrate. In contrast, the other tacks became trackless around 20 to 30 minutes at 25°C, 5 to 15 minutes at 40°C, and less than 10 minutes at 60°C. Aside from the control and Tack F, the test did not consistently distinguish and rank the tacks at different temperatures. The researchers recommend measuring the track-free time at 25°C as that temperature has the lowest overall variation (Figure 4-5) and a clear separation from the control. A test criteria of 35 minutes track-free time is also suggested.

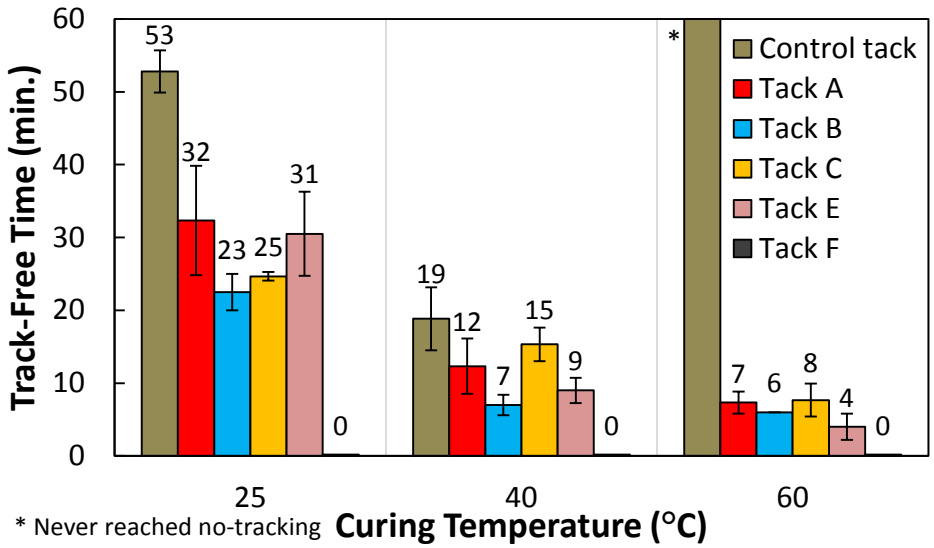

Figure 4-4. Track-Free Time Results.

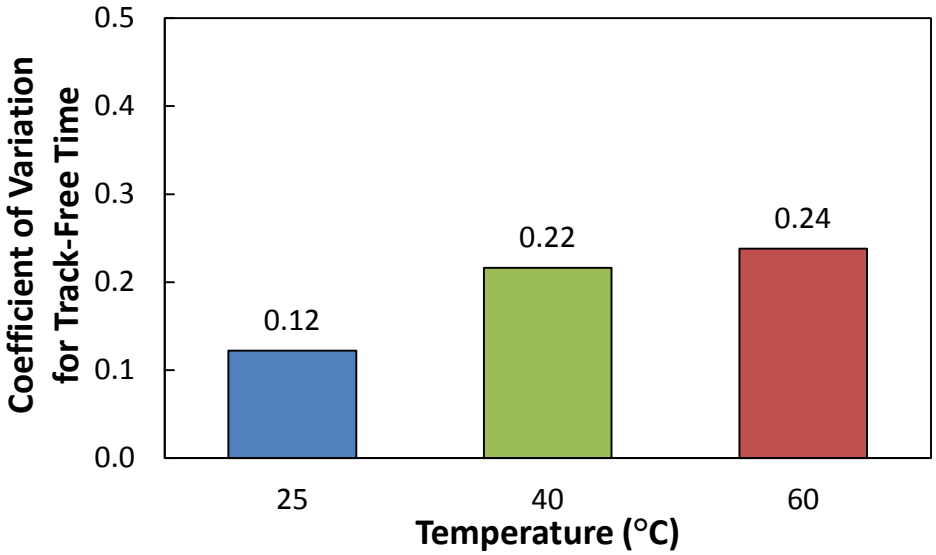

Figure 4-5. Coefficient of Variation of Track-Free Time.

DSR Tackiness Test on Residue

Figure 4-6 describes the change in tack energy and failure mode of Tack B at different temperatures. At lower temperatures, the tack was solid-like and not sticky. When the temperature was raised to 28°C, the tack became sticky but still showed a clean adhesive failure with the DSR tip. The tack energy was the highest just before cohesive failure started. After this point, the tack energy sharply decreased, and cohesive failure governed. As a consequence, there was high sensitivity in response of tackiness around the period when the tack initiated to fail cohesively. At higher temperatures over 40°C, the tack was liquid-like, and the tip was fully covered with tack. In addition, the tack energy did not change significantly.

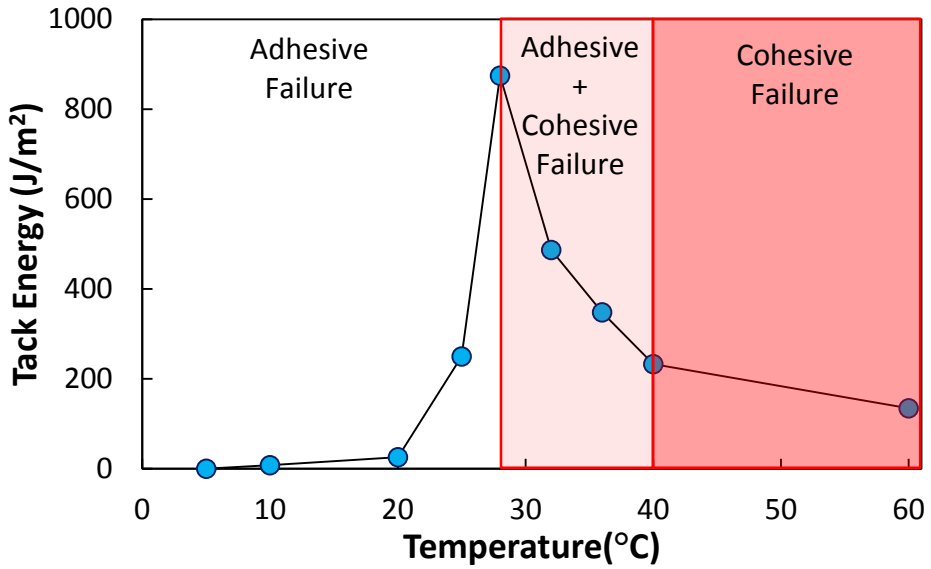

Figure 4-6. Change in Tack Energy and Failure Mode of Tack B over Temperatures.

Figure 4-7 presents the tack energy of all tack residues tested at three different temperatures. At 25°C, all trackless tack materials except the control tack had clean tips and mostly low tack energy. At 40°C, there was a clear distinction between the soft-residue (control tack and Tacks A, B, and C) and stiff-residue (Tacks D, E, and F) groups. Whereas the tacks in the soft-residue group exhibited cohesive failure, the tacks in the stiff-residue group failed adhesively. All tacks at 60°C were softened and showed cohesive failure. In addition, the rank of tack energy at 60°C was matched with the ranking of rheological properties for all tacks except Tack E.

Using this test, the researchers recommend the following criteria for trackless tack: when tested at 40°C, the result will either (1) show adhesive failure or (2) have tack energy higher than 200 J/m^2. At this time, the criteria are not stringent, allowing all current products marketed as trackless tack to qualify. With further experience, these criteria could be refined.

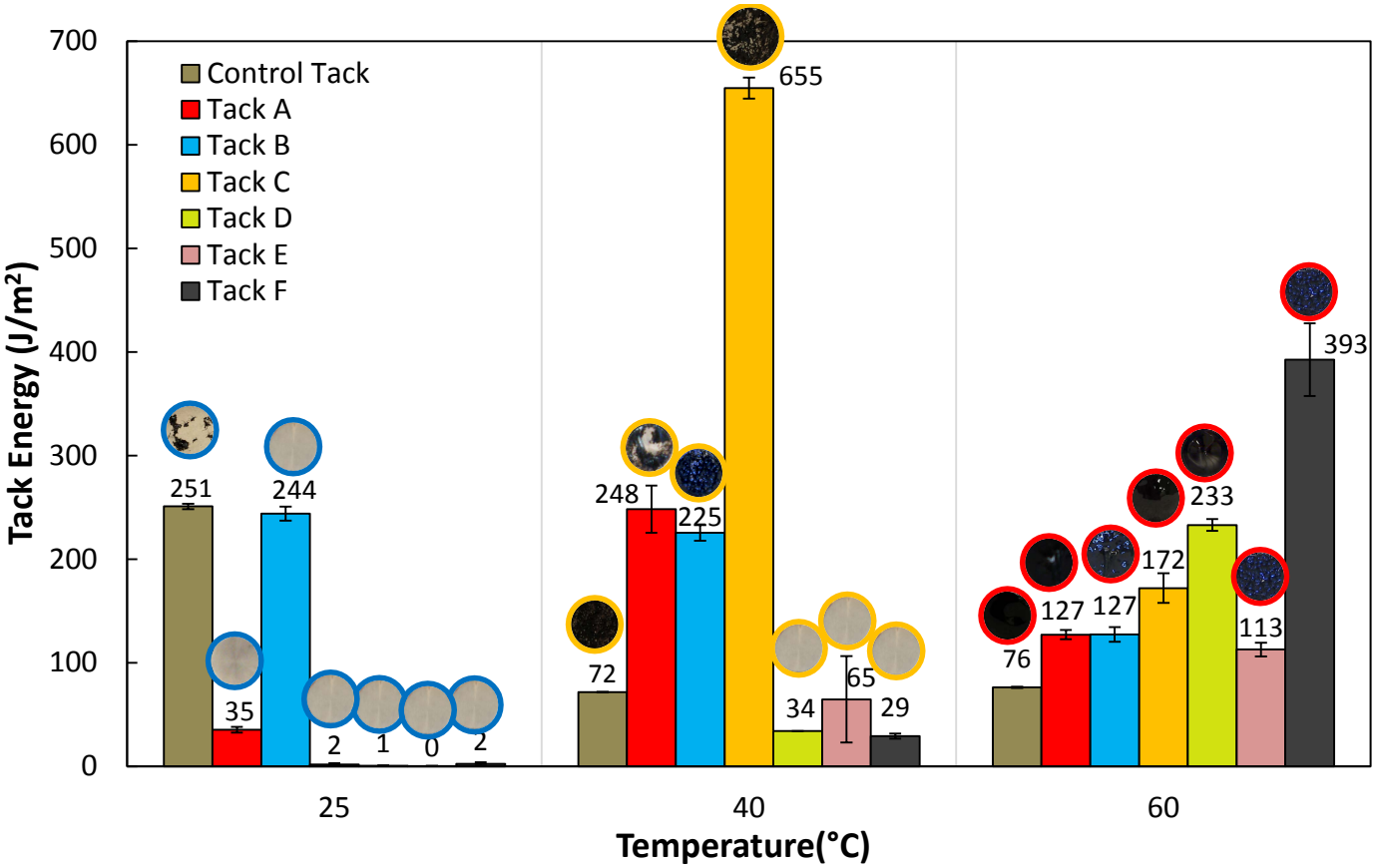

Figure 4-7. Tack Energy of All Tack Residues Tested at Different Temperatures.

SUMMARY

Trackless tacks play a key role in bonding pavement layers while avoiding the tracking problems associated with traditional tacks. While various trackless tack products were introduced to the market, the test methods for their tackiness/tracking resistance have not been established in TxDOT. The objective of this task, therefore, was to develop and assess tests for measuring tracking resistance and track-free time: the track-free time test and the DSR tackiness test. These methods were evaluated using seven tack materials and three temperatures, and were used on tack throughout curing and on tack residue.

The key results of this task are as follows:

- The track-free time test could distinguish between the control tack and trackless tacks at 25 and 60°C. The test could not distinguish among the different trackless tack types except for Tack F.
- Testing uncured emulsion in the DSR tackiness test was difficult and less reliable than testing emulsion residue.
- The DSR tackiness test on emulsion residue distinguished among the control tack, soft-residue trackless tacks, and stiff-residue trackless tacks. Both the tack energy and the sample failure mode are required to evaluate performance.

CHAPTER 5
LABORATORY BOND STRENGTH AND CRACKING RESISTANCE TESTING

This chapter reports on laboratory testing of bonded pavement layers. The objectives were to:

1. Compare different laboratory bond strength test methods and recommend one test for general use.
2. Identify factors that influence bond strength.
3. Compare cracking resistance of bonded layers using different trackless tacks.

TEST PROCEDURES

Materials

Most laboratory samples consisted of an overlay bonded to a substrate layer with tack. Table 5-1 lists the materials of each layer. Two substrate materials were used: Superpave Type D HMA and Portland cement concrete. The overlay was a thin overlay mix (TOM) Type C HMA, sampled from a maintenance job on US 71 in Cedar Park, Texas. Table 5-2 summarizes the raw aggregate substrates for the pneumatic adhesive tensile test instrument (PATTI).

Table 5-1. Materials of Laboratory Samples.

Layer	Mixture Type		
Substrate	Superpave Type D HMA		
	Portland Cement Concrete		
Overlay	TOM Type C HMA		
Tack	**Tack Index**	**Material Type**	**Residue Category***
	Control	Conventional emulsion (cationic)	Soft
	A	Trackless emulsion (cationic)	Soft
	B	Trackless emulsion (cationic)	Soft
	C	Trackless emulsion (anionic)	Soft
	D	Trackless emulsion (anionic)	Stiff
	E	Trackless emulsion (anionic)	Stiff
	F	Trackless hot-applied	Stiff

* Chapter 3 material characterization results

Table 5-2. Aggregates for PATTI Test.

Aggregate ID	Source	Composition
Type A	Delta	Dolomite with minor quartz
Type B	Spicewood	Calcite and quartz
Type C	Marble Falls	Dolomite

Testing Plan

Bond Strength between Pavement Layers

The laboratory testing plan was a series of small-scale experiments, each focusing on a subset of variables. The first experiment was to identify which bond strength test method would be used for further investigation. Table 5-3 shows the test matrix. The recommended test method was determined based on the measurement sensitivity, the measurement repeatability, and overall practicality. Once the optimal test method was determined, the effects of several factors on bond strength and bond energy were investigated. The small-scale experiments, given in Table 5-4, focus on tack type, substrate type, compaction effort, and tack reactivation temperature. Appendix C lists the test matrix for each factor. Many of these factors were selected to address an observed discrepancy between laboratory results and field results.

Table 5-3. Test Matrix – Bond Strength Test Method.

Test Method	Tack Type
Pull-off tensile strength	No Tack
	Tack E
	Tack F
Interface shear strength	No Tack
	Tack E
	Tack F
Arcan	No Tack
	Tack E
	Tack F
Torque	No Tack
	Tack E
	Tack F

Constants: Moderate rate, Aged HMA

Table 5-4. Test Matrix – Four Bond Strength Experiments.

Experiment	Variable	Value
Tack Type	Tack type	No Tack, Control, Tack A, Tack B, Tack C, Tack E, Tack F
Substrate Type	Tack type	No Tack, Tack E
	Substrate type	Aged, New, Concrete
Compaction Effort	Tack type	No Tack, Tack E
	Compaction angle (°)	1, 1.25
	Overlay temperature (°F)	275, 300
	Substrate temperature (°F)	60, 77, 104
Tack Reactivation Temperature	Tack type	No Tack, Tack C, Tack E, Tack F
	Overlay temperature (°F)	275, 300
	Substrate temperature (°F)	60, 77, 104

Constants: Moderate rate, Aged HMA for all but "Substrate Type" Experiment, 1.25° for all but "Compaction Effort" Experiment

** Not full-factorial

Bond Strength between Binder and Aggregate

One additional bond strength test method was evaluated, the pneumatic adhesive tensile test instrument test. Unlike the initial four tests, which focused on bonded pavement layer samples, the PATTI was used to measure the bond between binder and raw aggregate. The results of the PATTI test, therefore, should not be compared to the previous tests. Table 5-5 lists the test matrix for this experiment.

Table 5-5. Test Matrix – PATTI Test.

Tack Type	Aggregate Type
Control	Type A
	Type B
	Type C
Tack B	Type A
	Type B
	Type C
Tack C	Type A
	Type B
	Type C
Tack E	Type A
	Type B
	Type C

Cracking Resistance

Testing was done to address the susceptibility of trackless tack to brittle cracking failure. Two tests were used in this study: (1) a modified Texas overlay test, and (2) a modified beam fatigue test. Table 5-6 shows the test matrix.

Table 5-6. Test Matrix – Crack Resistance.

Test Type	Tack Type	Test Temperature (°F)
Modified Texas Overlay Test	No Tack	77
		40
	Control	77
		40
	Tack B	77
		40
	Tack C	77
		40
	Tack E	77
		40
	Tack F	77
		40
Modified Beam Fatigue	No Tack	77
		60
	Tack E	77
		60
	Tack F	77
		60

Constants: Moderate rate, Aged HMA for overlay, New HMA for beam

Sample Preparation

Most samples were prepared with the Superpave gyratory compactor (SGC). A 6-in. (150 mm) diameter substrate was compacted with 60 gyrations, to a height of approximately 2 in. In most cases, the substrate surface was artificially aged (polished) using an orbital sander with medium (80) and fine (220) grit paper, and subsequently cleaned with an ultrasonic water bath. "New" samples were briefly conditioned with medium grit paper and cleaned. Once dry, heated tack was applied to the substrate with a brush at a "moderate" rate recommended by the vendor (between 0.04 and 0.06 gal/sy for emulsions and 0.12 gal/sy for hot-applied tack). The samples were set to cure for 30 to 60 minutes at 140°F then allowed to stabilize at the specified substrate temperature. The samples were reinserted into the mold and the overlay mix was compacted with

25 gyrations. For each sample configuration, three replicate samples were prepared, except for the pull-off test in which three measurements could be made on one sample.

Beam fatigue samples were prepared in a linear kneading compactor (Figure 5-1). The substrate was compacted to 1.5-in. (38.1 mm) thick. Once cooled, the tack was applied and cured for at least 30 minutes. The slab was reinserted into the compactor and the overlay was compacted on top. The same densities achieved in the SGC were targeted in the slab samples. Triplicate prism samples were cut from the slabs for each measurement.

Figure 5-1. Linear Kneading Compactor.

Bond Strength Testing between Pavement Layers

The following tests focused on measuring the bond strength of bonded pavement layers. The direct shear test was performed with the PINE interface shear strength apparatus presented in Figure 5-2. The sample is inserted with the bond interface oriented vertically. One side of the apparatus holds the specimen rigidly while the other is free to slide vertically. A load was applied to the free-sliding side at a rate of 0.2 in./min (5 mm/min) until failure, and the peak load was recorded. The shear test result can be influenced by aggregate interlock of two layers since the direction of applied shear is parallel to the bond interface.

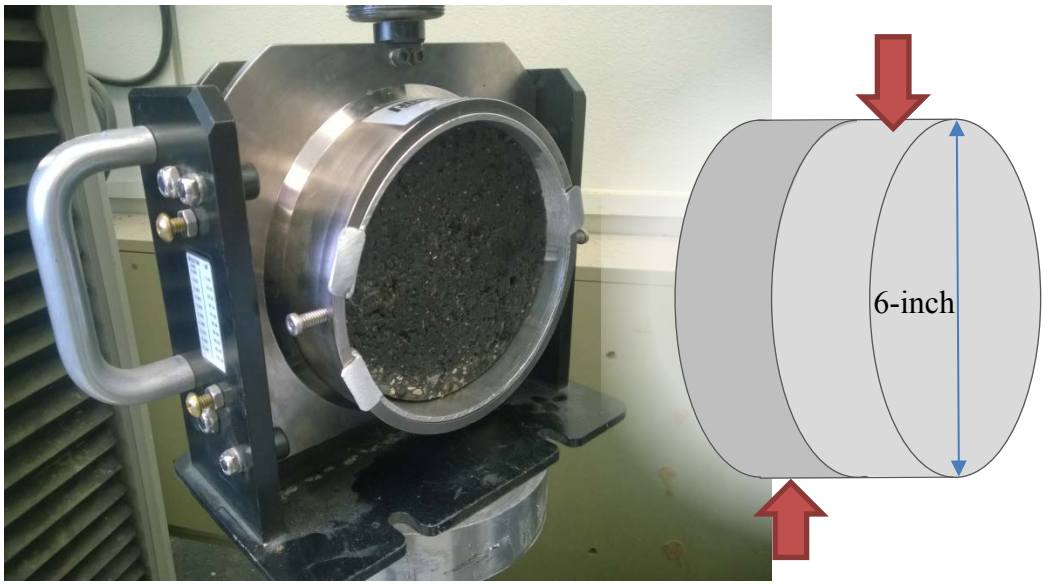

Figure 5-2. PINE Interface Shear Strength Apparatus.

The pull-off tension test was employed with the Proceq DY-206 as illustrated in Figure 5-3. The test involves coring through the overlay and partway into the bottom layer with a 2-in. diameter core barrel. Three measurements can fit on one 6-in. core. Steel pull stubs were glued to the top surface and loaded in tension at a rate of 5 psi/sec until failure. The failure location was then noted as either at the bond or in the upper or lower layers. One drawback of this test is that when the failure occurs in either the top or lower layers the actual bond strength cannot be determined. Also, in many cases the ratio of HMA lift thickness to maximum aggregate size is beyond the 3:1 ratio, which is the minimum requirement for consideration of appropriate representative volume element (RVE).

Figure 5-3. Proceq DY-206 Pull-Off Tester.

Figure 5-4 shows the Arcan test. The bonded sample was trimmed to the dimensions shown and notched at the bond interface. The top and bottom surfaces were bonded to metal plates and fixed in a loading frame. The unique design of the Arcan test allows a sample to be tested at various orientations. A sample could be tested in direct tension, direct shear, or a combination of both. In this study, the samples were tested at 45°, which should represent a compromise between shear and tensile testing approaches, while the loading rate was 0.2 in./min.

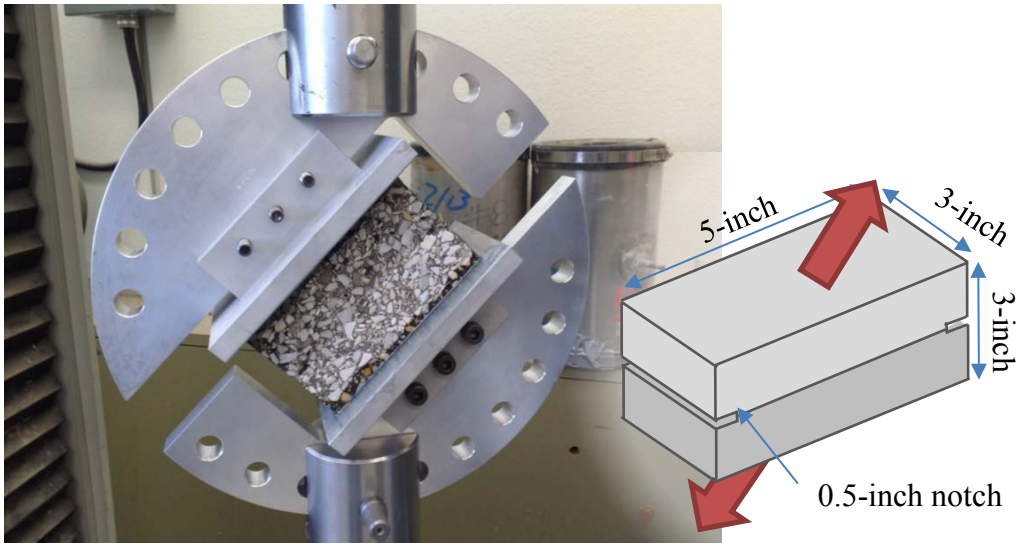

Figure 5-4. Arcan Test.

The last bond strength test considered was the torque test shown in Figure 5-5. In this approach, the base of sample is fixed and a torque wrench is mounted to the top layer. The operator manually applies load at a constantly increasing rate until failure. The maximum load is recorded by the torque wrench. Since the upper limit of torque is 147ft-lb, samples were cored with a 2-in. diameter core barrel as in the pull-off tension test.

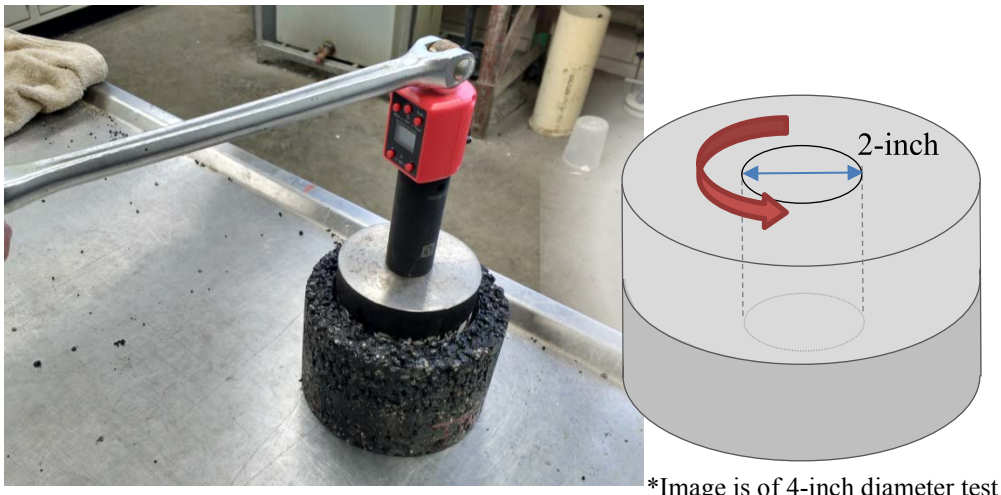

*Image is of 4-inch diameter test

Figure 5-5. Torque Test.

Bond Strength Testing between Binder and Aggregate

The PATTI test (Figure 5-6) was used to measure the bond strength between asphalt and residue binders and raw aggregate in contrast with all other tests that focus on the performance of pavement layers bonded with tack. A metal stub is adhered to a substrate with binder and is then pulled off using pneumatic force. The test was performed in accordance with AASHTO TP 91-11 Determining Asphalt Binder Bond Strength by Means of the Asphalt Bond Strength (ABS) Test. The substrate was prepared by cutting a 0.25-in. slice from a large rock. The slice was smoothed with a lapidary wheel, cleaned in an ultrasonic water bath, and then dried in an oven at 230°F. The substrate was then preheated to 104°F in preparation for residue application. Binder samples were poured and then cooled down in silicon molds with a 0.315-in. (8 mm) diameter hole. The residue was pressed on metal stubs preheated at 175°F, and the stubs were pushed onto the substrates. After stabilizing at room temperature, the sample was tested at a rate of 90±5 psi/sec. Triplicate samples were tested.

Figure 5-6. Pneumatic Adhesive Tensile Test Instrument.

Cracking Resistance

Two tests were considered to evaluate cracking resistance. The first is the Texas overlay test presented in Figure 5-7. The bonded sample was notched on the bottom and glued to the overlay plates. The test was run at two temperatures, 40 and 77°F, at a rate of one complete cycle every 10 seconds, and an opening gap of 0.02 in. The test was terminated when the maximum load for a given cycle had dropped more than 93 percent of the initial maximum load, or after 1000 cycles.

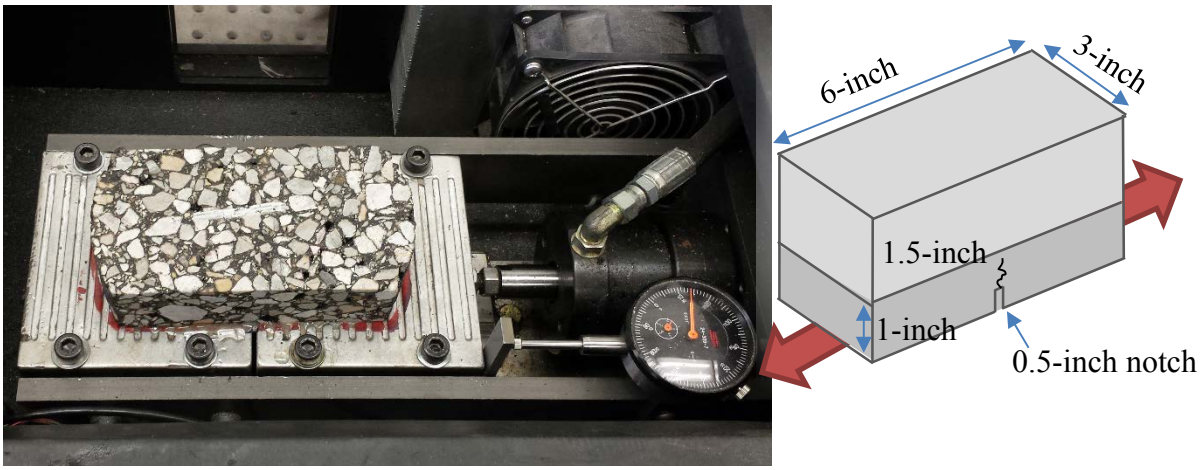

Figure 5-7. Modified Texas Overlay Test.

The second test is the modified beam fatigue test (Figure 5-8). The modified beam fatigue test was run in general accordance with AASHTO TP8-94. To avoid equipment failure with the standard beam fatigue device, a simplified device was designed that fixes the beam with free rotation at two points, rather than four. The test was run in load-controlled mode because earlier failure happens in stress-controlled mode than in strain-controlled mode (*27*).

The composite beam specimens compacted by the linear kneading compactor were sawn into 2.5-in. wide by 15-in. long by 2.0-in. thick beam specimens. The samples were loaded with a haversine waveform without a rest period at 60 and 77°F testing temperatures. A frequency of 1 Hz was applied rather than the specified frequency of 5 to 10 Hz due to a technical defect at high frequency of the uniform testing machine (UTM) used for this test. An input load level was determined as 25 percent of the peak force measured from a monotonic test at a loading rate of 0.025 in./min until failure. A constant cyclic load of 13.5 lbf (0.06 kN) was applied in the center until failure or during 24 hours. The displacement of the actuator was recorded, and the data indicate the deflection inside the clamp.

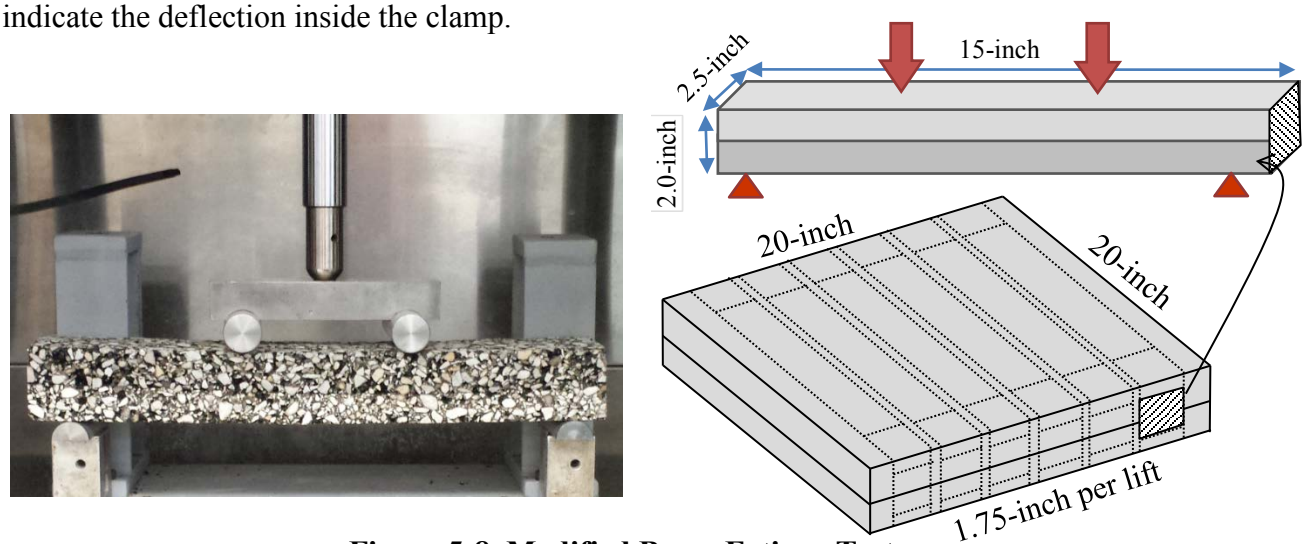

Figure 5-8. Modified Beam Fatigue Test.

The detailed calculations of the flexural stiffness, as well as the dimension and the maximum stress of each beam sample are described in Appendix D. Additionally, the bulk specific gravity of the end part of the tested sample was measured because the variance of air void in the mixture may affect the cracking résistance.

Statistical Analysis

Several analyses of variance (ANOVAs) were performed to identify which factors were most influential to the interlayer bond strength. A *p*-value of 0.05 was chosen for the ANOVA test to define statistical significance.

LABORATORY RESULTS

The research team focused on bond strength and bond energy to evaluate bonding performance. Bond energy is the total work per unit area during the test and is calculated as the area under the stress–strain curve. Note that when measuring bond strength and energy, the cross-sectional area of fracture was used instead of the uneven fracture area. The failure mode can also indicate bonding performance. For example, a sample that failed at the interface exhibits a flat surface (Figure 5-9a), and a sample that failed within the mix has more surface area of fracture (Figure 5-9b). When the sample fails in the mix, this indicates that the bond strength is greater than the internal strength of the layers.

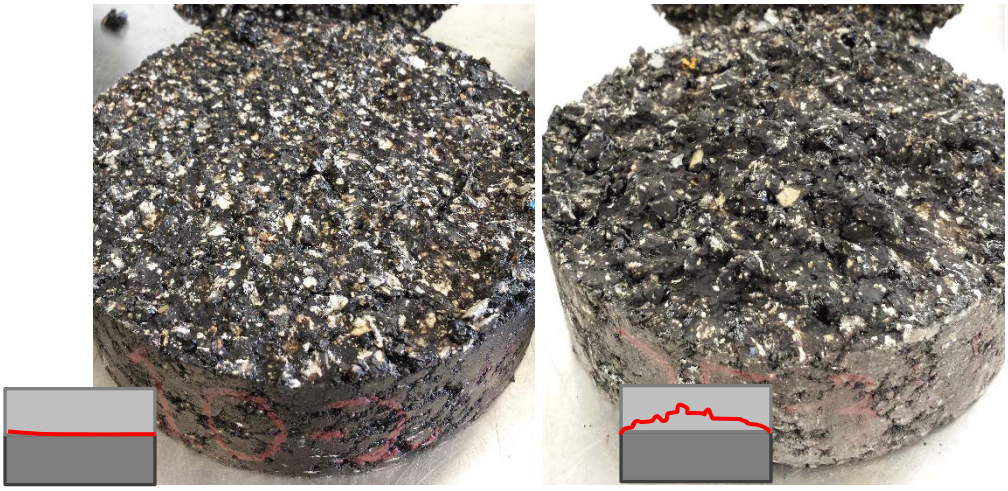

(a) **(b)**

Figure 5-9. Failure Location at (a) Interface and (b) Top Layer.

Bond Strength Testing between Pavement Layers

The first study was to compare four different bond strength tests. Table 5-7 shows the results of sensitivity and variability of bond strength by test type. None of the tests had significant bond strength sensitivity versus tack type. This is likely because the lab-molded samples all had high

bond strengths, even for samples without tack. Still, the pull-off and shear tests were closest to correctly distinguishing samples with tack from samples without tack. The tests with the lowest variability were the shear test and the Arcan test.

Table 5-7. Results of Sensitivity Analysis of Test Methods to Tack Type.

Test Type	Bond Strength	
	COV*	*p*-value
Pull-off	0.21	0.14
Interface Shear	0.07	0.12
Arcan	0.11	0.63
Torque	0.14	0.9

* Coefficient of Variance

Table 5-8 summarizes a comparison of all the test methods. The interface shear test well represents the failure mode in the field, is quick and easy to perform, and has a low cost. The only drawback of the shear test is it must be performed in the lab using a loading frame. Overall, the interface shear test is the most practical and reliable test to evaluate the bonding performance. The remainder of the testing in this section, therefore, used the shear test.

Table 5-8. Characteristics of Test Type.

Test Type	Representation of Field Condition	Sample Preparation	Cost	Test Time (Prep/Test)	Test Rate	Advantage/ Disadvantage
Pull-off	Fair	Easy	$5,000	24 hrs/ 5 min	5 psi/ sec	- Possibility of failed test (no result). - Tensile force not representative of field conditions.
Interface Shear	Good	Easy	$5,000	None / 5 min	0.2 in. /min	- Possibility of damaging apparatus. - Requires loading frame.
Arcan	Very Good	Moderate	$3,000	24 hrs/ 20 min	0.2 in. /min	- Consideration of two loading mechanisms. - Complicated installation. - Requires loading frame. - Device is custom built.
Torque	Good	Easy	$500	24 hrs/ 5 min	Manual	- Difficult to only load in torque. - Inconsistent loading rate.

Table 5-9 summarizes the statistical results of shear bond strength and bond energy for each experiment. The table indicates which variables were significant as noted by highlighted cells. Variables that were significant for both performance indicators are both highlighted and bolded. In the laboratory study, bond energy was the preferred performance indicator as it reflected both

the overall bond strength and the failure mode (samples with interface failure had lower bond energy than samples failing in the mix.) The modeled results are shown in the subsequent discussion and the final statistical models for each experiment are in Appendix E.

Table 5-9. Statistical Analysis of Bond Strength and Bond Energy.

Experiment	Explanatory Variable	Shear Bond Strength (psi)			Shear Bond Energy (ft-lb/in^2)		
		Variable *p*-value	Model *p*-value	Model R^2	Variable *p*-value	Model *p*-value	Model R^2
Tack Type	Tack	>0.05	–	–	0.009	0.009	0.69
Surface Type	**Tack**	<0.001	<0.001	0.97	<0.001	<0.001	0.89
	Surface	<0.001			<0.001		
	Tack*Surface	<0.001			>0.05		
Compaction Effort	Tack	R	<0.001	0.83	R	–	–
	Comp. Angle	0.03			>0.05		
	Temp	R			R		
	Comp. Angle *Temp	>0.05			>0.05		
	Comp Angle *Tack	>0.05			>0.05		
	Tack*Temp	R			>0.05		
Tack Reactivation Temperature	**Tack**	<0.001	<0.001	0.77	<0.001	<0.001	0.84
	Temp	<0.001			<0.001		
	Temp*Tack	<0.001			>0.05		

Bold	Variable significant for **both** performance metrics
Not bold	Variable significant for only one performance metric
>0.05	Variable not significant and was removed from the model
"–"	Value not calculated
R	Variable was significant but removed from model since main effect of interest was not significant

Figure 5-10 shows the effect of tack type on bond performance. Bond strengths for all samples, including samples with No Tack, were excellent. Bond strengths from field samples rarely reach above 100 psi, while these laboratory sample strengths ranged from 150 to over 180 psi. Statistically speaking, the bond strengths for all samples were not different, even though the No Tack samples had a noticeably lower average strength. But when considering the failure mode, the stiff-residue group trackless tacks never had an interface failure. The effect of failure mode is better represented in the bond energy graph, and in subsequent discussion only bond energy results will be presented. Tack F had the highest bond energy (3.9 ft-lb/in^2) followed by Tack E at 3.1 ft-lb/in^2. Both these tacks are in the stiff-residue group. The bond energies for all soft-residue groups (including the control) were statistically similar (between 1.8 and 2.6 ft-lb/in^2). The No Tack sample had the lowest bond energy at 1.3 ft-lb/in^2.

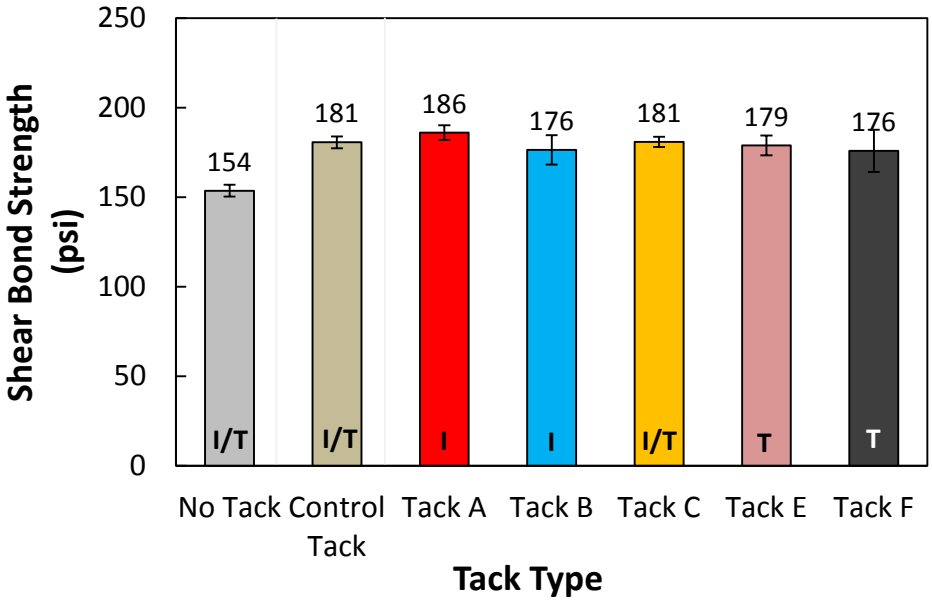

(a)

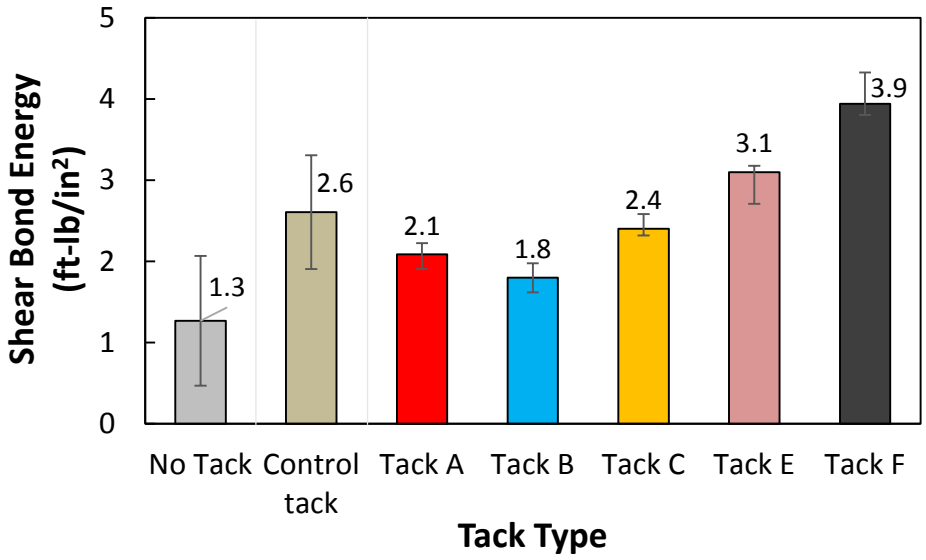

(b)

Figure 5-10. Modeled Effect of Tack Type: (a) Shear Strength and (b) Bond Energy.

Figure 5-11 shows the effect of surface type on bond energy using samples with Tack E and without tack. The bond energy of samples with aged (lab-polished) HMA and new HMA were not statistically different. The laboratory polishing procedure, therefore, was inadequate to represent an actual aged substrate. The presence of tack made a significant difference. HMA samples without tack had bond energies of 2 ft-lb/in^2 and samples with Tack E had bond strengths of 3 ft-lb/in^2. The bond energies of concrete surface samples were dramatically lower

than HMA surface samples. No Tack and Tack E concrete samples had bond energies of 0.04 and 0.8 ft-lb/in^2. While the concrete bond energy appears unacceptably low, the actual bond strength was above 100 psi. Overall, both surface type and the presence of tack had a high impact on bond performance.

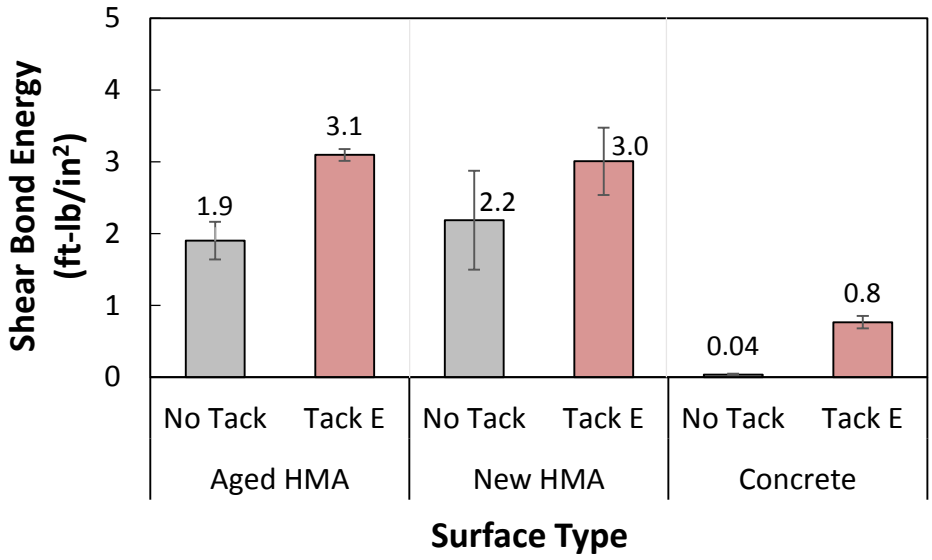

Figure 5-11. Modelled Effect of Surface Type on Bond Energy.

Based on the statistical results in Table 5-9, compaction angle did have an effect on bond strength but not bond energy. The difference in bond strength, while statistically significant, was not practically significant. Therefore, the researchers considered this variable to have only a marginal effect on bond performance.

Table 5-9 indicates that the bonding performance was strongly dependent on the tack reactivation temperature. In this study, tack reactivation temperature was defined as the average of the surface temperature and the mixture temperature. The shear bond energy results are presented in Figure 5-12. Overall, modeled bond energies ranged from 0.5 to 5 ft-lb/in^2. Bond energy increased at higher tack reactivation temperatures for all samples. Within the tested range of 160 to 212°F, bond energy increased by 2 ft-lb/in^2 for a given sample type. Bond energy was highest for Tack F (hot-applied, stiff-residue tack). Next highest was Tack E (stiff-residue tack), then Tack C (soft-residue tack), and lastly No Tack.

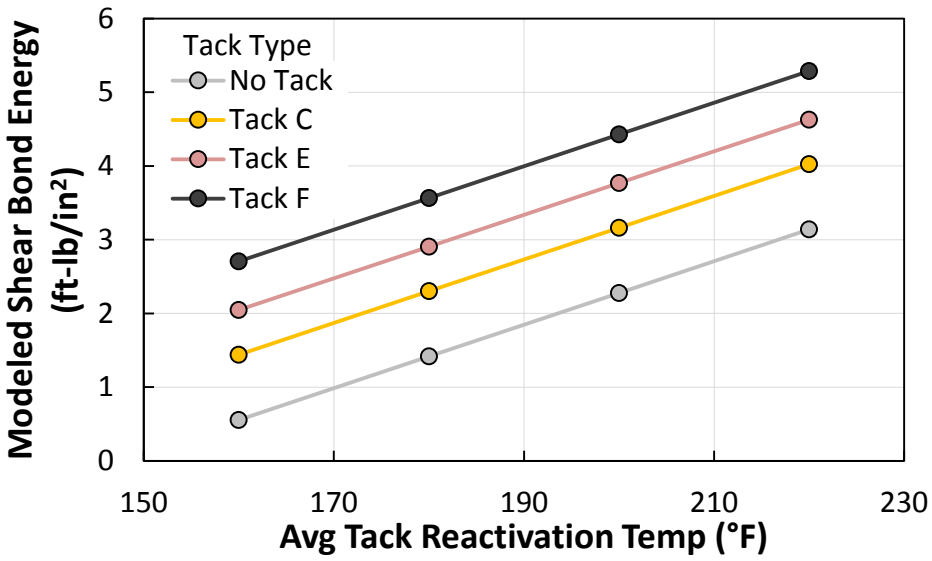

Figure 5-12. Modeled Effect of Tack Reactivation Temperature and Tack Type on Shear Bond Energy.

Bond Strength between Binder and Aggregate

Early in the project, the research team evaluated the effect of different tack types spread on various aggregate types in dry condition on the bond strength using the PATTI test. Cohesive failure inside the residue was prominent in all the test results, implying that the bond between binder and aggregate was stronger than the internal bond of the tack itself. The results in Figure 5-13 show that there was no significant difference between aggregate types in terms of pull-off strength, whereas the bond strength was highly dependent on tack type.

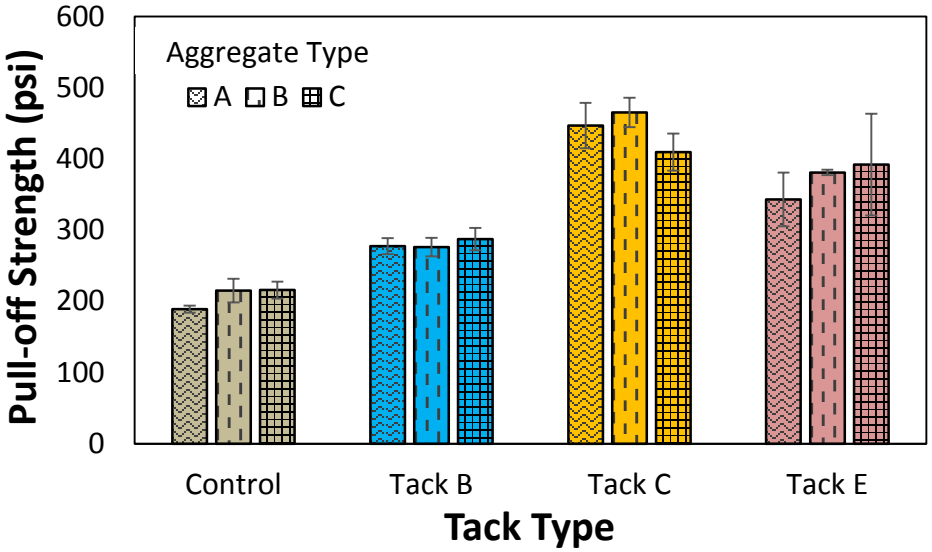

Figure 5-13. Pull-Off Strength of Tack Residues on Three Aggregate Types.

Although Tack C is softer than Tack E, the pull-off strength was higher. This project did not consider moisture conditioning, which may reveal an interaction between aggregate type and bond strength.

Cracking Resistance

Cracking resistance was evaluated with results from the overlay tester and the modified beam fatigue test. In overlay testing, the performance indicators were the maximum load and the number of failure cycles. Table 5-10 indicates the results of statistical analysis for different tacks tested at different temperatures. The test temperature was the only statistically significant variable influencing the maximum load and number of failure cycles; however, the *p*-value for tack type was 0.06. Since tack type was not statistically significant, either tack type is not important for cracking resistance, or the test was not appropriate for this study.

Table 5-10. Statistical Analysis of the Overlay Test Results. (Maximum Load and Number of Failure Cycles)

Explanatory Variable	Maximum Load			Number of Failure Cycles*		
	p-value	Model *p*-value	Model R^2	*p*-value	Model *p*-value	Model R^2
Tack Type	>0.05	<0.001	0.88	>0.05	<0.001	0.92
Test Temp	**<0.001**			**<0.001**		
Tack*Temp	>0.05			>0.05		

Bold	Variable significant for **both** performance metrics
Not bold	Variable significant for only one performance metric
>0.05	Variable not significant and was removed from the model
*	In logarithmic scale

Figure 5-14 describes the number of failure cycles at two different test temperatures. The number of failure cycles at 77°F in Figure 5-12(a) was plotted in logarithmic scale. The samples with stiff tack residues (i.e., Tacks E and F) failed sooner than soft tack residues (i.e., the control tack and Tack B); however, the result of Tack C was closer to stiff-residue group. It was demonstrated that the brittleness has an impact on cracking resistance. At 40°F, all specimens became so brittle that failure at the first cycle occurred except for one sample that had No Tack. For all samples at both test temperatures, the crack propagated upward through the overlay HMA, with no debonding at the interface. This suggests that all samples, even No Tack samples, had adequate bond strength and were not susceptible to low-temperature cracking.

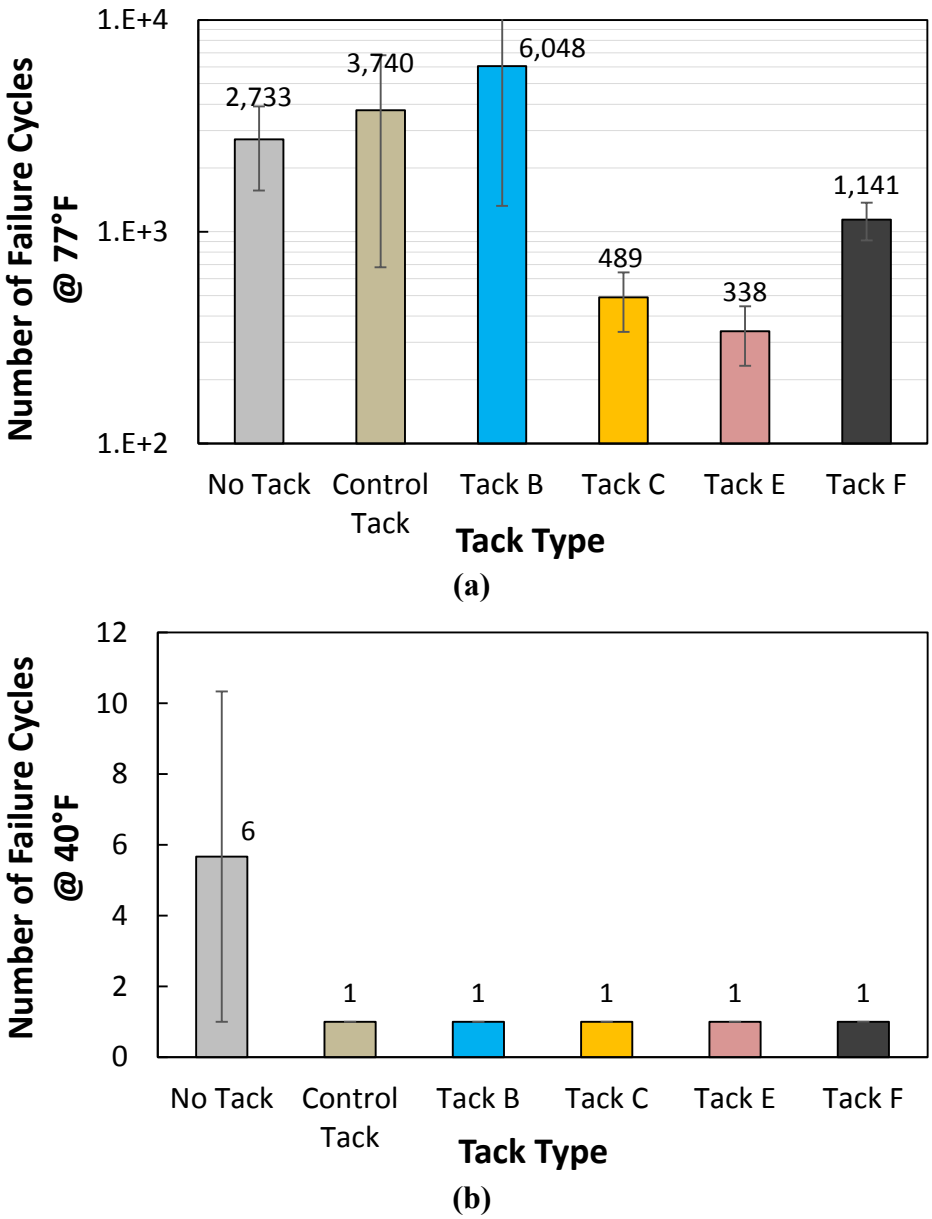

Figure 5-14. Overlay Results, Number of Failure Cycles: (a) 77°F and (b) 40°F.

Figure 5-15 exhibits the maximum load at the first cycle of samples tested at 40 and 77°F for various tacks. The peak load at the first cycle of samples tested at the lower temperature was much greater than at room temperature.

In the modified beam fatigue test, the failure cycles and initial stiffness were evaluated for each beam sample. Figure 5-16 describes the determination of initial stiffness and failure cycle of a beam sample. The power function was best fitted to the data where the constants of this mathematical form were needed to predict the failure cycle.

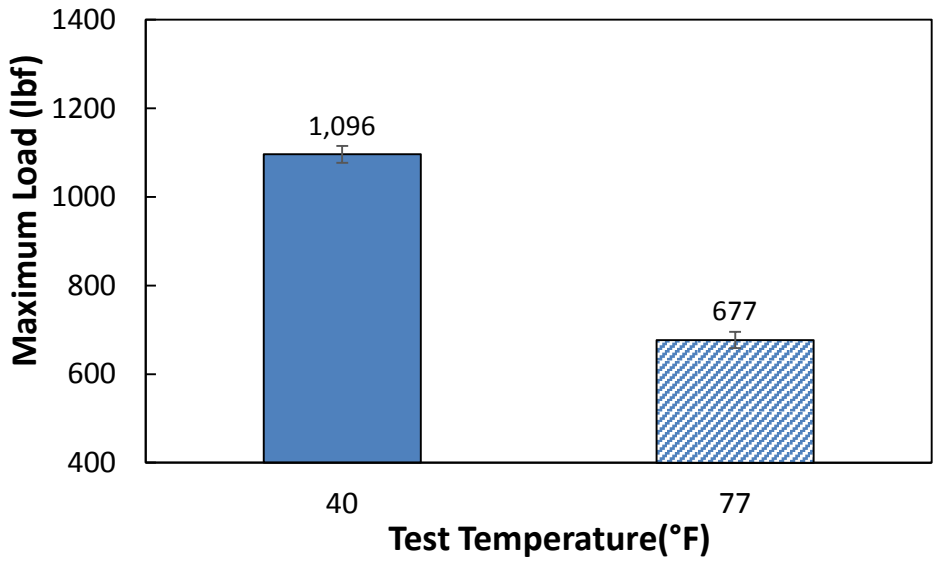

Figure 5-15. Beam Fatigue Results, Maximum Load at First Cycle.

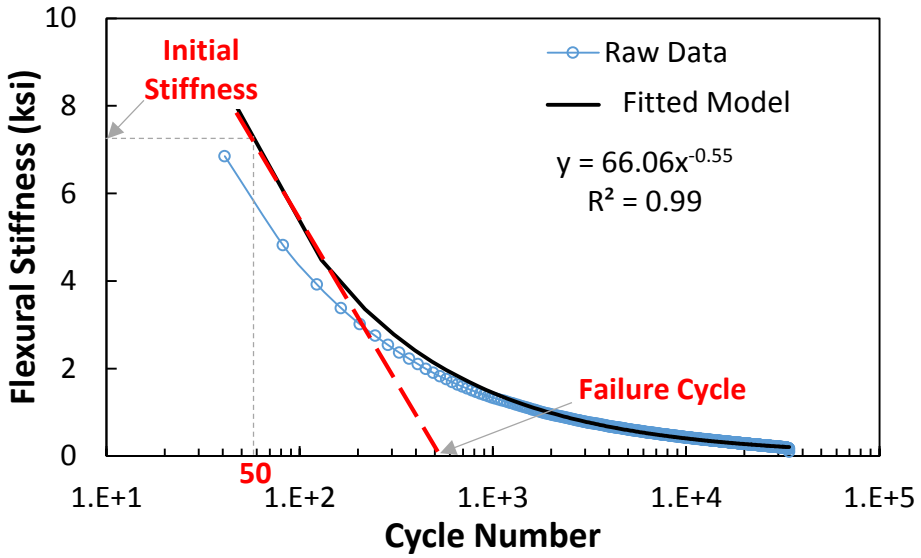

Figure 5-16. Determination of Initial Stiffness and Failure Cycle for Beam Fatigue Test.

The initial stiffness was determined as the stiffness at the 50th load cycle to represent a reference. The failure life in the stress-controlled mode is traditionally regarded as the stiffness reduction of 10 percent; however, in this study, the failure cycle was defined as the inflection point in which the stiffness stops decreasing rapidly. The point is located where a line having the slope of change in stiffness at the 50th load cycle meets the x-axis. To determine the failure cycle, the natural number of flexural stiffness is plotted against the number of cycles in logarithmic scale. In the curve, the failure cycle is determined as the intercept of a tangent line at the 50th load cycle. The detailed description for calculating the failure cycle is included in Appendix D.

The results of the statistical analysis of the beam fatigue test are summarized in Table 5-11. The effect of tack type was not significant in terms of initial stiffness, but the failure cycle was noticeably influenced by both tack type and temperature.

Table 5-11. Statistical Analysis of Beam Fatigue Results.
(Failure Cycle and Initial Stiffness)

Explanatory Variable	Failure Cycle			Initial Stiffness		
	p-value	Model *p*-value	Model R^2	*p*-value	Model *p*-value	Model R^2
Tack Type	0.003	<0.001	0.82	>0.05	0.039	0.35
Test Temp	**0.004**			**0.039**		
Tack*Temp	0.002			>0.05		

Bold	Variable significant for **both** performance metrics
Not bold	Variable significant for only one performance metric
>0.05	Variable not significant and was removed from the model

Figure 5-17 presents the failure cycles of beam samples with different tacks tested at different temperatures. The failure cycles of samples at 77°F were similar regardless of tack type. The results at 60°F showed that the samples with Tack E had the most resistance to fatigue cracking, followed by Tack F and No Tack samples, respectively. Also, debonding at the interface did not occur in any sample, suggesting that cold-weather delamination is not a concern.

The exact reason the Tack F sample failed before Tack E is still unknown. It may be related to the tack type alone or to non-uniform tack application of Tack F. The researchers found that the bulk specific gravity of samples with Tack F were higher than for the Tack E and No Tack samples. Further study is needed to answer this question.

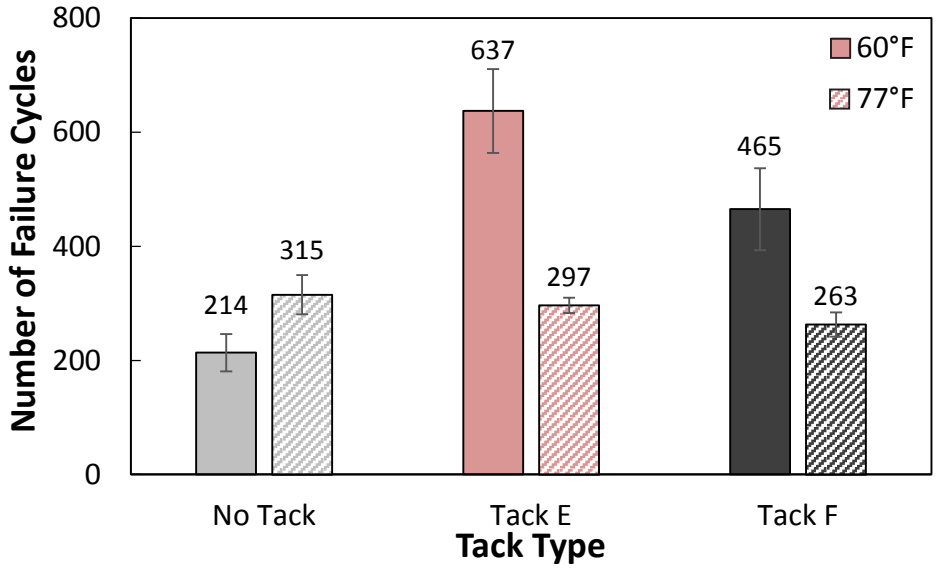

Figure 5-17. Failure Cycles of Beam Samples with Different Tacks and Test Temperature.

Table 5-12. Bulk Specific Gravity of Beam Samples with Different Tacks.

Tack Type	Bulk Specific Gravity (G_{mb})	
	Average	St. Dev.
No Tack	2.06	0.01
Tack E	2.08	0.02
Tack F	2.18	0.14

SUMMARY

The objective of this task was to measure the performance of bonded pavement layers through extensive laboratory evaluations. The properties evaluated in the laboratory were bonding strength and cracking resistance. Several devices were considered in the bond strength analysis: pull-off tester, interlayer shear strength apparatus, Arcan test, and torque test. The shear test proved the most promising and was used for further evaluations of tack type, substrate type, compaction effort, and tack reactivation temperature. The cracking resistance tests were done using the overlay tester and flexural beam fatigue test.

The key results are as follows:

- Based on test characteristics and statistical results, the interlayer shear test is the most practical and repeatable test to evaluate pavement layer bonding.
- The bond strength of laboratory samples was high, between 100 and 200 psi. In many cases, samples failed in the HMA layer, meaning the bond strength was higher than the layer strength.
- The effect of the following factors on shear bond strength and bond energy were tested:
    - **Tack type** had a significant impact on bond performance. All samples had acceptable bond strengths. Samples with stiff-residue tacks had higher bond energy than samples with soft-residue tacks. All tack samples had higher bond energies than samples with no tack.
    - **Surface type** had a high impact on bond performance. New HMA surface samples had higher bond energy than concrete surface samples.
    - **Compaction angle** marginally influenced bond performance.
    - **Reactivation temperature** (the average temperature between the existing surface and the loose HMA) significantly affected bond performance. As the temperature increased, so did the bond strength and bond energy. Again, stiff-residue tack samples had higher bond energy than soft-residue tack samples.
- Based on the PATTI test results, tack type had a significant impact on bond strength. Aggregate type was not a significant factor; however, the aggregate sample size was small in this study. In addition, the effect of moisture conditioning was not considered.

- Cracking resistance results from the overlay test were influenced by temperature and marginally influenced by tack type. At low temperatures, the maximum load was higher and samples failed after one cycle. Based on the number of cycles to failure at 77°F, the samples could be roughly divided into soft- and stiff-residue groups.
- From the beam fatigue test, tack type and test temperature have significant impact on the number of cycles to failure. At the low test temperature, samples with trackless tack had more cycles to failure than samples without tack.
- In both the overlay and beam fatigue tests, none of the samples had interface debonding, indicating that the samples are resistant to low-temperature delamination.

CHAPTER 6
FIELD SECTIONS AND BOND STRENGTH TESTING

This chapter reports on the construction of test sections and subsequent testing. The objectives of field testing were to:

1. Construct test sections with different existing surface types, tack materials, and application rates.
2. Compare the bond strengths in each test section and identify influential factors.
3. Provide general assistance to TxDOT to test bond strength on various projects.

PROJECTS

US 183, Cedar Park

This project location is on US 183, between FM 1431 and Osage Drive (Figure 6-1). US 183 is a four-lane principal arterial that runs through an urban area on the south and lighter urban area on the north. The south half has closely spaced signals and an average annual daily traffic (AADT) of 35,000 with 9 percent trucks, while the north half has few signals and an AADT of 23,000 with 9 percent trucks.

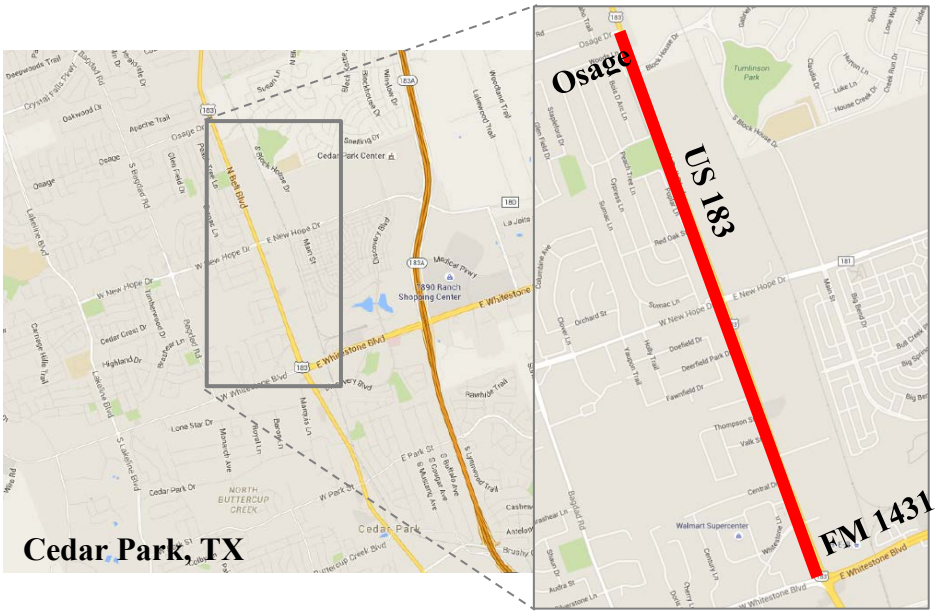

Figure 6-1. Project Location on US 183.

The project had three surface types. Figure 6-2 presents the existing polished surface condition after years of traffic and climate exposure. A portion of the project was milled and inlayed with new HMA. A picture of this surface is not available. On the southern end, the pavement was milled to meet curb and gutter requirements (Figure 6-3a). Some areas of the milled section had "scabbing," a condition where the milling is inconsistent, leaving a cut surface in some areas and exposing a smooth aged surface in others (Figure 6-3b). During construction, the milled surface was cleaned prior to tack applications, though the researchers noted that cleaning was insufficient in some locations.

Figure 6-2. Existing Surface Condition.

(a) **(b)**

Figure 6-3. Surface Condition of Milled Section: (a) Uniform and (b) Scabbed.

Table 6-1 shows the testing plan for this project. It consisted of three tack types (Tacks B, C, and E), three surface types (existing, new, and milled), and three target tack rates (low, moderate, and high). The actual tack rates are shown in the table, and were measured using ASTM D2995 (Standard Practice for Estimating Application Rate and Residual Application Rate of Bituminous Distributors) (Figure 6-4). In a few sections, the rate was not measured and instead was estimated based on measurements from similar sections. Samples with No Tack were taken at the location where tack rate was measured, and were not part of a full-scale test section.

Table 6-1. US 183-Leander Testing Plan.

Tack Type	Surface Type	Tack Rate (gal/sy)		
		Level	Average Residual	Residual at Core Location
None*	Existing	-	0	0
	New	-	0	0
	Milled	-	0	0
Tack B	Existing	Low	0.02	0.02
		Moderate	0.04	0.04
		High	0.05	0.05
	New	Low	0.02	0.02**
		Moderate	0.04	0.05
		High	0.05**	0.05**
	Milled	Moderate	0.04**	0.04**
		High	0.06**	0.06**
Tack C	Existing	Low	0.03	0.03
		Moderate	0.04	0.05
		High	0.05	0.05
	New	Low	0.02	0.02
		Moderate	0.05	0.05
		High	0.06	0.06
	Milled	Moderate	0.03	0.03
		High	0.06**	0.06**
Tack E	Existing	Low	0.02	0.02
		Moderate	0.03	0.04
		High	0.04	0.05
	New	Low	0.02	0.03
		Moderate	0.03	0.04
		High	0.04	0.05
	Milled	Moderate	0.04	0.04
		High	0.06	0.07

* Not a full-scale test section
** Estimated value

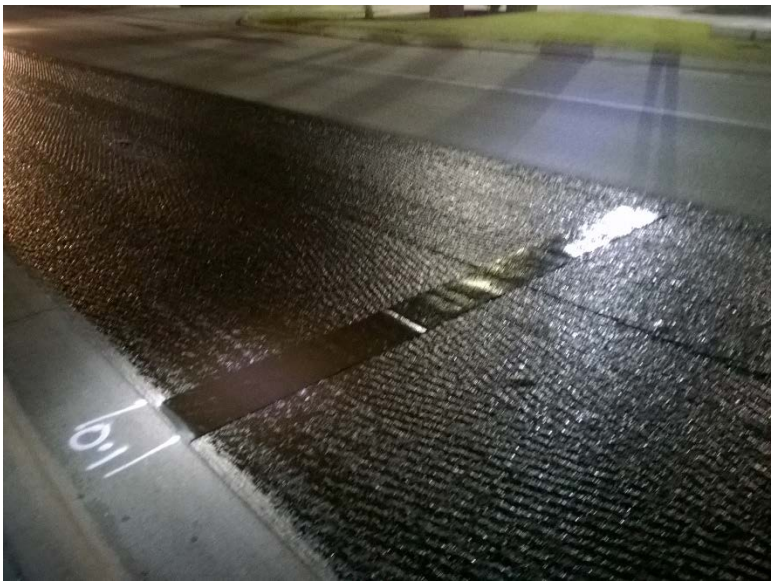

Figure 6-4. Measurement of Tack Application Rate (ASTM D2995).

All construction was performed during the night, with a given tack type being used each night. The average air temperature was 77 to 90°F. The humidity was 45 percent when applying Tack B, 79 percent for Tack C, and 60 percent for Tack E. The wind speed was 7 mph for Tack B, and 3–4 mph for Tacks C and E. In most cases, tack was applied uniformly. For Tack C, however, the distributor had some problems with pump pressure and spray uniformity (Figure 6-5). Tack was allowed to cure at least 30 minutes before HMA laydown.

A material transfer vehicle (MTV) was used to deliver the mix from the trucks to the paver. Thin overlay mix was laid down with the target thickness of 1 in. The HMA was compacted by two 10-ton rollers. The first roller was operated with low vibration while the next roller was run only with static loading and no vibration. Both rollers applied one down-and-back pass on the left, right, and middle of the mat.

Samples were cored from the center of the wheel path for subsequent laboratory testing (Figure 6-6). Four cores were taken from each section: three for the shear test and one for the pull-off test. For the Tack E sections, core locations with uniform density were selected with the rolling density meter (ground penetrating radar). Because of time constraints, core locations for other sections were chosen randomly. Cores over the milled section were marked to denote the direction of traffic.

Figure 6-5. Non-Uniformity of Tack C Application.

Figure 6-6. Coring Samples.

SH 336, McAllen

Figure 6-7 shows the test site located on SH 336 in McAllen, Texas. At this site, Tack B and RC-250 were used. RC-250 is a cut-back in which asphalt binder is dissolved with petroleum solvent. Only one surface type was studied: an aged and polished gravel surface with low angularity (Figure 6-8). The tack materials were applied on different days. The humidity was 80 percent for Tack B, and 87 percent for RC-250. On both days, a very light rain was falling for a few minutes. The average wind speed was 1 mph for Tack B, and 3.5 mph for RC-250. The air temperature for both tacks was around 77°F. Table 6-2 summarizes the testing plan for this project.

Figure 6-7. Project Location on SH 336.

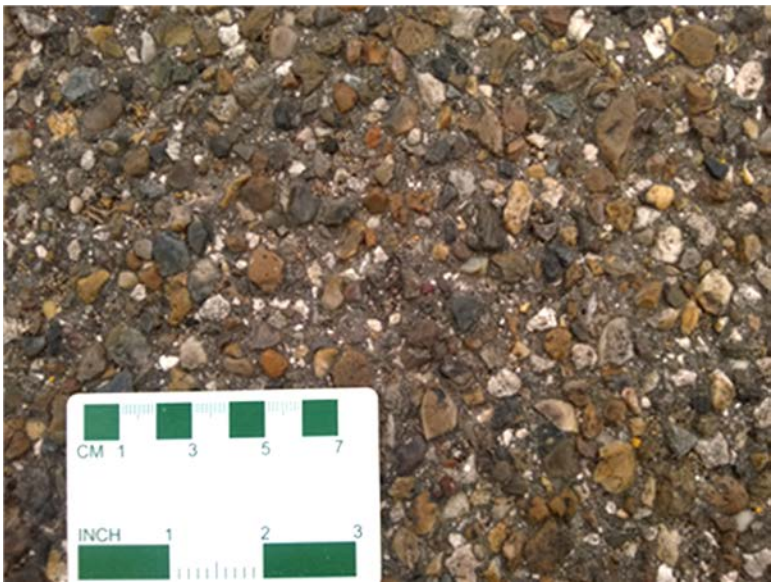

Figure 6-8. Existing Surface.

Table 6-2. SH 336-McAllen Testing Plan.

Test Section	Tack Type	Surface Type	Tack Rate (gal/sy)		
			Level	Average Residual	Residual at Core Location
SH 336	Tack B	Existing	Low	0.04	0.04
			Moderate	0.04	0.05
			High	0.09	0.10
	RC-250		Low	0.04	0.04
			Moderate	0.06	0.05
			High	0.07	0.07

The track-free time test was conducted for each tack applied at moderate shot rate to measure the time when the tack was cured and would not track. On SH 336, Tack B became trackless after 30 minutes, but RC-250 kept tracking for over one hour. Figure 6-9 presents the tack condition after construction vehicles passed. The tack would still track some under heavy, slow-moving construction equipment, especially for the RC-250 section.

The number of field cores collected from SH 336 was limited because of very low bond strengths. Tack B cores were collected the night after construction, but RC-250 cores could not be sampled intact. A few cores of the existing pavement were taken from the center turn-lane.

Figure 6-9. Tack Condition after Trucks Passing, RC-250 in SH 336.

US 96, Browndell

This project was located on US 96, 12 miles north of Jasper and running north to the county line (Figure 6-10). The specific test section locations were constructed in the northbound lane near milepost 382. The project was a Type D stone-matrix asphalt (SMA), laid 1.5-in. thick using the Tack E trackless tack. The existing pavement was an aged HMA with a moderate-smooth surface texture and low angularity (Figure 6-11).

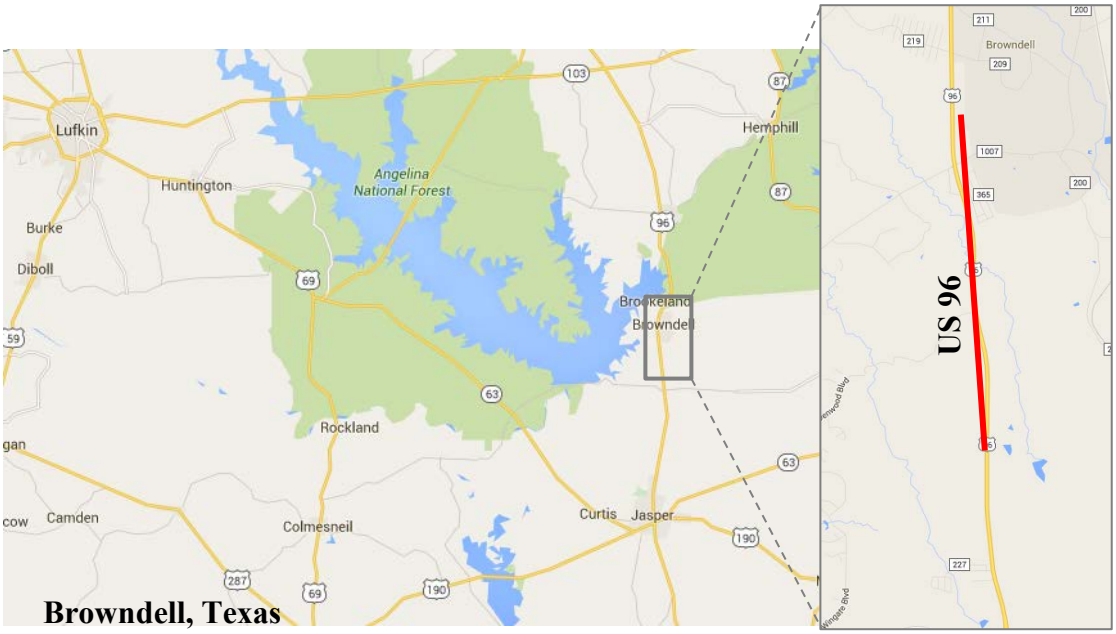

Figure 6-10. Project Location on US 96.

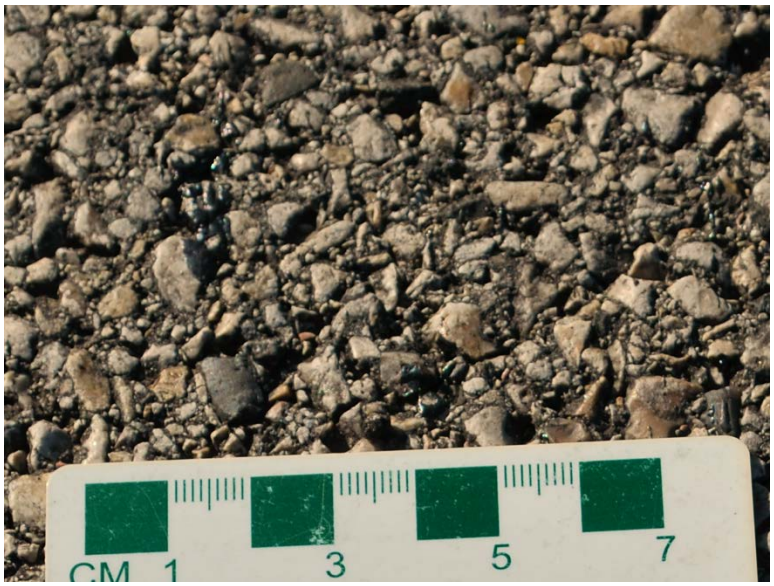

Figure 6-11. US 96 Surface Texture.

Construction was done on February 26, 2016. The pavement temperature for construction was between 70 and 80°F. Three test sections had low, moderate, and high tack application rates (Table 6-3). Tack uniformity was not ideal at the beginning of the day, but once the tack was heated adequately, uniformity was greatly improved. Samples from the original 0.05 section could not be cored because of traffic control issues, so samples were cored from a different part of the project with a similar expected application rate. The loose HMA was loaded into the paver by a material transfer vehicle and the HMA was compacted with tandem breakdown rollers and a finishing roller. Cores were sampled with a portable core drill with a 6-in. core barrel. Two samples were taken of the unpaved shoulder.

Table 6-3. US 96-Browndell Testing Plan.

Test Section	Tack Type	Surface Type	Tack Rate (gal/sy)		
			Level	Average Residual	Residual at Core Location
US 96	Tack E	Existing	Low	0.03*	0.03*
			Moderate	0.04	0.05
			High	0.06	0.06

* Estimated rate

FIELD RESULTS

Bond strengths from field cores were considerably lower (15–94 psi) than bond strengths from laboratory molded samples (100–200 psi). Most field cores failed at the interface. During testing, only the bond strength was measured and not the bond energy.

Figure 6-12 presents the average bond strengths from each project. The US 96 project on an existing HMA surface had the highest bond strength (71 psi). On US 183, the overall average

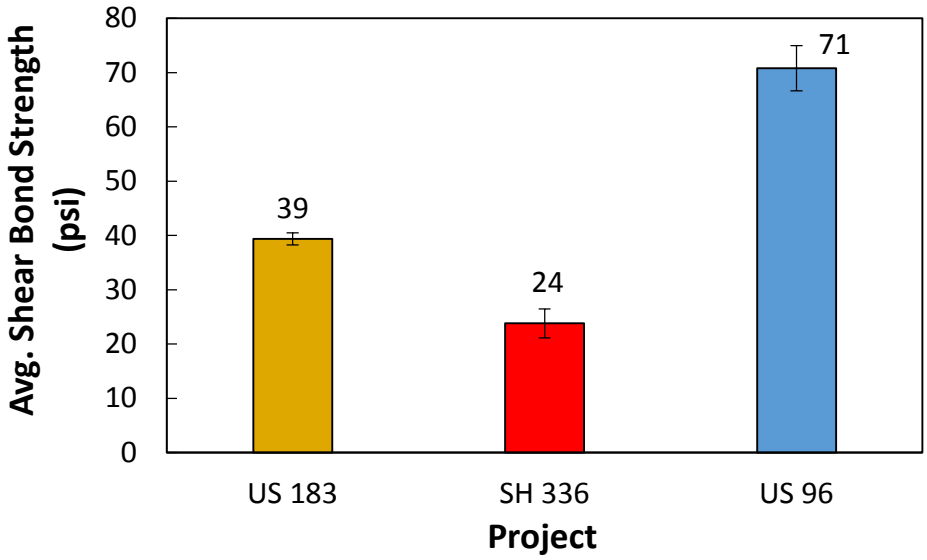

Figure 6-12. Bond Strength of the Three Field Projects.

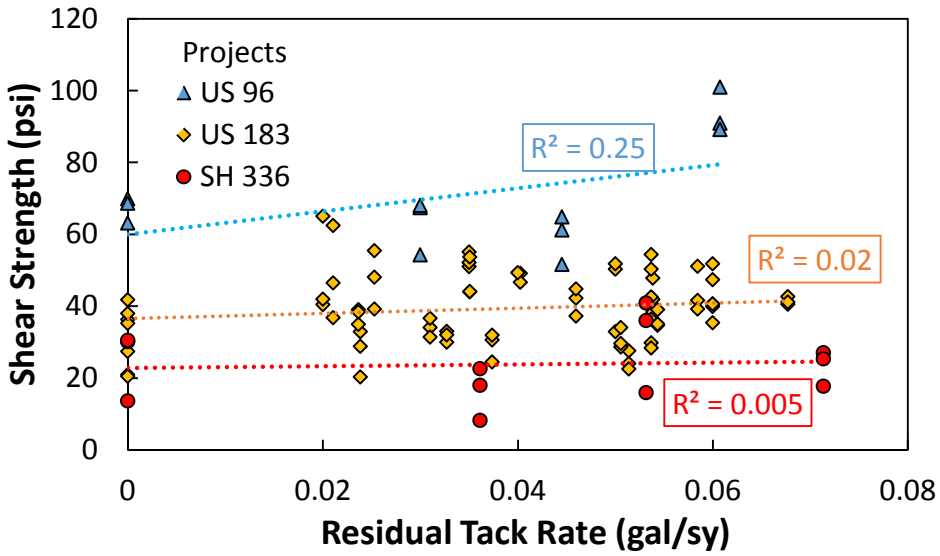

Figure 6-13. Effect of Tack Rate on Shear Strength on All Sections of Three Projects.

strength was low (39 psi), which includes sections with existing, milled, and new HMA surfaces and different tack types. The SH 336 project with an existing HMA surface had very low bond strengths (24 psi). The projects have different tack types, though the range in performance is likely related to the surface condition, construction parameters (i.e., temperature, compaction effort), and overlay mix type.

Figure 6-13 shows the distribution of bond strengths versus tack rate for the three projects. Overall, tack residual rate was not a statistically significant factor. There is little indication that a particular tack rate yielded better or worse bond performance; however, on US 96, the highest tack rate (0.06 gal/sy) did have higher bond strength (94 psi) than other tack rates (59–67 psi). The effect of tack rate on bond performance may be more evident over a longer time period.

Focusing now on US 183, Table 6-4 summarizes the model results, Figure 6-14 illustrates the model, and Table 6-5 shows the statistical groupings of the results. Shear strength was influenced by tack type and surface type. Samples with No Tack had the lowest strengths (23–28 psi) and Tack E samples had the highest strength (44–48 psi). Samples with Tacks B and C were between 28 to 39 psi on average and not statistically different. Samples from aged existing pavement had the lowest bond strengths in most of cases, and samples from milled and new HMA sections had similar bond strengths. In the statistical groupings, all Tack E and most of Tack B results were in the highest bond strength group. Tack C and No Tack samples were in the lower strength groups, as were most results for existing surface samples. No significant difference in the shear strength between surface types was observed for Tack E.

Table 6-4. Statistical Analysis Summary of US 183 Bond Strengths.

Explanatory Variable	*p*-value	Model *p*-value	Model R^2
Tack Type	<0.001	<0.001	0.68
Surface Type	<0.001		
Tack*Surface	<0.001		

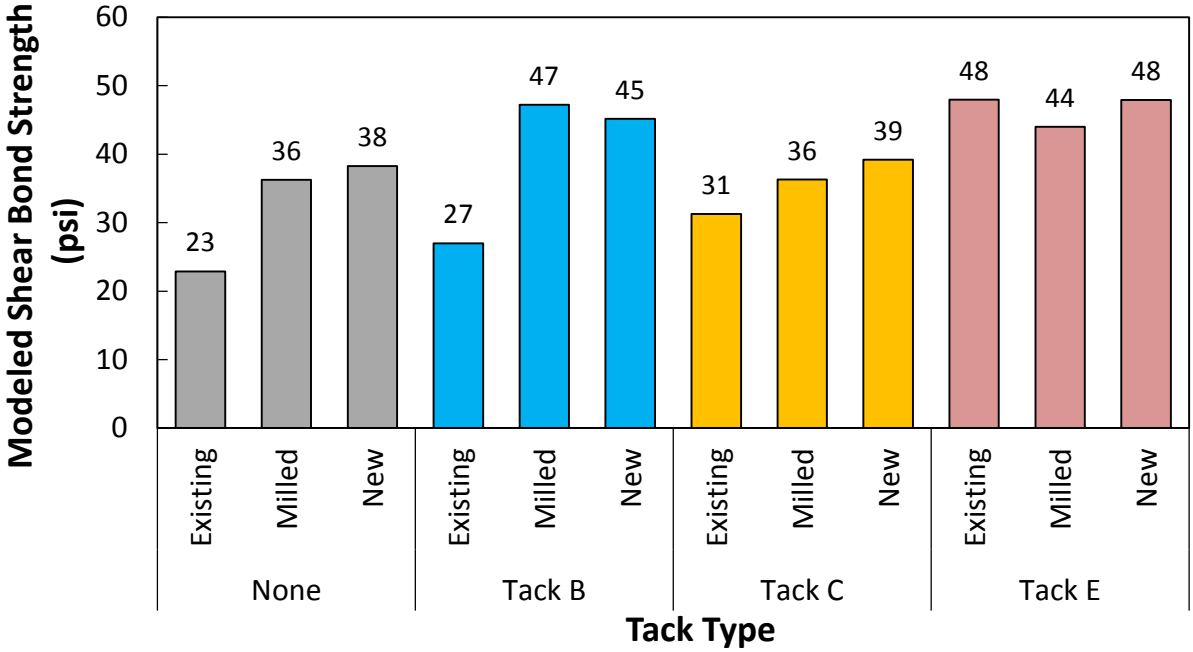

Figure 6-14. Modeled Shear Strength of US 183 Results.

Table 6-5. Statistical Grouping of Modeled Bond Strength Results on US 183.

Tack Type	Surface Type	Est. Bond Strength (psi)	Statistical Grouping*			
Tack E	Existing	48.0	A			
Tack E	New	47.9	A			
Tack B	Milled	47.2	A	B		
Tack B	New	45.2	A	B		
Tack E	Milled	44.0	A	B		
Tack C	New	39.2	A	B	C	
None	New	38.3	A	B	C	D
Tack C	Milled	36.3		B	C	D
None	Milled	36.2		B	C	D
Tack C	Existing	31.3			C	D
Tack B	Existing	27.0				D
None	Existing	22.9				D

* Tukey's HSD

Figure 6-15 shows the shear failure of different surface types. Unlike laboratory testing, the primary failure location was at the bond interface. In some cases, the substrate aggregate was exposed, suggesting an area where the tack did not adhere to the surface (adhesive failure). On the milled samples, this was observed more frequently, suggesting that the surface was poorly cleaned and that dirt within the grooves lowered the bond strength.

Figure 6-15. Interface Shear Failure of Different Surface Types: (a) Existing, (b) New, and (c) Milled Substrate.

On the SH 336 project, the researchers did not expect the samples to have such low bond strengths. The overall average bond strength was 24 psi (Figure 6-12). This value includes samples with low, moderate, and high rates of Tack B and samples with No Tack, and excludes the weaker RC-250 samples that could not be cored intact. The researchers molded samples in the laboratory to replicate the field samples using the materials collected in the field (cores of the existing surface, tack sampled from the field, and Type D mix from the field.) Tack was applied at a moderate rate with a brush, the overlay was compacted in the gyratory compactor, and the samples were tested for shear strength.

The results in Figure 6-16 show that the shear strength of lab-compacted samples was significantly greater than the bonded field samples, even when using identical materials,. The Tack B sample had a bond strength of 154 psi, almost five times the strength observed from the field samples. The RC-250 sample had the same bond strength as the No Tack sample—74 psi, which was three time greater than previously for No Tack. These observations highlight that bond strength is affected by factors beyond the tack coat materials. This could include compaction temperature, compaction effort, tack application technique, etc. The results also show that Tack B can yield a higher bond strength than RC-250 and No Tack.

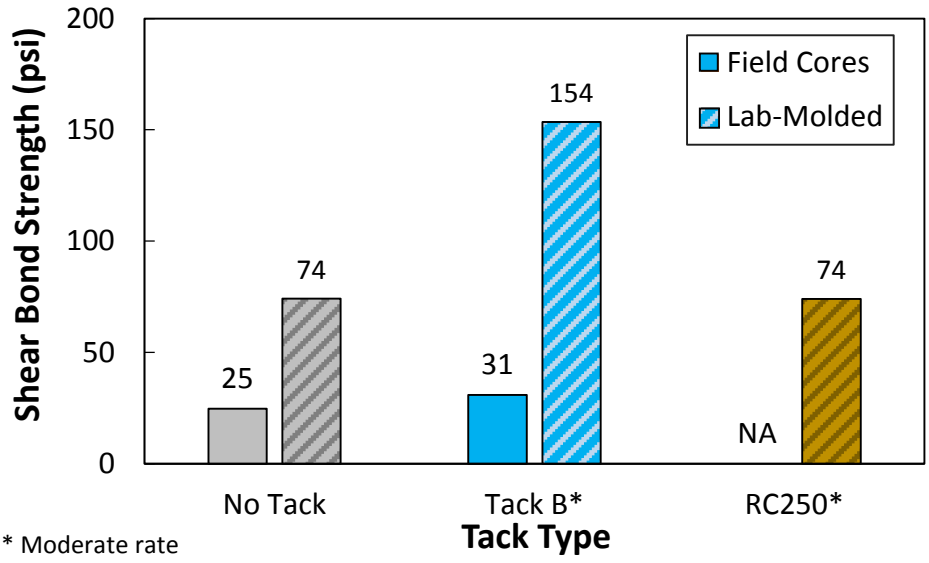

Figure 6-16. Bond Strength of Lab-Compacted Samples Using SH 336 Materials.

LAREDO, VARIOUS PROJECTS

Throughout the project, the researchers assisted the Laredo District by measuring bond strength on various projects. The projects had a wide range of tack types, tack rates, surface types, overlay designs, and pavement structures. Table 6-6 summarizes the project descriptions, and Figure 6-17 presents the results from bond strength tests. The shear bond strengths ranged from 25 to 94 psi. Because there are so many variables among sections, it is not feasible to draw conclusions about a given tack type or construction method as it relates to bond strength. What the results do show, however, is the wide range of bond strengths that can be expected in a field environment. This also underscores that bond strength is not simply a factor of the tack coat. Other variables like ambient and pavement temperature during construction, overlay temperature, compaction effort, overlay density, etc. will affect bond strength.

Table 6-6. Summary of Field Projects from Laredo.

Project ID	CSJ	Highway	Mix Type	Substrate Type	Tack	Tack Rate
1	0299-01-065	US 277	TOM TyC (76-22)	NA	CSS-1H	0.04 None
2	NA	NA	1-inch TOM	Type C	Conventional	0.04 0.08
3	2150-04-062	IH-35/ FM 468	SP Type D (70-22,SAC A)	Seal coat Glasgrid over seal coat	SS-1	0.07
4	1229-01-062	SH-85	TOM	Seal coat over HMA	CBC-1	0.02
5	0301-01-075	SH-85	SP (70-22)	Underseal	Not Applicable	NA
6	0037-09-029	NA	1.5-in. SP Type C	Type C	EBL	0.2
7	0276-05-026	NA	2-in. SP	Seal coat over Type C	EBL	0.2
8	0037-03-077	US 83, Zavala	SP Type C	NA	NA	NA
9	0037-10-033	US 83, Los Botines	SP Type C	NA	NA	NA
10	2150-04-055	I-35	SP Type C	NA	NA	NA
11	0018-04-051	NA	4-in. Type B (64-22)	4-in. Type B (64-22)	NA	NA None

NA – Not Available / Unknown

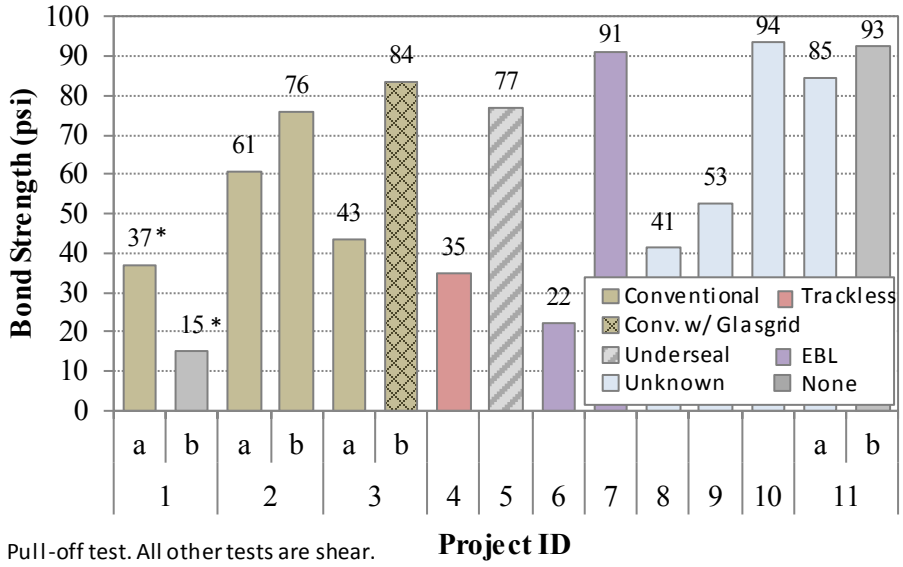

Figure 6-17. Bond Strengths from Laredo Projects.

SUMMARY

The objective of this task was to measure the performance of bonded pavement layers through field evaluations. The primary property evaluated in the field testing was bonding strength. In the field, test sections were constructed to evaluate the effect of different tack types, tack application rates, and surface conditions. Field samples were collected and tested for bond strength to validate the laboratory results. Bond strength testing was performed on a wide variety of projects from the Laredo District.

The key results from shear testing of field cores in all projects are as follows:

- Bond strengths from field samples were considerably lower (15–95 psi) than for lab-molded samples (100–200 psi).
- Bond strength varied significantly between projects. US 96 had the highest bond strengths (60–95 psi), US 183 had low strengths (25–50 psi), and SH 336 had very low strengths (15–30 psi). The range in bond strength is related to different pavement surface types, different HMA overlay designs, and different compaction temperatures.
- In most cases, tack rate did not influence bond strength.
- In the US 183 project, the milled and new HMA sections had higher bond strengths than the existing HMA sections. Also, sections with Tack E had higher strengths than sections with Tack B, Tack C, and No Tack.
- Bond strengths from various projects in the Laredo District ranged between 25 and 94 psi. The results underscore that bond strength is not simply a factor of the tack coat, but is influenced by many other factors, such as ambient and pavement temperature during construction, overlay temperature, compaction effort, and overlay density.

CHAPTER 7
CONCLUSION AND RECOMMENDATIONS

REPORT SUMMARY

Trackless tack is a popular material for bonding pavement layers. While conventional tack tends to be sticky and messy, trackless tack hardens quickly at ambient temperatures and then reactivates when HMA is spread and compacted. Several trackless tack products have come to market in Texas; however, there are currently no specifications to ensure the products have trackless properties and adequate bond strength.

The objectives of this project were to:

1. Evaluate the tracking resistance of different trackless tack products.
2. Evaluate bond strength of different trackless tack products and other construction parameters (i.e., surface type, tack reactivation temperature, and compaction effort).
3. Construct trackless tack test sections in the field and evaluate initial performance.
4. Develop a set of specifications for trackless tack and test procedures.

The tack materials were first characterized with advanced binder tests. Then, the researchers compared two potential tracking resistance tests for tack: a track-free time test and a DSR tackiness test. Researchers also compared four bond strength tests: interface shear, pull-off, torque, and Arcan. Using the recommended bond strength test, the researchers compared the bond strengths and bond energies achieved with different trackless tack types, surface types, reactivation temperatures (i.e., average of surface and HMA temperature), and compaction efforts. Researchers also assessed the susceptibility of bonded samples to cracking using the overlay and beam fatigue tests.

On three overlay projects, located on US 183, SH 336, and US 96, test sections were constructed with different tack types, application rates, and surface types. The researchers collected cores and measured bond strength in the laboratory. The researchers also measured core bond strengths from a wide range of overlay projects in the Laredo District.

FINDINGS

The key findings from this research are as follows.

Chapter 3: Material Characterization

- According to the DSR frequency sweep test, the control tack is the softest tack followed by Tack A, B and C respectively. These materials are classified as in the soft-residue group. Tacks D, E, and F belong to stiff-residue group.

- The MSCR test revealed that the percent recovery decreases with increase in stress level for all material types. For the soft-residue group, considerable changes in percent recovery and non-recoverable creep compliance were observed at high stress level conditions. However, the percent recovery and non-recoverable creep of the stiff-residue group did not decrease significantly under this condition.
- The LAS test showed that Tack F has the most resistance to fatigue cracking and Tack E has the lowest resistance to fatigue cracking at the corresponding intermediate temperatures.

Chapter 4: Tracking Resistance Testing

- The track-free time test could distinguish between the control tack and trackless tacks at 25 and 60°C. The test could not distinguish among the different trackless tack types except for Tack F.
- Testing uncured emulsion in the DSR tackiness test was difficult and less reliable than testing emulsion residue.
- The DSR tackiness test on emulsion residue distinguished among the control tack, soft-residue trackless tacks, and stiff-residue trackless tacks. Both the tack energy and the sample failure mode are required to evaluate performance.

Chapter 5: Laboratory Bond Strength and Cracking Resistance Testing

- Based on test characteristics and statistical results, the interlayer shear test is the most practical and repeatable test to evaluate pavement layer bonding.
- The bond strength of laboratory samples was high, between 100 and 200 psi. In many cases, samples failed in the HMA layer, meaning the bond strength was higher than the layer strength.
- The effect of the following factors on shear bond strength and bond energy were tested:
    - **Tack type** had a significant impact on bond performance. All samples had acceptable bond strengths. Samples with stiff-residue tacks had higher bond energy than samples with soft-residue tacks. All tack samples had higher bond energies than samples with No Tack.
    - **Surface type** had a high impact on bond performance. New HMA surface samples had higher bond energy than concrete surface samples.
    - **Compaction angle** marginally influenced bond performance.
    - **Reactivation temperature** (the average temperature between the existing surface and the loose HMA) significantly affected bond performance. As the temperature increased, so did the bond strength and bond energy. Again, stiff-residue tack samples had higher bond energy than soft-residue tack samples.

- Based on the PATTI test results, tack type had a significant impact on bond strength. Aggregate type was not a significant factor; however, the aggregate sample size was small in this study. In addition, the effect of moisture conditioning was not considered.
- Cracking resistance results from the overlay test were influenced by temperature and marginally influenced by tack type. At low temperatures, the maximum load was higher and samples failed after one cycle. Based on the number of cycles to failure at 77°F, the samples could be roughly divided into soft- and stiff-residue groups.
- From the beam fatigue test, tack type and test temperature have significant impact on the number of cycles to failure. At the low test temperature, samples with trackless tack had more cycles to failure than samples without tack.
- In both the overlay and beam fatigue tests, none of the samples had interface debonding, indicating that the samples are resistant to low-temperature delamination.

Chapter 6: Field Sections and Bond Strength Testing

- Bond strengths from field samples were considerably lower (15–95 psi) than for lab-molded samples (100–200 psi).
- Bond strength varied significantly between projects. US 96 had the highest bond strengths (60–95 psi), US 183 low strengths (25-50 psi), and SH 336 had very low strengths (15–30 psi). The range in bond strength is related to different pavement surface types, different HMA overlay designs, and different compaction temperatures.
- In most cases, tack rate did not influence bond strength.
- In the US 183 project, the milled and new HMA sections had higher bond strengths than the existing HMA sections. Also, sections with Tack E had higher strengths than sections with Tack B, Tack C, and tack.
- Bond strengths from various projects in the Laredo District ranged between 25 psi to 94 psi. The results underscore that bond strength is not simply a factor of the tack coat, but is influenced by many other factors, such as ambient and pavement temperature during construction, overlay temperature, compaction effort, overlay density, etc.

RECOMMENDATIONS

The researchers recommend adopting the DSR tackiness test to qualify trackless tack materials. The recommended test criteria are (a) no cohesive failure at 40°C (DSR tip must be clean) or (b) tack energy higher than 200 J/m^2 at 40°C. These criteria qualify both stiff- and soft-group trackless tacks in the present market. In the future, TxDOT may consider tightening the requirements by only permitting materials with no cohesive failure at 40°C. The researchers predict this will ensure the best overall performance. Using the track-free time test, the researchers recommend a maximum of 35 minutes for track-free time at 25°C. The test procedures are contained in Appendix G and the recommended draft trackless tack specification is found in Appendix H.

The researchers also recommend adopting the interlayer shear strength test to measure bond strength between pavement layers. The proposed test method is in Appendix G. For routine testing, bond strength should be used as the performance indicator. At the research level, both bond strength and bond energy should be used.

TxDOT should promote trackless tack as providing good bond strength, better than conventional tack. District engineers should be aware that the performance of stiff-residue tacks is superior to soft-residue tacks in both bond strength and tracking resistance; though, good bond strengths can be achieved by all trackless and conventional tack types in the study under ideal situations.

To achieve higher bond strengths, the researchers recommend compacting at higher temperatures (both ambient and overlay mix temperatures). The existing surface is also a critical factor for bond strength. For bonding thin lifts to heavily polished pavements, TxDOT may consider using an underseal or milling to ensure a better bond. Construction over new HMA likely does not require tack as long as the compaction temperatures are high enough. The emphasis on tack application rate should be reduced; rather, more emphasis should be placed on tack uniformity. Overlay designs with higher binder contents may also improve bond strength.

Finally, the researchers recommend long-term evaluation of the test sections built during this project. Tack type and application rate may be more significant over time, mitigating moisture-related damage and increasing bond strength through age hardening.

REFERENCES

1. Mohammad, L. N., M. A. Elseifi, A. Bae, N. Patel, J. Button, and J. A. Scherocman. *Optimization of Tack Coat for HMA Placement*. NCHRP Report 712. Transportation Research Board, Washington, DC, 2012.

2. Weston, J. *Tech Notes: Issues Related to Tack Coat.* Materials Laboratory, Washington State Department of Transportation. http://www.wsdot.wa.gov/NR/rdonlyres/DC652B96-0298-45CD-9345-0960BBC3D39D/0/TackCoatTN2007.pdf. Accessed April 17, 2015.

3. Khweir, K., and D. Fordyce. Influence of Layer Bonding on the Prediction of Pavement Life. *Proceedings of the Institution of Civil Engineers-Transport,* Vol. 156, No. 2, 2003, pp. 73-83.

4. Tran, N., R. Willis, and G. Julian. *Refinement of the Bond Strength Procedure and Investigation of a Specification*. NCAT Report 12-04. National Center for Asphalt Technology, Auburn, AL, 2012.

5. West, R. C., J. Zhang, and J. Moore. *Evaluation of Bond Strength between Pavement Layers*. NCAT Report 05-08. National Center for Asphalt Technology, Auburn, AL, 2005.

6. Al-Qadi, I. L., K. I. Hasiba, A. Salinas Cortina, H. Ozer, Z. Leng, D. C. Parish, and S. J. Worsfold. *Best Practices for Implementation of Tack Coat: Part I-Laboratory Study*. FHWA-ICT-12-004. Illinois Center for Transportation, Rantoul, IL, 2012.

7. Tran, N., D. Timm, B. Powell, G. Sholar, and R. Willis. Effectiveness of Heavier Tack Coat on Field Performance of Open-Graded Friction Course. In *Transportation Research Record: Journal of the Transportation Research Board*, Transportation Research Board of the National Academies, Washington, DC, 2013. pp. 1-8.

8. Clark, T. M., T. M. Rorrer, and K. K. McGhee. *Trackless Tack Coat Materials: A Laboratory Evaluation for Performance Acceptance*. VCTIR 12-R14. Virginia Center for Transportation Innovation and Research, Charlottesville, VA, 2012.

9. Chen, Y., G. Tebaldi, R. Roque, and G. Lopp. Effects of Trackless Tack Interface on Pavement Top-Down Cracking Performance. *Procedia-Social and Behavioral Sciences,* Vol. 53, No. 3, 2012, pp. 432-439.

10. McGhee, K. K., and T. M. Clark. *Bond Expectations for Milled Surfaces and Typical Tack Coat Materials Used in Virginia*. VTRC 09-R21. Virginia Transportation Research Council, Charlottesville, VA, 2009.

11. Gorsuch, C., S. Hogendoorn, C. Daranga, and J. McKay. Measuring Surface Tackiness of Modified Asphalt Binders and Emulsion Residues Using a Dynamic Shear Rheometer. *Proceedings of the 58th Annual Conference of the Canadian Technical Asphalt Association (CTAA)*, Newfoundland and Labrador, Canada, 2013, pp. 121-138.

12. Raab, C., and M. N. Partl. Investigation into a Long-Term Interlayer Bonding of Asphalt Pavements. *Baltic Journal of Road and Bridge Engineering,* Vol. 3, No. 2, 2008, pp. 65-70.

13. Scullion, T., S. Sebesta, C. K. Estakhri, P. Harris, C. Shon, O. Harvey, and K. Rose-Harvey. *Full-Depth Reclamation: New Test Procedures and Recommended Updates to Specifications*. TX-11/0-6271-2. Texas Transportation Institute, Texas A&M University, College Station, TX, 2012.

14. Germann, F. P., and R. L. Lytton. *Methodology for Predicting the Reflection Cracking Life of Asphalt Concrete Overlays*. TX-79/09-207-5. Texas Transportation Institute, Texas A&M University, College Station, TX, 1979.

15. Zhou, F., and T. Scullion. *Upgraded Overlay Tester and its Application to Characterize Reflection Cracking Resistance of Asphalt Mixtures*. TX-04/0-4467-1. Texas Transportation Institute, Texas A&M University, College Station, TX, 2003.

16. Zhou, F., and T. Scullion. *Overlay Tester: A Rapid Performance Related Crack Resistance Test*. TX-05/0-4467-2. Texas Transportation Institute, Texas A&M University, College Station, TX, 2005.

17. Clyne, T. R., M. O. Marasteanu, and A. Basu. *Evaluation of Asphalt Binders Used for Emulsions*. MN/RC – 2003-24. University of Minnesota, Minneapolis, MN, 2003.

18. Anderson, R. M. Understanding the MSCR Test and its Use in the PG Asphalt Binder Specification. Presented at Webinar of the Asphalt Institute, 2011.

19. Hanz, A., Z. Arega, and H. U. Bahia. Rheological Evaluation of Emulsion Residues Recovered Using Newly Proposed Evaporative Techniques. Presented at 88th Annual Meeting of Transportation Research Board, Washington, DC, 2009.

20. Zhou, F., W. Mogawer, H. Li, A. Andriescu, and A. Copeland. Evaluation of Fatigue Tests for Characterizing Asphalt Binders. *Journal of Materials in Civil Engineering,* Vol. 25, No. 5, 2012, pp. 610-617.

21. Mogawer, W., A. Austerman, M. E. Kutay, and F. Zhou. Evaluation of Binder Elastic Recovery on HMA Fatigue Cracking Using Continuum Damage and Overlay Test Based Analyses. *Road Materials and Pavement Design,* Vol. 12, No. 2, 2011, pp. 345-376.

22. Bahia, H. U., D. Hanson, M. Zeng, H. Zhai, M. Khatri, and R. Anderson. *Characterization of Modified Asphalt Binders in Superpave Mix Design*. NCHRP Report 459. Transportation Research Board, Washington, DC, 2001.

23. Hintz, C., R. Velasquez, C. Johnson, and H. Bahia. Modification and Validation of Linear Amplitude Sweep Test for Binder Fatigue Specification. In *Transportation Research Record: Journal of the Transportation Research Board, No. 2207*, TRB, National Research Council, Washington, DC, 2011, pp. 99-106.

24. Johnson, C. M. *Estimating Asphalt Binder Fatigue Resistance Using an Accelerated Test Method.* Ph.D dissertation. University of Wisconsin–Madison, Madison, WI, 2010.

25. Gent, A. N., and A. J. Kinloch. Adhesion of Viscoelastic Materials to Rigid Substrates. III. Energy Criterion for Failure. *Journal of Polymer Science Part A-2: Polymer Physics,* Vol. 9, No. 4, 1971, pp. 659-668.

26. Andrews, E. H., and A. J. Kinloch. Mechanics of Adhesive Failure. I. *Proceedings of the Royal Society of London A: Mathematical, Physical and Engineering Sciences,* Vol. 332, No. 1590, 1973, pp. 385-399.

27. Artamendi, I., and H. Khalid. Different Approaches to Depict Fatigue of Bituminous Materials. *Proceedings of the 15th European Conference of Fracture – Advanced Fracture Mechanics for Life and Safety Assessments, ECF-15*, Sweden, 2004.

28. Marasteanu, M. O., and D. A. Anderson. Establishing Linear Viscoelastic Conditions for Asphalt Binders. In *Transportation Research Record: Journal of the Transportation Research Board, No. 1728*, TRB, National Research Council, Washington, DC, 2000. pp. 1-6.

29. Clyne, T. R., and M. O. Marasteanu. *Inventory of Properties of Minnesota Certified Asphalt Binders*. MN/RC-2004-35. University of Minnesota, Minneapolis, MN, 2004.

30. Marasteanu, M., and D. Anderson. Improved Model for Bitumen Rheological Characterization. Presented at Eurobitume Workshop on Performance Related Properties for Bituminous Binders, Brussels, Belgium, 1999.

31. Schapery, R. A. Theory of Crack Initiation and Growth in Viscoelastic Media. *International Journal of Fracture,* Vol. 11, No. 1, 1975, pp. 141-159.

32. Kim, Y., H. Lee, D. Little, and Y. R. Kim. A Simple Testing Method to Evaluate Fatigue Fracture and Damage Performance of Asphalt Mixtures (With Discussion). *Journal of the Association of Asphalt Paving Technologists,* Vol. 75, 2006, pp. 755-787.

APPENDIX A:
ANALYSIS OF ADVANCED CHARACTERIZATION RESULTS

DSR FREQUENCY SWEEP

A master curve was created based on the time–temperature superposition concept and assumption of thermorheologically simple behavior for tested materials (*28*). The desired master curve forms a single curve for the complex shear modulus versus reduced frequency. This curve is created such that the computed frequency at the reference temperature equals the loading frequency of the test condition (*29*). The reduced frequency can be expressed as follows:

$$f_r = f \times a(T_i) \tag{2}$$

where,

$a(T_i)$ = shift factor as a function of temperature.
T_i = testing temperature.
f = loading frequency at the testing temperature of interest.
f_r = reduced frequency at the loading frequency and temperature of interest.

Here, the shift factor forms a second-order polynomial relationship in terms of temperature. This relationship is shown in Equation (3):

$$\log a(T_i) = aT_i^2 + bT_i + c \tag{3}$$

where,

a, b, c = coefficients of the second-order polynomial.

The master curve mathematical formulation adopted in this study is based on the Christensen-Anderson-Marasteanu (CAM) model (*30*). The CAM model is introduced in the following equation:

$$|G^*| = G_g \left[1 + \left(\frac{f_c}{f_R}\right)^k\right]^{-\frac{m_e}{k}} \tag{4}$$

where,

$|G^*|$ = dynamic shear modulus (Pa).
G_g = glassy modulus (10^9 Pa).
f_c, m_e, k = fitting coefficients.
f_R = reduced frequency of loading.

The typical value of glassy modulus is 10^9 Pa. This parameter indicates the limiting stiffness obtained at very low temperatures and high frequencies where physical hardening of viscoelastic

materials is dominant. Three shift factor coefficients in Equation (3) and three model parameters in Equation (4) are simultaneously determined using the Solver tool in Microsoft Excel. The model parameters fitted to the data can be used to predict the value of complex shear modulus or phase angle at any desired temperature and frequency of loading within the range of testing conditions.

MULTIPLE-STRESS CREEP-RECOVERY

The parameters determined by the MSCR test are the average percent recovery and the non-recoverable creep compliance. The percent recovery is defined as the delayed elastic response of a binder and calculated through the following equation:

$$\%\text{Recovery} = \frac{\gamma_r}{\gamma_p} \times 100 \tag{5}$$

where,

γ_r = recoverable shear strain.
γ_p = peak shear strain.

The non-recoverable creep compliance (J_{nr}) represents the residual strain after repeated loading with respect to the stress level. J_{nr} is a parameter representing the resistance to permanent deformation under repeated loading. The non-recoverable creep compliance is determined using Equation (6):

$$J_{nr} = \frac{\gamma_u}{\tau_{Applied}} \tag{6}$$

where,

γ_u = non-recoverable shear strain.
$\tau_{Applied}$ = applied shear stress.

These two parameters were used to assess the material properties of the binder related to the fatigue resistance as well as rutting.

LINEAR AMPLITUDE SWEEP

To analyze LAS test results, the viscoelastic continuum damage concept was used to calculate the fatigue resistance of the sample. The damage growth in viscoelastic materials is defined as the change in energy potential (W) relative to the change in the damage intensity (D), following Paris' Law suggested by Schapery (*31*), as shown in Equation (7):

$$\frac{\mathrm{d}D}{\mathrm{d}t} = \left(-\frac{\partial W}{\partial D} \right)^{\alpha} \tag{7}$$

where,

α = energy release rate (=$1/m$).
W = work potential.
D = damage intensity.
t = time.

The parameter α can be obtained using *m*-value, which is the slope of the storage modulus versus the angular frequency curve on the logarithmic scale. Thus, the frequency sweep data need to be converted into time domain by using the interconversion method (*24*). The storage modulus is calculated using Equation (8):

$$G'(\omega) = \left|G^*\right|(\omega) \times \cos\delta(\omega) \tag{8}$$

where,

ω = angular frequency (rad/sec).
G' = storage modulus.
$|G^*|$ = complex shear modulus.
δ = phase angle.

The work potential is determined using dissipated energy subjected to loading in strain-controlled mode (*32*). The dissipated energy is defined as follows:

$$W = \pi . I_D . \gamma_o^2 . \left|G^*\right| . \sin\delta \tag{9}$$

where,

W = dissipated energy.
I_D = initial undamaged value of $|G^*|$.
γ_0 = shear strain.

The damage intensity (D) is determined by integrating Equation (7) after Equation (9) is substituted as follows:

$$D(t) \cong \sum_{i=1}^{N} \left[\pi I_D \gamma_o^2 \left(\left|G^*\right| \sin\delta_{i-1} - \left|G^*\right| \sin\delta_i \right) \right]^{\frac{a}{1+a}} \left(t_i - t_{i-1}\right)^{\frac{1}{1+a}} \tag{10}$$

The material parameter $|G^*| \sin\delta$ is plotted against damage intensity, D, and the following mathematical formulation is fitted to the data:

$$\left|G^*\right|\sin\delta = C_0 - C_1\left(D\right)^{C_2} \tag{11}$$

where,

C_0, C_1 and C_2 = model coefficients.

Equation (11) can be substituted into Equation (9) and then the derivative of dissipated energy in Equation (9) can be determined with respect to damage intensity (D). The following equation is found after this substitution:

$$\frac{\mathrm{d}W}{\mathrm{d}D} = \pi I_D C_1 C_2 \left(D\right)^{C_2-1}\left(\gamma_{max}\right)^2 \tag{12}$$

Once Equation (12) is substituted into Equation (7), it is integrated to obtain the relationship between the number of cycles to failure, N_f, and the strain amplitude, γ_{max}. The simplified relationship can be found through the following equation:

$$N_f = A\left(\gamma_{max}\right)^{-2\alpha} \tag{13}$$

where,

$$A = \frac{f\left(D_f\right)^k}{k\left(\pi C_1 C_2\right)^{\alpha}} \ . \tag{14}$$

$$\mathrm{k} = 1 + (1 - C_2)\alpha \ . \tag{15}$$

D_f = damage accumulation at failure.

Using Equation (13), the fracture life can be determined at any strain level under a given damage intensity. Hence, the LAS test enables the prediction of fatigue resistance under various conditions (*23*).

APPENDIX B:
RESULTS OF ADVANCED CHARACTERIZATION RESULTS

DSR FREQUENCY SWEEP

Table B-1. Shift Factor Coefficients and Model Parameters.

Binder Type	*Shift Factor*			CAM Model Parameter		
	a	*b*	*c*	f_c	m_e	*k*
Control Tack	7.84E-04	−0.153	4.31	2.43E+01	6.55E-02	1.48
A	7.41E-04	−0.153	4.34	8.19E-04	5.59E-02	1.83
B	7.36E-04	−0.157	4.49	8.93E-02	5.96E-02	1.58
C	7.56E-04	−0.161	4.60	7.74E-02	6.21E-02	1.57
D	3.16E-04	−0.134	4.20	7.62E-02	5.65E-02	1.25
E	3.22E-04	−0.140	4.40	1.05E-01	6.64E-02	1.46
F	4.02E-04	−0.148	4.58	1.07E-01	5.71E-02	1.25

LINEAR AMPLITUDE SWEEP (LAS)

Table B-2. Shear Strain at Maximum Shear Stress.

Tack Type	Shear strain at maximum shear stress	
	Average	Std Dev
Control Tack	9.0	0.05
A	9.4	0.20
B	9.5	0.20
C	9.1	0.15
D	9.3	0.70
E	9.2	0.30
F	9.4	0.66

Table B-3. Calibration of Fatigue Parameter A and B.

Tack Type	Fatigue Parameter	
	A	B
Control Tack	4.49E+06	−4.19
A	2.60E+06	−4.00
B	2.87E+06	−3.99
C	8.83E+05	−3.52
D	1.93E+06	−4.03
E	2.41E+05	−3.06
F	5.76E+06	−4.36

APPENDIX C:
TEST MATRICES

Table C-1. Test Matrix – Tack Type.

Tack Type
No Tack
Control Tack
Tack A
Tack B
Tack C
Tack E
Tack F

Constants: Moderate rate, Aged HMA

Table C-2. Test Matrix – Substrate Type.

Tack Type	Substrate Type
No Tack	Lab-Aged
	New
	Concrete
Tack E	Lab-Aged
	New
	Concrete

Constants: Moderate rate, Aged HMA

Table C-3. Test Matrix – Compaction Effort.

Tack Type	Compaction Angle	Overlay Temp (°F)	Substrate Temp (°C)	Avg. Temp (°C)
No Tack	1	300	25	87
		275	25	80
			15	75
	1.25	300	25	87
		275	25	80
			15	75
Tack E	1	300	25	87
		275	25	80
			15	75
	1.25	300	25	87
		275	25	80
			15	75

Constants: Moderate rate, Aged HMA

Table C-4. Test Matrix – Tack Reactivation Temperature.

Tack Type	Overlay Temp (°F)	Substrate Temp (°C)	Avg. Temp (°C)
No Tack	300	40	94.5
		25	87
		15	82
	275	25	80
		15	75
Tack C	300	40	94.5
		25	87
		15	82
	275	25	80
		15	75
Tack E	300	40	94.5
		25	87
		15	82
	275	25	80
		15	75
Tack F	300	40	94.5
		25	87
		15	82
	275	25	80
		15	75

Constants: Moderate rate, Aged HMA

APPENDIX D:
FOUR-POINT BENDING BEAM

FLEXURAL STIFFNESS

A beam has a long span compared to its cross-sectional dimension. It is assumed that the beam is subjected to pure bending, and its transverse sections remain plane before and after loading. Also, the flexural stiffness of a four-point bending beam was obtained using a linear solution for simplifying the calculation.

The maximum stress is generally expressed as in Equation (16):

$$\sigma_{\max} = \frac{Mc}{I} \tag{16}$$

where,

M = moment.
c = distance from neutral axis to bottom surface of beam.
I = second moment of area (moment of inertia).

Here, the second moment of area for a rectangular section is $bh^3/12$, and the distance from the neutral axis to the bottom surface of a beam is $h/2$. The moment between two loading points is $PL/6$.

Hence, the maximum tensile stress for a four-point bending beam is as follows:

$$\sigma_{\max} = \frac{PL}{bh^2} \tag{17}$$

where,

P = load applied by actuator.
L = length of beam between two supports.
b = average width.
h = average height.

Assume the modulus, E, of two layers in a composite beam to be the same. When the length between an outside and inside clamp is referred to as a, the deflection at a point is:

$$\delta = \frac{Px}{12EI}(3La - 3a^2 - x^2) \text{ for } \boldsymbol{x < a} \tag{18}$$

$$= \frac{Pa}{12EI}\left(3Lx - 3x^2 - a^2\right) \text{ for } \boldsymbol{a < x < (L - a)} \tag{19}$$

Thus, the deflection at the inside clamp and at the center of a beam is:

$$\delta_{x=a} = \frac{Pa^2}{12EI}\left(3L - 4a\right) \tag{20}$$

$$\delta_{x=\frac{L}{2}} = \frac{Pa}{48EI}\left(3L^2 - 4a^2\right) \tag{21}$$

Since the deflection at the inside clamp was recorded in this study, the ratio of the deflection at the center of a beam to the one at the inside clamp should be calculated to obtain the maximum tensile strain. The ratio of the deflection is presented in Equation (22):

$$R_\delta = \frac{\delta_{x=\frac{L}{2}}}{\delta_{x=a}} = \frac{\left(3L + 4a\right)}{4a} \tag{22}$$

Because a is one-third of L, the ratio of the deflection at the center of a beam to the one at the inside clamp becomes $13/4$. Finally, the maximum deflection at the center can be calculated by multiplying the ratio into the deflection at the inside clamp coming from the displacement of the actuator.

The maximum tensile strain is:

$$\varepsilon_{max} = \frac{12\delta_{x=\frac{L}{2}} h}{3L^2 - 4a^2} \tag{23}$$

Then, the flexural stiffness is expressed as the maximum tensile stress divided by the maximum tensile strain.

FAILURE CYCLE

As mentioned previously in Chapter 5, the power function expressed in Equation (24) was used as a best-fitting curve for the collected data.

$$\mathrm{y} = \mathrm{A}x^B \tag{24}$$

In this equation, A and B are constants. When taking the logarithm from both sides of the equation, it becomes:

$$\log y = \log A + \mathrm{B}\log x \tag{25}$$

Substituting $\log A$ into $\bar{A}$ and $\log x$ into $\bar{x}$, the following equation is derived:

$$\log y = \bar{A} + \mathrm{B}\bar{x} \tag{26}$$

The relationship of y and $\bar{x}$ is transformed into Equation (27):

$$\mathrm{y} = 10^{\bar{A} + \mathrm{B}\bar{x}} \tag{27}$$

The slope of this form at any point can be found by taking the derivative of y with respect to $\bar{x}$, as shown in Equation (28):

$$\mathrm{y}' = 10^{\bar{A} + \mathrm{B}\bar{x}} \times \ln 10 \times B \tag{28}$$

Then, the stiffness at the 50th load cycle is:

$$\mathrm{y}(\log 50) = 10^{\bar{A} + \mathrm{B}\log 50} \tag{29}$$

The slope at the 50th load cycle becomes:

$$\mathrm{y}'(\log 50) = 10^{\bar{A} + \mathrm{B}\log 50} \times \ln 10 \times B \tag{30}$$

Finally, the equation of a line having this slope through the stiffness at the 50th load cycle and $\bar{x} = log50$ becomes:

$$y = \left(10^{\bar{A} + B\log 50} \times \ln 10 \times B\right)\left(\bar{x} - \log 50\right) + 10^{\bar{A} + B\log 50} \tag{31}$$

The failure cycle is estimated when the line meets the x-axis. That value is the x-intercept of the line as follows:

$$\bar{x} = \frac{-10^{\bar{A} + B\log 50}}{10^{\bar{A} + B\log 50} \times \ln 10 \times B} + \log 50 \tag{32}$$

Since $\bar{x}$ is the logarithm of the x value, the number of failure cycles can be found in Equation (33):

$$x = 10^{\bar{x}} = 10^{\frac{-10^{\bar{A}+B\log 50}}{10^{\bar{A}+B\log 50}\times \ln 10\times B}+\log 50} \tag{33}$$

APPENDIX E:
LABORATORY AND FIELD DATA

Table E-1. Results of Track-Free Time Test.

Tack	Test Temp (°C)	Track-Free Time (min.)
Control	25	50
		56
		52
Control	40	18
		24
		15
Control	60	> 60*
		> 60*
Tack A	25	29
		28
		41
Tack A	40	14
		15
		8
Tack A	60	9
		6
		7
Tack B	25	23
		20
		25
Tack B	40	8
		6
		6
Tack B	60	6
		6
		6
Tack C	25	24
		25
		25
Tack C	40	14
		18
		14
Tack C	60	8
		6
		10
Tack E	25	29
		26
		37
Tack E	40	10
		10
		7
Tack E	60	6
		3
		4
Tack F	25	0
Tack F	40	0
Tack F	60	0

* Never reached no-tracking

Table E-2. Results of DSR Tackiness Test.

Tack	Test Temp (°C)	Tack Energy (J/m^2)
Control	25	253.5
		248.4
Control	40	71.3
		71.9
Control	60	75.8
		76.8
Tack A	25	322.5
		215.9
Tack A	40	201.5
		119.9
Tack A	60	102.4
		92.3
Tack B	25	250.9
		237.4
Tack B	40	232.9
		217.9
Tack B	60	134.6
		120.3
Tack C	25	0.5
		3.1
Tack C	40	644.4
		664.9
Tack C	60	186.5
		157.7
Tack D	25	1.1
		0.3
Tack D	40	34.2
		34.2
Tack D	60	238.8
		227.3
Tack E	25	0.8
		0.0
Tack E	40	23.1
		106.3
Tack E	60	106.3
		119.4
Tack F	25	4.0
		1.0
Tack F	40	31.6
		26.8
Tack F	60	357.5
		427.7

Table E-3. Results of PATTI Test.

Tack	Aggregate	Pull-off Strength (psi)
Control	Type A	198
		188
		181
Control	Type B	211
		246
		188
Control	Type C	240
		202
		205
Tack A	Type B	252
		184
		264
Tack B	Type A	285
		293
		256
Tack B	Type B	294
		285
		251
Tack B	Type C	303
		272
Tack C	Type A	508
		400
		433
Tack C	Type B	464
		502
		431
Tack C	Type C	358
		432
		439
Tack D	Type B	375
		228
		374
Tack E	Type A	271
		398
		361
Tack E	Type B	378
		389
		377
Tack E	Type C	464
		321
Tack F	Type B	669
		435
		689

Table E-4. Results of Overlay Test.

Tack	Test Temp (°C)	Maximum Load @ 1st cycle (lbf)	Failure Cycles
None	5	1181	15
		1111	1
		1045	1
None	25	704	1814
		675	1328
		443	5058
Control	5	1086	1
		1197	1
		974	1
Control	25	668	747
		558	9861
		708	613
Tack B	5	927	1
		963	1
		1124	1
Tack B	25	739	1875
		685	795
		621	15473
Tack C	5	1099	1
		1115	1
		1130	1
Tack C	25	676	287
		720	393
		711	788
Tack E	5	1117	1
		1109	1
		1192	1
Tack E	25	805	132
		723	399
		693	484
Tack F	5	1040	1
		1117	1
		1205	1
Tack F	25	684	703
		648	1487
		730	1233

Table E-5. Results of Modified Beam Fatigue Test.

Tack	Test Temp (°C)	Failure Cycles	Initial Stiffness (ksi)	Stiffness @Failure (ksi)
None	15	154	954.4	351.1
		266	106.5	39.2
		221	195.2	71.8
None	25	359	15.0	5.5
		247	19.1	7.0
		339	12.8	4.7
Tack E	15	512	125.8	46.3
		766	54.8	20.1
		634	453.8	166.9
Tack E	25	271	56.5	20.8
		305	52.3	19.2
		315	375.7	138.2
Tack F	15	534	588.6	216.5
		540	569.7	209.6
		321	735.5	270.6
Tack F	25	278	465.1	171.1
		290	354.6	130.4
		221	611.9	225.1

Table E-6. Comparison of Test Methods.

Test Method	Tack	Peak Strength	Failure Location	
			Top HMA	Bond
Pull-off	None	127.6	100	0
		56.7	0	100
		142.4	100	0
Pull-off	Tack E	180.1	100	0
		150.3	100	0
		159.4	100	0
Pull-off	Tack F	135.5	100	0
		146.3	100	0
		168.7	100	0
Shear	None	150.6	40	60
		160.3	30	70
		150.0	10	90
Shear	Tack E	169.6	60	40
		188.8	50	50
		178.2	50	50
Shear	Tack F	163.3	100	0
		199.5	100	0
		164.9	100	0
Arcan	None	138.3	0	100
		123.6	100	0
		129.0	0	100
Arcan	Tack E	136.0	100	0
		122.2	100	0
		152.4	35	65
Arcan	Tack F	131.4	100	0
		129.1	100	0
		170.7	100	0
Torque	None	401.0	60	40
		374.4	55	45
		495.1	50	30
Torque	Tack E	398.2	82	20
		463.7	100	0
		364.9	100	0
Torque	Tack F	444.7	100	0
		480.8	100	0
		366.8	100	0

Table E-7. Results of Interlayer Shear Test on Lab-Compacted Samples.

Tack	Substrate	Overlay Temp (°F)	Substrate Temp (°F)	Comp. Angle (deg.)	Bond Strength (psi)	Bond Energy (ft-lb/in.^{2})
None	"Aged" HMA	300	77	1	179.8	44.3
					156.1	35.0
					160.9	32.6
None	"Aged" HMA	300	77	1.25	160.3	57.2
					150.0	43.3
					187.8	59.2
None	"Aged" HMA	300	104	1.25	176.4	57.2
					190.4	60.9
None	New HMA	300	77	1.25	163.0	76.0
					164.5	39.6
None	Concrete	300	77	1.25	12.4	0.4
					25.4	1.1
					31.3	1.5
Tack B	"Aged" HMA	300	77	1.25	174.5	45.4
					181.9	55.9
					185.6	105.4
Tack B	"Aged" HMA	300	77	1.25	189.5	52.1
					178.4	52.5
					161.2	38.1
Tack A	"Aged" HMA	300	77	1.25	194.2	61.9
					180.9	54.2
					183.0	49.3
Tack E	"Aged" HMA	275	60	1	161.4	70.9
					152.4	59.9
					134.0	52.4
Tack E	"Aged" HMA	275	60	1.25	159.3	57.2
					157.0	52.8
					164.2	59.9
Tack E	"Aged" HMA	275	77	1	143.0	77.5
					141.5	60.2
					140.9	65.1
Tack E	"Aged" HMA	275	77	1.25	149.5	65.8
					166.5	77.1
					162.8	86.5
Tack E	"Aged" HMA	300	60	1.25	162.3	98.0
					165.7	67.6
					182.0	68.0
Tack E	"Aged" HMA	300	77	1	189.1	113.5
					152.3	80.1
					168.7	87.6
Tack E	"Aged" HMA	300	77	1.25	169.6	81.2
					188.8	85.9
					178.2	78.5
Tack E	"Aged" HMA	300	104	1.25	170.0	103.7
					159.4	95.9
					195.5	115.4
Tack E	New HMA	300	77	1.25	164.3	67.1
					171.1	67.2
					164.2	104.3
Tack E	Concrete	300	77	1.25	125.4	24.9
					96.0	18.0
					112.4	18.0

Table E-7. Results of Interlayer Shear Test on Lab-Compacted Samples (cont.).

Tack	Substrate	Overlay Temp (°F)	Substrate Temp (°F)	Comp. Angle (deg.)	Bond Strength (psi)	Bond Energy (ft-lb/in.^{2})
Tack F	"Aged" HMA	275	60	1.25	201.3	80.5
					181.6	76.6
					182.0	64.2
Tack F	"Aged" HMA	275	77	1.25	0.0	0.0
					222.0	130.2
					221.8	93.9
					158.0	55.7
Tack F	"Aged" HMA	300	60	1.25	226.2	115.6
					226.9	97.9
					202.0	77.8
Tack F	"Aged" HMA	300	77	1.25	163.3	92.9
					199.5	124.5
					164.9	94.9
Tack F	"Aged" HMA	300	104	1.25	247.4	126.7
					236.1	115.7
					249.8	111.8
Tack C	"Aged" HMA	275	60	1.25	181.9	52.5
					173.2	50.5
					168.9	44.1
Tack C	"Aged" HMA	275	77	1.25	200.1	60.7
					187.4	66.2
					194.5	61.5
Tack C	"Aged" HMA	300	60	1.25	181.6	59.0
					174.1	51.0
					0.5	0.0
					174.8	51.9
Tack C	"Aged" HMA	300	77	1.25	184.0	72.0
					175.1	63.0
					183.4	55.4
Tack C	"Aged" HMA	300	104	1.25	178.0	90.6
					177.1	87.0
					199.8	92.6
None	"Aged" HMA	275	60	1	93.7	14.6
					70.0	10.8
					89.1	16.8
None	"Aged" HMA	275	60	1.25	127.7	37.8
					116.3	27.5
					90.5	20.9
None	"Aged" HMA	275	77	1	127.3	37.3
					127.2	36.0
					130.1	36.7
None	Concrete	275	77	1.25	142.1	47.4
					139.1	43.0
					141.2	39.1
None	"Aged" HMA	300	60	1.25	170.0	48.3
					142.5	29.9
					154.8	31.6

Table E-8. Results of Interlayer Shear Test on Field Cores.

Project	Tack Type	Surface Type	Target Tack Rate	Residual Tack Rate (gal/sy)	Peak Strength (psi)
US 183	Tack E	Existing	Low	0.02	36.8
				0.02	62.5
				0.02	46.5
US 183	Tack E	Existing	Moderate	0.04	50.9
				0.04	55.1
				0.04	52.1
US 183	Tack E	Existing	High	0.05	38.3
				0.05	47.8
				0.05	41.8
US 183	Tack E	Milled	Moderate	0.04	49.1
				0.04	46.6
US 183	Tack E	Milled	High	0.07	42.6
				0.07	40.5
				0.07	41.1
US 183	Tack E	New	Low	0.03	39.1
				0.03	55.4
				0.03	48.1
US 183	Tack E	New	Moderate	0.04	43.9
				0.04	53.7
				0.04	44.0
US 183	Tack E	New	High	0.05	54.4
				0.05	42.5
				0.05	50.3
US 183	Tack B	Existing	Low	0.02	28.8
				0.02	32.9
				0.02	20.3
US 183	Tack B	Existing	Moderate	0.04	24.5
				0.04	30.6
				0.04	31.9
US 183	Tack B	Existing	High	0.05	24.0
				0.05	22.5
				0.05	27.6
US 183	Tack B	Milled	Moderate	0.04	49.3
US 183	Tack B	Milled	High	0.06	51.7
				0.06	47.3
				0.06	40.5
US 183	Tack B	New	Low	0.02	40.4
				0.02	41.9
				0.02	65.0
US 183	Tack B	New	Moderate	0.05	37.3
				0.05	42.2
				0.05	44.7
US 183	Tack B	New	High	0.05	32.9
				0.05	50.2
				0.05	51.7
US 183	Tack C	Existing	Low	0.03	29.9
				0.03	32.9
				0.03	32.0
US 183	Tack C	Existing	Moderate	0.05	28.6
				0.05	29.6
				0.05	34.1

Table E-8. Results of Interlayer Shear Test on Field Cores (cont.).

Project	Tack Type	Surface Type	Target Tack Rate	Residual Tack Rate (gal/sy)	Peak Strength (psi)
US 183	Tack C	Existing	High	0.05	36.3
				0.05	29.7
				0.05	28.3
US 183	Tack C	Milled	Moderate	0.03	34.0
				0.03	36.6
				0.03	31.4
US 183	Tack C	Milled	High	0.06	39.9
				0.06	35.4
				0.06	40.6
US 183	Tack C	New	Low	0.02	39.0
				0.02	34.9
				0.02	38.3
US 183	Tack C	New	Moderate	0.05	34.6
				0.05	35.0
				0.05	39.0
US 183	Tack C	New	High	0.06	41.5
				0.06	51.1
				0.06	39.1
US 183	None	Existing	None	0.00	27.3
				0.00	20.9
				0.00	20.4
US 183	None	Milled	None	0.00	36.2
US 183	None	New	None	0.00	35.2
				0.00	41.7
				0.00	37.9
US 96	None	Existing	None	0.00	69.9
				0.00	68.6
				0.00	63.2
US 96	Tack E	Existing	Low	0.03	54.2
				0.03	67.4
				0.03	68.0
US 96	Tack E	Existing	Moderate	0.04	64.8
				0.04	61.1
				0.04	51.6
US 96	Tack E	Existing	High	0.06	90.9
				0.06	89.2
				0.06	101.0
SH 336	None	Existing	None	0.00	13.6
				0.00	30.2
				0.00	30.5
SH 336	Tack B	Existing	Low	0.04	22.6
				0.04	8.2
				0.04	17.9
SH 336	Tack B	Existing	Moderate	0.05	36.0
				0.05	16.0
				0.05	40.9
SH 336	Tack B	Existing	High	0.07	17.7
				0.07	27.0
				0.07	25.3

APPENDIX F:
STATISTICAL ANALYSIS RESULTS

Statistical Analyses of Bond Test Failure Mode (by Test Methods)

Column1=Pull-off

Source	DF	Sum of Squares	Mean Square	F Value	Pr > F
Model	2	2222.222222	1111.111111	1.00	**0.421875**
Error	6	6666.666667	1111.111111		
Corrected Total	8	8888.888889			

R-Square	Coeff Var	Root MSE	A/B Mean
0.250000	300.0000	33.33333	11.11111

Source	DF	Type I SS	Mean Square	F Value	Pr > F
Tack	2	2222.222222	1111.111111	1.00	0.421875

Source	DF	Type III SS	Mean Square	F Value	Pr > F
Tack	2	2222.222222	1111.111111	1.00	0.421875

Parameter	Estimate		Standard Error	t Value	Pr > |t|
Intercept	0.00000000	B	19.24500897	0.00	1
Tack E	0.00000000	B	27.21655270	0.00	1
Tack No Tack	33.33333333	B	27.21655270	1.22	0.26657
Tack F	0.00000000	B	.	.	.

Column1=Shear

Source	DF	Sum of Squares	Mean Square	F Value	Pr > F
Model	2	8266.666667	4133.333333	46.50	**0.000223**
Error	6	533.333333	88.888889		
Corrected Total	8	8800.000000			

R-Square	Coeff Var	Root MSE	A/B Mean
0.939394	23.57023	9.428090	40.00000

Source	DF	Type I SS	Mean Square	F Value	Pr > F
Tack	2	8266.666667	4133.333333	46.50	0.000223

Source	DF	Type III SS	Mean Square	F Value	Pr > F
Tack	2	8266.666667	4133.333333	46.50	0.000223

Parameter	Estimate		Standard Error	t Value	Pr > |t|
Intercept	0.00000000	B	5.44331054	0.00	1
Tack E	46.66666667	B	7.69800359	6.06	0.000914
Tack No Tack	73.33333333	B	7.69800359	9.53	7.63E-05
Tack F	0.00000000	B	.	.	.

Column1=Arcan

Source	DF	Sum of Squares	Mean Square	F Value	Pr > F
Model	2	6938.88889	3469.44444	2.20	**0.192569**
Error	6	9483.33333	1580.55556		
Corrected Total	8	16422.22222			

	R-Square	Coeff Var	Root MSE	A/B Mean
	0.422530	135.0211	39.75620	29.44444

Source	DF	Type I SS	Mean Square	F Value	Pr > F
Tack	2	6938.888889	3469.444444	2.20	0.192569

Source	DF	Type III SS	Mean Square	F Value	Pr > F
Tack	2	6938.888889	3469.444444	2.20	0.192569

Parameter	Estimate		Standard Error	t Value	Pr > |t|
Intercept	0.00000000	B	22.95325362	0.00	1
Tack E	21.66666667	B	32.46080257	0.67	0.529292
Tack No Tack	66.66666667	B	32.46080257	2.05	0.085794
Tack F	0.00000000	B	.	.	.

Column1=Torque

Source	DF	Sum of Squares	Mean Square	F Value	Pr > F
Model	2	2516.666667	1258.333333	19.70	**0.00231**
Error	6	383.333333	63.888889		
Corrected Total	8	2900.000000			

	R-Square	Coeff Var	Root MSE	A/B Mean
	0.867816	53.28702	7.993053	15.00000

Source	DF	Type I SS	Mean Square	F Value	Pr > F
Tack	2	2516.666667	1258.333333	19.70	0.00231

Source	DF	Type III SS	Mean Square	F Value	Pr > F
Tack	2	2516.666667	1258.333333	19.70	0.00231

Parameter	Estimate		Standard Error	t Value	Pr > |t|
Intercept	0.00000000	B	4.61479103	0.00	1
Tack E	6.66666667	B	6.52630007	1.02	0.346422
Tack No Tack	38.33333333	B	6.52630007	5.87	0.001078
Tack F	0.00000000	B	.	.	.

Statistical Analysis of Shear Test Failure Mode

(a) Tack Type

Linear Models

e: A/B

Source	DF	Sum of Squares	Mean Square	F Value	Pr > F
Model	6	22840.47619	3806.74603	7.27	0.001119
Error	14	7333.33333	523.80952		
Corrected Total	20	30173.80952			

R-Square	Coeff Var	Root MSE	A/B Mean
0.756964	33.61011	22.88689	68.09524

Source	DF	Type I SS	Mean Square	F Value	Pr > F
Tack	6	22840.47619	3806.74603	7.27	0.001119

Source	DF	Type III SS	Mean Square	F Value	Pr > F
Tack	6	22840.47619	3806.74603	7.27	0.001119

Parameter	Estimate		Standard Error	t Value	Pr > |t|
Intercept	98.33333333	B	13.21374945	7.44	3.15E-06
Tack Control	-31.66666667	B	18.68706369	-1.69	0.112274
Tack E	-51.66666667	B	18.68706369	-2.76	0.015196
Tack C	-6.66666667	B	18.68706369	-0.36	0.726596
Tack No Tack	-25.00000000	B	18.68706369	-1.34	0.202281
Tack F	-98.33333333	B	18.68706369	-5.26	0.00012
Tack A	1.66666667	B	18.68706369	0.09	0.930196
Tack B	0.00000000	B	.	.	.

(b) Surface Type

Linear Models

e: A/B

Source	DF	Sum of Squares	Mean Square	F Value	Pr > F
Model	1	3500.694444	3500.694444	9.07	0.008265
Error	16	6172.916667	385.807292		
Corrected Total	17	9673.611111			

	R-Square	Coeff Var	Root MSE	A/B Mean
Bad	0.361881	24.46752	19.64198	80.27778

Source	DF	Type I SS	Mean Square	F Value	Pr > F
Substrate-Revised	1	3500.694444	3500.694444	9.07	0.008265

Source	DF	Type III SS	Mean Square	F Value	Pr > F
Substrate-Revised	1	3500.694444	3500.694444	9.07	0.008265

Parameter	Estimate		Standard Error	t Value	Pr > |t|
Intercept	70.41666667	B	5.67015058	12.42	1.25E-09
Substrate-Revised Concrete	29.58333333	B	9.82098890	3.01	0.008265
Substrate-Revised HMA	0.00000000	B	.	.	.

(c) Compaction Angle + (d) Tack Reactivation Temperature

Linear Models

: A/B

Source	DF	Sum of Squares	Mean Square	F Value	Pr > F
Model	7	28423.55499	4060.50786	7.91	4.79E-07
Error	70	35912.66296	513.03804		
Corrected Total	77	64336.21795			

R-Square	Coeff Var	Root MSE	A/B Mean
0.441797	28.06556	22.65034	80.70513

Source	DF	Type I SS	Mean Square	F Value	Pr > F
Tack	3	11200.38462	3733.46154	7.28	0.000256
Avg Temp	1	12134.67678	12134.67678	23.65	6.85E-06
Avg Temp*Tack	3	5088.49360	1696.16453	3.31	0.025086

Source	DF	Type II SS	Mean Square	F Value	Pr > F
Tack	3	4385.98009	1461.99336	2.85	0.043543
Avg Temp	1	12134.67678	12134.67678	23.65	6.85E-06
Avg Temp*Tack	3	5088.49360	1696.16453	3.31	0.025086

Source	DF	Type III SS	Mean Square	F Value	Pr > F
Tack	3	4385.98009	1461.99336	2.85	0.043543
Avg Temp	1	11736.52827	11736.52827	22.88	9.27E-06
Avg Temp*Tack	3	5088.49360	1696.16453	3.31	0.025086

Parameter	Estimate		Standard Error	t Value	Pr > |t|
Intercept	155.0310889	B	74.0600654	2.09	0.039946
Tack E	193.9802790	B	96.2811998	2.01	0.047776
Tack C	172.8093722	B	104.7367489	1.65	0.103436
Tack None	-16.0187120	B	96.2811998	-0.17	0.868342
Tack F	0.0000000	B	.	.	.
Avg Temp	-0.9720958	B	0.8820644	-1.10	0.274207
Avg Temp*Tack E	-2.4476734	B	1.1533397	-2.12	0.037357
Avg Temp*Tack C	-1.9093115	B	1.2474275	-1.53	0.130375
Avg Temp*Tack None	0.4440630	B	1.1533397	0.39	0.701387
Avg Temp*Tack F	0.0000000	B	.	.	.

Statistical Analysis of Overlay Test (Cycles-Log-Transformed)

Linear Models

The GLM Procedure

Class Level Information		
Class	Levels	Values
Tack	6	Control Tack E Tack C None Tack F Tack B
Temperature	2	5 25

Number of Observations Read	36
Number of Observations Used	36

Generated by the SAS System ('Local', W32_7PRO) on May 31, 2016 at 3:25:01 PM

Linear Models

Dependent Variable: Log Cycles

Source	DF	Sum of Squares	Mean Square	F Value	Pr > F
Model	1	64.69448634	64.69448634	405.05	<.0001
Error	34	5.43042429	0.15971836		
Corrected Total	35	70.12491064			

R-Square	Coeff Var	Root MSE	Log Cycles Mean
0.922561	23.62334	0.399648	1.691750

Source	DF	Type I SS	Mean Square	F Value	Pr > F
Temperature	1	64.69448634	64.69448634	405.05	<.0001

Source	DF	Type III SS	Mean Square	F Value	Pr > F
Temperature	1	64.69448634	64.69448634	405.05	<.0001

Parameter	Estimate		Standard Error	t Value	Pr > |t|
Intercept	3.032297755	B	0.09419789	32.19	<.0001
Temperature 5	-2.681096093	B	0.13321593	-20.13	<.0001
Temperature 25	0.000000000	B	.	.	.

Note: The X'X matrix has been found to be singular, and a generalized inverse was used to solve the normal equations. Terms whose estimates are followed by the letter 'B' are not uniquely estimable.

Statistical Analysis of Overlay Test (Peak Load)

Linear Models

The GLM Procedure

Class Level Information		
Class	Levels	Values
Tack	6	CSS-1H Tack E Tack C None Tack F Tack B
Temperature	2	25 25

Number of Observations Read	36
Number of Observations Used	36

Generated by the SAS System ('Local', W32_7PRO) on May 31, 2016 at 3:22:07 PM

Linear Models

Dependent Variable: 1st cycle

Source	DF	Sum of Squares	Mean Square	F Value	Pr > F
Model	1	1580202.273	1580202.273	253.24	<.0001
Error	34	212156.519	6239.898		
Corrected Total	35	1792358.792			

R-Square	Coeff Var	Root MSE	1st cycle Mean
0.881633	8.908414	78.99302	886.7238

Source	DF	Type I SS	Mean Square	F Value	Pr > F
Temperature	1	1580202.273	1580202.273	253.24	<.0001

Source	DF	Type III SS	Mean Square	F Value	Pr > F
Temperature	1	1580202.273	1580202.273	253.24	<.0001

Parameter	Estimate		Standard Error	t Value	Pr > |t|
Intercept	677.2136124	B	18.61883399	36.37	<.0001
Temperature 5	419.0203221	B	26.33100755	15.91	<.0001
Temperature 25	0.0000000	B	.	.	.

Note: The X'X matrix has been found to be singular, and a generalized inverse was used to solve the normal equations. Terms whose estimates are followed by the letter 'B' are not uniquely estimable.

Statistical Analysis of Beam Fatigue Test (Initial Stiffness)

Linear Models

The GLM Procedure

Class Level Information		
Class	Levels	Values
Test Temp	2	15 25
Sample	3	Tack E No Tack Tack F

Number of Observations Read	18
Number of Observations Used	18

Generated by the SAS System ('Local', W32_7PRO) on May 31, 2016 at 2:58:48 PM

Linear Models

Dependent Variable: Initial stiffness, ksi

Source	DF	Sum of Squares	Mean Square	F Value	Pr > F
Model	2	10509.54139	5254.77070	4.04	0.0394
Error	15	19494.38304	1299.62554		
Corrected Total	17	30003.92443			

R-Square	Coeff Var	Root MSE	Initial stiffness, ksi Mean
0.350272	77.84714	36.05032	46.30911

Source	DF	Type I SS	Mean Square	F Value	Pr > F
Sample	2	10509.54139	5254.77070	4.04	0.0394

Source	DF	Type III SS	Mean Square	F Value	Pr > F
Sample	2	10509.54139	5254.77070	4.04	0.0394

Parameter	Estimate		Standard Error	t Value	Pr > |t|
Intercept	80.38434588	B	14.71748131	5.46	<.0001
Sample Tack E	-53.33858059	B	20.81366167	-2.56	0.0216
Sample No Tack	-48.88712577	B	20.81366167	-2.35	0.0330
Sample Tack F	0.00000000	B	.	.	.

Note: The X'X matrix has been found to be singular, and a generalized inverse was used to solve the normal equations. Terms whose estimates are followed by the letter 'B' are not uniquely estimable.

Statistical Analysis of Beam Fatigue Test (Failure Cycle-Log Transformed)

Linear Models

The GLM Procedure

Class Level Information		
Class	Levels	Values
Test Temp	2	15 25
Sample	3	Tack E No Tack Tack F

Number of Observations Read	18
Number of Observations Used	18

Generated by the SAS System ('Local', W32_7PRO) on May 31, 2016 at 3:02:11 PM

Linear Models

Dependent Variable: Failure Cycles_log

Source	DF	Sum of Squares	Mean Square	F Value	Pr > F
Model	5	373950.5399	74790.1080	11.13	0.0004
Error	12	80664.4034	6722.0336		
Corrected Total	17	454614.9433			

R-Square	Coeff Var	Root MSE	Failure Cycles_log Mean
0.822565	22.45119	81.98801	365.1834

Source	DF	Type I SS	Mean Square	F Value	Pr > F
Test Temp	1	97331.8820	97331.8820	14.48	0.0025
Sample	2	123130.0426	61565.0213	9.16	0.0038
Test Temp*Sample	2	153488.6154	76744.3077	11.42	0.0017

Source	DF	Type III SS	Mean Square	F Value	Pr > F
Test Temp	1	97331.8820	97331.8820	14.48	0.0025
Sample	2	123130.0426	61565.0213	9.16	0.0038
Test Temp*Sample	2	153488.6154	76744.3077	11.42	0.0017

Parameter	Estimate		Standard Error	t Value	Pr > |t|
Intercept	263.0058000	B	47.33579905	5.56	0.0001
Test Temp 15	202.1064000	B	66.94292900	3.02	0.0107
Test Temp 25	0.0000000	B	.	.	.
Sample Tack E	33.6991667	B	66.94292900	0.50	0.6238
Sample No Tack	52.2301333	B	66.94292900	0.78	0.4504
Sample Tack F	0.0000000	B	.	.	.
Test Temp*Sample 15 Tack E	138.5571667	B	94.67159810	1.46	0.1690
Test Temp*Sample 15 No Tack	-303.6692000	B	94.67159810	-3.21	0.0075
Test Temp*Sample 15 Tack F	0.0000000	B	.	.	.
Test Temp*Sample 25 Tack E	0.0000000	B	.	.	.
Test Temp*Sample 25 No Tack	0.0000000	B	.	.	.
Test Temp*Sample 25 Tack F	0.0000000	B	.	.	.

Note: The X'X matrix has been found to be singular, and a generalized inverse was used to solve the normal equations. Terms whose estimates are followed by the letter 'B' are not uniquely estimable.

Statistical Analysis of All Field Project Bond Strengths

Linear Models

The GLM Procedure

Class Level Information		
Class	Levels	Values
Project	3	SH 336 US 183 US 96

Number of Observations Read	100
Number of Observations Used	100

Generated by the SAS System ('Local', W32_7PRO) on June 03, 2016 at 11:32:46 AM

Linear Models

Dependent Variable: Peak Strength (psi)

Source	DF	Sum of Squares	Mean Square	F Value	Pr > F
Model	2	14420.08920	7210.04460	66.25	<.0001
Error	97	10557.13549	108.83645		
Corrected Total	99	24977.22469			

R-Square	Coeff Var	Root MSE	Peak Strength (psi) Mean
0.577330	25.26819	10.43247	41.28697

Source	DF	Type I SS	Mean Square	F Value	Pr > F
Project	2	14420.08920	7210.04460	66.25	<.0001

Parameter	Estimate		Standard Error	t Value	Pr > |t|
Intercept	70.83595611	B	3.01159493	23.52	<.0001
Project SH 336	-47.02841416	B	4.25903840	-11.04	<.0001
Project US 183	-31.45470252	B	3.24064231	-9.71	<.0001
Project US 96	0.00000000	B	.	.	.

Note: The X'X matrix has been found to be singular, and a generalized inverse was used to solve the normal equations. Terms whose estimates are followed by the letter 'B' are not uniquely estimable

Statistical Analysis of US 183 Bond Strength

Linear Models

Class Level Information		
Class	Levels	Values
Tack Type	4	Tack E Tack C None Tack B
Surface Type	3	Existing Milled New
Actual Tack Rate	7	0.00 0.02 0.03 0.04 0.05 0.06 0.07

Number of Observations Read	76
Number of Observations Used	76

Dependent Variable: Peak Load (psi)

Source	DF	Sum of Squares	Mean Square	F Value	Pr > F
Model	11	4837.925698	439.811427	12.84	<.0001
Error	64	2192.691081	34.260798		
Corrected Total	75	7030.616779			

R-Square	Coeff Var	Root MSE	Peak Load (psi) Mean
0.688123	14.86309	5.853272	39.38125

Source	DF	Type I SS	Mean Square	F Value	Pr > F
Tack Type	3	2214.569204	738.189735	21.55	<.0001
Surface Type	2	1387.191040	693.595520	20.24	<.0001
Tack Type*Surface Ty	6	1236.165454	206.027576	6.01	<.0001

Source	DF	Type III SS	Mean Square	F Value	Pr > F
Tack Type	3	1696.994230	565.664743	16.51	<.0001
Surface Type	2	1387.553899	693.776949	20.25	<.0001
Tack Type*Surface Ty	6	1236.165454	206.027576	6.01	<.0001

Parameter	Estimate		Standard Error	t Value	Pr > |t|
Intercept	45.15027070	B	1.95109081	23.14	<.0001
Tack Type Tack E	2.78130465	B	2.75925908	1.01	0.3173
Tack Type Tack C	-5.96381223	B	2.75925908	-2.16	0.0344
Tack Type None	-6.87423233	B	3.90218162	-1.76	0.0829
Tack Type Tack B	0.00000000	B	.	.	.
Surface Type Existing	-18.16237394	B	2.75925908	-6.58	<.0001
Surface Type Milled	2.07589857	B	3.51737898	0.59	0.5571
Surface Type New	0.00000000	B	.	.	.
Tack Type*Surface Ty Tack E Existing	18.20633174	B	3.90218162	4.67	<.0001
Tack Type*Surface Ty Tack E Milled	-5.99975324	B	4.79904885	-1.25	0.2158
Tack Type*Surface Ty Tack E New	0.00000000	B	.	.	.
Tack Type*Surface Ty Tack C Existing	10.24287848	B	3.90218162	2.62	0.0108
Tack Type*Surface Ty Tack C Milled	-4.95749585	B	4.67855141	-1.06	0.2933
Tack Type*Surface Ty Tack C New	0.00000000	B	.	.	.
Tack Type*Surface Ty None Existing	2.76574115	B	5.51851817	0.50	0.6180
Tack Type*Surface Ty None Milled	-4.10372116	B	7.61925318	-0.54	0.5920
Tack Type*Surface Ty None New	0.00000000	B	.	.	.
Tack Type*Surface Ty Tack B Existing	0.00000000	B	.	.	.
Tack Type*Surface Ty Tack B Milled	0.00000000	B	.	.	.
Tack Type*Surface Ty Tack B New	0.00000000	B	.	.	.

APPENDIX G:
TRACKLESS TACK AND BOND STRENGTH TEST PROCEDURES

DRAFT Test Procedure for

DYNAMIC SHEAR RHEOMETER TACKINESS

TxDOT Designation: Tex-XXX-X

Date: June 2016

1. SCOPE

1.1 Use this test to measure the tackiness of tack residue. It is specifically used to qualify non-tracking products.

1.2 This test is derived from a test method by researchers at Akzo Nobel and Blacklidge Emulsions (*1*). Tackiness is measured by lowering a DSR tip onto a tack residue sample and then measuring the tensile force as the testing tip retracts.

1.3 The values given in parentheses (if provided) are not standard and may not be exact mathematical conversions. Use each system of units separately. Combining values from the two systems may result in nonconformance with the standard.

2. APPARATUS

2.1 *Dynamic Shear Rheometer (DSR) Test System* – As specified in AASHTO 315 (Determining the Rheological Properties of Asphalt Binder Using a Dynamic Shear Rheometer), with the following additional requirements:

2.1.1 *Test Plates* – an 8 mm diameter stainless steel upper plate (tip) and a 25 mm diameter stainless steel base plate.

2.1.2 *Loading Device* – Capable of applying a controlled normal compressive load of 10.5±0.1 N and removing the load at a constant rate of 1.0 mm/second.

2.1.3 *Control and Data Acquisition System* – Capable of recording the normal load to an accuracy of 0.1 N. Capable of programming the load, delay time, and loading rates so the test procedures are automated.

2.2 *Specimen Mold* – 20 mm diameter silicone mold with an approximate depth of 1.25 mm.

2.3 *Oven* – Capable of heating to between 70 and 100°C.

3. MATERIALS

3.1 20 g of tack residue collected with ASTM D7497 (Standard Practice for Recovering Residue from Emulsified Asphalt Using Low Temperature Evaporative Technique) or AASHTO PP72 Method B. The tack should be sampled from the terminal mill.

4. PROCEDURES

4.1 Measurements of three samples constitute a single test.

4.2 *Prepare the DSR system.*

4.2.1 Clean all contact surfaces with an asphalt solvent and then with acetone.

4.2.2 Establish the zero gap – Close the gap and observe the normal force. After establishing contact between the plates, set the zero gap at approximately zero normal force.

NOTE: Reset the gap when testing at different temperatures.

4.2.3 Move the plates apart and preheat the system.

4.3 *Mold residue samples* – Heat the residue until it is just liquid and pour into the silicone molds. A target final specimen thickness of 1.0 mm is desired when the sample is cooled. As needed, the cooled sample can be compressed manually between calipers to achieve the target thickness.

4.4 Invert the residue sample onto the base plate and remove the mold.

4.5 Preheat the sample and plates to 60°C for 5 to 10 minutes to prevent debonding at interface between the sample and the bottom plate, and then condition at the specified test temperature ±0.2°C for 5 minutes.

4.6 Lower the top plate at 1 mm/second and touch the sample with 10.5 N compressive force, and maintain contact for 10 seconds.

4.7 Detatch the tip at a rate of 1 mm/second.

4.8 Observe the failure mode on the upper plate and note it as cohesive (dirty tip), adhesive (clean tip), or both.

5. CALCULATIONS

5.1 The DSR software will produce a graph similar to Figure 1.

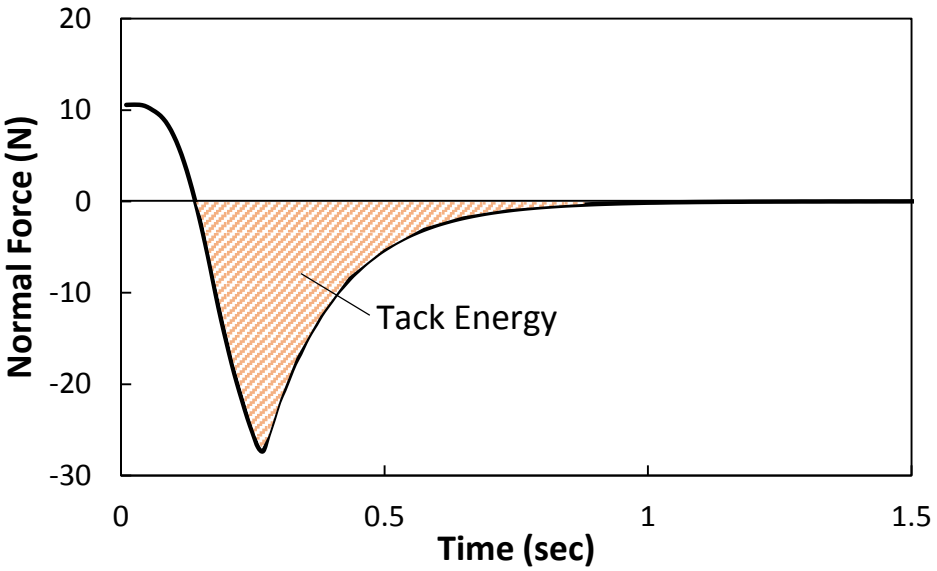

Figure 1. Example Tackiness Result.

5.2 Calculate the total tack energy (area between the tensile normal force and 0.0 N) as follows:

$$G = \frac{r}{A}\int F(t)dt$$

G = Tack energy (J/m^2)
$\frac{r}{A}$ = Pull-off speed (m/s) / Contact area (m^2) = 19.89 /s-m
F = Normal force (N)
t = Time (s)

5.2.1 Average the tack energy of three samples.

6. REPORT

6.1 Report the following:

- Average tack energy and standard deviation.
- Failure modes.

7. REFERENCES

[1] Gorsuch, C., S. Hogendoorn, C. Daranga, and J. Mckay. Measuring Surface Tackiness of Modified Asphalt Binders and Emulsion Residues Using a Dynamic Shear Rheometer. *Proceedings of the 58th Annual Conference of the Canadian Technical Asphalt Association (CTAA)*, Newfoundland and Labrador, Canada, 2013. pp. 121–138.

DRAFT Test Procedure for

TRACK-FREE TIME OF TACK MATERIAL

TxDOT Designation: Tex-XXX-X

Draft Date: June 2016

1. SCOPE

1.1 Use this test to estimate the track-free time of tack material. It is specificially used to qualify trackless tack products.

1.2 This test is derived from ASTM D7711 (Standard Test Method for No-Pick-Up Time of Traffic Paint).

1.3 The values given in parentheses (if provided) are not standard and may not be exact mathematical conversions. Use each system of units separately. Combining values from the two systems may result in nonconformance with the standard.

2. APPARATUS

2.1 *Steel Cylinder with Rubber O-Rings and Ramp* – Cylinder rolls down the ramp, through a tack sample, and onto a piece of white tracking paper.

2.1.1 The device is the same specified in ASTM D7711. The cylinder shall be 12 lb with a diameter of 3.75 in. The ramp has a slope of 1:6 with a horizontal running length of 3 7/8 in.

2.1.2 The replaceable O-rings shall be made of synthetic rubber or rubber-like material meeting the requirements of HK 715 or Classification D2000. Standards for O-rings and rubber products are also found in Test Methods ASTM D1414 and Classification D2000.

2.1.3 The O-rings have an outside diameter of 4 1/8 in., inside diameter of 3 3/8 in., and cross section of 3/8 in.

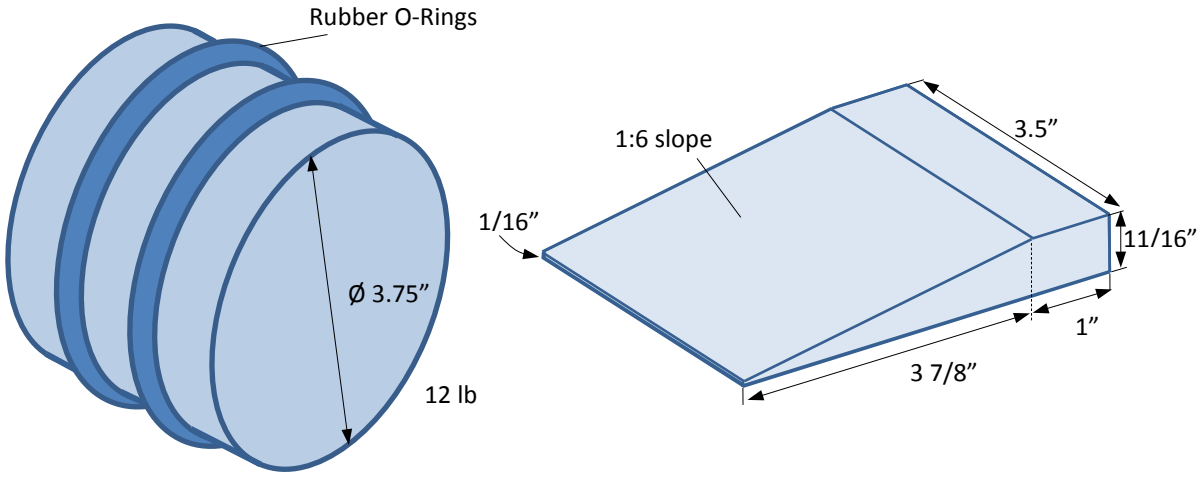

Figure 1. Roller and Ramp Apparatus.

2.2 *Thin-Film Applicator* – A draw-down rod, bar, adjustable knife applicator, etc. capable of uniformly spreading a thin liquid film at 15 ±2 mils.

NOTE: To achieve 15 mils, the applicator path depth should be approximately 30 mils.

2.3 *Thin-Film Thickness Gauge* – Resolution of 2 mils or better.

2.4 Oven capable of maintaining a temperature between 150 ±5 and 300 ±10°F.

2.5 *Tracking paper* – White medium-weight poster paper. At least one side should *have* a matte (non-glossy) finish.

2.6 *Stopwatch.*

3. MATERIALS

3.1 Tack sampled from a terminal mill or distributor truck.

4. PROCEDURES

4.1 Measurements of two specimens constitute a single test.

4.2 Substrate Board Preparation

4.2.1 Cut 1/2-in.-thick plywood (or similar) into 4-in.-wide by 12-in.-long (or longer) pieces.

4.2.2 Cut #30 roofing felt (asphalt paper) into pieces of matching size.

4.2.3 Flatten the felt pieces by keeping them at an elevated temperature (between 100 and 200°F) with a weight on top for several hours or overnight.

4.2.4 Adhere flattened felt pieces to boards using an all-purpose spray adhesive (e.g., 3M 77).

4.2.5 If using a draw-down method with unconfined edges (e.g., draw-down rod), use masking tape to frame a 3-in.-wide path on the paper.

4.3 *Tack Application*

4.3.1 Pre-heat an 8 fl-oz tack sample to the manufacturer's recommended application temperature in a covered (but not sealed) container.

4.3.2 Remove any surface film and stir the tack before applying.

4.3.3 Pour a small quantity of tack (approximately 30 g) on one end of the substrate board. Use more tack if applying a longer specimen.

4.3.4 Spread the tack at a uniform rate of 15 ±2 mils using a thin-film applicator. Use a smooth, continuous motion with a rate of 12 in./sec.

NOTE: To achieve 15 mils, the applicator depth could be as high as 30 mils. This will depend on the material viscosity. A trial run should be performed before the actual test.

NOTE: To maintain tack uniformity, the applicator will run off the end of the specimen board. A rag, paper towels, etc. should be placed under the end of the board to catch excess tack.

4.3.5 Start the stopwatch.

4.3.6 Measure the film thickness in three locations and record the average. All measurements should within 15 ±2 mils.

4.4 *Testing*

4.4.1 Allow the specimen to rest at 77 ±1°F and with no ambient air movement.

4.4.2 After 10 minutes, place the ramp, tack specimen, and tracking paper in the configuration shown in Figure 2. The ramp and tracking paper will be on a piece of plywood of the same thickness as the substrate board. The surface should be level.

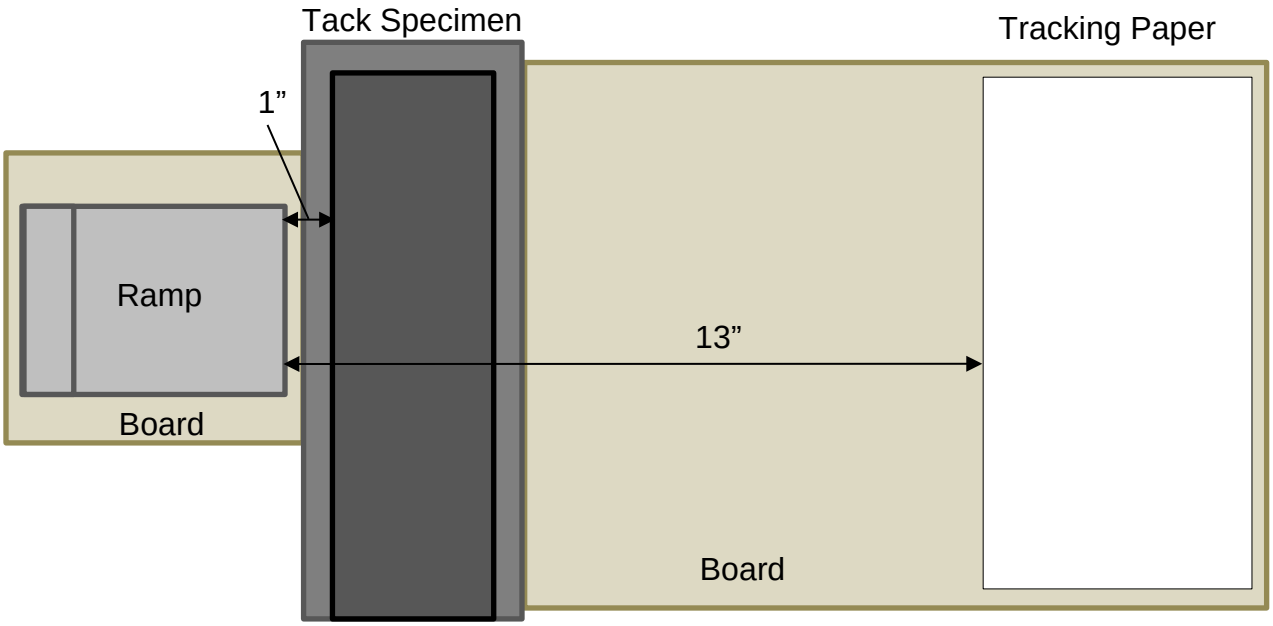

Figure 2. Tack Tracking.

4.4.3 Place the roller on the top of the ramp and allow the roller to run down the ramp, through the tack, and over the tracking paper. Label each track path with the test time from the stopwatch.

NOTE: Ensure that a clean portion of the O-ring is used for each test. When positioned on the ramp, the top of the roller will be the first point to contact the tack.

4.4.4 Allow the sample to continue curing at 77°F, and clean the O-rings as needed with an asphalt solvent and then acetone.

4.4.5 Repeat roller testing every 5 to 10 minutes on an untracked location until the track-free time. When nearing this point, test every 1 or 2 min.

5. CALCULATIONS

5.1 Using time measurements for 4 unique wheel paths (2 per sample), calculate the average track-free time as follows:

$$\text{Track-Free Time, minutes} = \frac{\sum t_{No\ tracking,i}}{4}$$

$t_{No\ tracking,i}$ = Track-free time for each wheel path, minutes

6. REPORT

6.1 Report the following:

- Average track-free time
  or
  "Not Available" if the sample did not stop tracking after 60 minutes.

DRAFT Test Procedure for

SHEAR BOND STRENGTH TEST

TxDOT Designation: Tex-XXX-X

Draft Date: May 2016 (Updated), August 2014 (Original)

1. SCOPE

1.1 Use this test to determine the shear strength between two bonded pavement layers. Specimens are most often cores from the field, but bonded laboratory specimens may also be tested.

1.2 The values given in parentheses (if provided) are not standard and may not be exact mathematical conversions. Use each system of units separately. Combining values from the two systems may result in nonconformance with the standard.

2. APPARATUS

2.1 *Interlayer Shear Strength Apparatus* – Holds a cylindrical core horizontally and consists of two parts: (1) a ridged sleeve to hold one side of the specimen and to provide a reaction force; and (2) a sliding sleeve holding the other side of the specimen that moves perpendicular to the core's vertical axis and produces the shear load. While testing, the sliding sleeve must only move vertically.

2.1.1 The device should accommodate 6-in. diameter cores and, optionally, 4-in. diameter cores with the use of reducer sleeves.

2.1.2 Core shims are required when testing cores that are more than 1/8 in. smaller than the target diameter. Shim thicknesses may range from 1/16- to 1/2-in. thick.

2.1.3 The gap between the sliding and reaction sleeves should be 1/4 in., and optionally adjust to accommodate larger gaps.

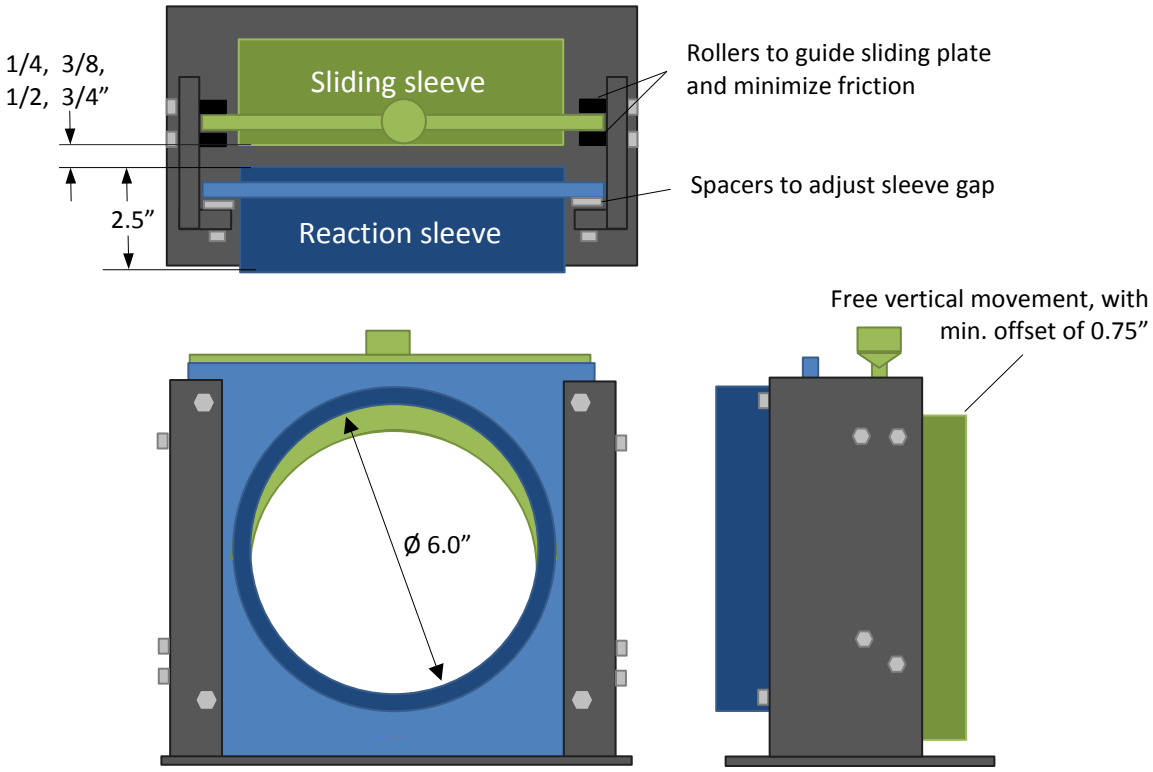

Figure 1 – Interlayer Shear Strength Apparatus.

2.2 *Loading Frame* – Must apply a uniform vertical displacement rate of 0.2 in. (5 mm)/minute. The displacement should be accurate within 0.02 in. (0.5 mm). The load cell should have a working range of 200–5,000 lb (8.9–22.2 kN) with an accuracy of 1%. A higher working range up to 7,500 lb may be needed for unique scenarios.

2.3 *Core Drill and 4-in. Core Barrel* – May be used to reduce the diameter of core specimens when testing layer thicknesses less than 1.0 in. (25 mm).

3. SPECIMENS

3.1 Measurements on three specimens constitute a single test.

3.2 *Core Specimens* — Specimen diameter must be between 6 and 5.5 in. (150–140 mm) or 4 and 3.5 in. (100–90 mm). Specimens with diameters that are more than 1/8 in. smaller than 6 or 4 in. must use core shims. There is no specific density requirement.

3.2.1 Mark the direction of traffic on the surface prior to coring.

3.2.2 Carefully remove the core to minimize stress to the bond and surrounding layers. Make a note if the core debonds at the interface in question during sampling.

3.2.3 Trim cores so the thickness between the bond and either specimen end is no more than 3 in.

3.2.4 Allow specimens to fully dry after coring and trimming.

---

4. PROCEDURE

4.1 *Testing*

4.1.1 Measure the specimen diameter three times to the nearest 0.06 in. (0.002 mm) and average.

4.1.2 Slide the specimen into the shearing apparatus and position the interface in question in the center of the gap. Orient the specimen so the traffic direction is vertical. As needed, insert core shims and/or use the 4-in. diameter reducer sleeves.

NOTE: To aid in locating the bond, clearly mark the bond before placing it in the apparatus. Ensure that core shims do not interfere with the shearing gap.

4.1.3 Position the apparatus in the loading frame and apply the shearing load at a constant rate of displacement of 0.2 in. (5 mm)/minute and stop after the maximum load is achieved and the load has decreased substantially.

NOTE: Ensure the sliding half of the shear apparatus does not bottom-out during testing. This will damage the equipment.

4.1.4 Record the maximum load.

4.1.5 Note the location of the failure (at the bond interface or in the adjacent layers).

4.2 *Calculation*

4.2.1 The maximum shear strength is calculated using the following equation:

$$Shear_{max} = 4 * F_{Max}/(\pi D^2)$$

$Shear_{max}$ = Maximum shear strength, psi
F_{Max} = Maximum load, lb
D = Average specimen diameter, in.

---

5. REPORT

5.1 Report the following for each specimen

- Maximum shear strength for individual specimens
- Note samples that fail at a location other than the bond
- Average shear strength and standard deviation of the three speciemens.

APPENDIX H:
TRACKLESS TACK SPECIFICATION

ITEM XXX
TRACKLESS TACK (DRAFT SPECIFICATION)

XXX.1. Description. Provide polymer-modified asphalt or emulsified asphalt for a tack coat that is resistant to tracking and has adequate bond strength. This specification is to be used in conjunction with Item 300 (Asphalts, Oils, and Emulsions).

XXX.2. Materials. In Item 300, amend Table 3 and Table 9 with the following.

Table 3
Polymer-Modified Asphalt Cement for Trackless Tack

Property	Test Procedure	Trackless	
		Min	Max
Polymer		–	–
Viscosity, 275°F, cP	T 316	–	3000
Penetration, 77°F, 100 g, 5 sec	T 49	–	25
Softening Point, °F	T 53	170	–
Dynamic Shear, G*/sin δ, 82°C, 10 rad/sec, kPa	T 315	1.0	–
Flash Point, C.O.C., °F	T 48	425	–
DSR Tackiness Test: Residue cohesive failure (dirty tip) or Tack Energy, J/m^2	Tex-XXX	–	None or 200
Lab Track-Free Time, 77°F, minutes	Tex-XXX	–	35

Table 9
Polymer-Modified Emulsified Asphalt for Trackless Tack

Property	Test Procedure	Trackless	
		Min	Max
Viscosity, Saybolt Furol, 77°F, sec	T 72	20	100
Storage Stability, 1 Day, %	T 59	–	1
Settlement, 5-day, %	T 59	–	5
Sieve Test, %	T 59	–	0.1
Distillation Test:[1] Residue by distillation, % by wt. Oil distillate, by volume of emulsion	T 59	 50 –	 – 1.0
Test on Residue from Distillation: Penetration, 77°F, 100 g, 5 sec Solubility in trichloroethylene, % Softening point, °F Dynamic shear, G*/sin(δ), 82°C, 10 rad/s, kPa	 T 49 T 44 T 53 T 315	 – 97.5 150 1.0	 75 – – –
DSR Tackiness Test, 40°C: Residue cohesive failure (dirty tip) or Tack Energy, J/m^2	Tex-XXX	–	None or 200
Lab Track-Free Time, 77°F, minutes	Tex-XXX	–	35

1. Exception to AASHTO T 59: Bring the temperature on the lower thermometer slowly to 350±10°F. Maintain at this temperature for 20 min. Complete total distillation in 60±5 min. from first application of heat.

XXX.3. Equipment. See Item 300.

XXX.4. Construction.

Amend Table 18 as follows.

Table 18
Typical Material Use

Material Application	Typically Used Materials
Tack coat	PG Binders, SS-1H, CSS-1H, EAP&T, Trackless Tack

B. Storage and Application Temperatures. Use temperatures as recommended by the manufacturer.

XXX.5. Payment. See Item 300.

Non-Tracking Tack Coat:
Materials, Construction, and Measurement

May be used to modify existing specifications (i.e., Item 334, 340, 341, 344, etc.)

XXX.1. Materials.

A. Non-Tracking Tack Coat. Furnish a non-tracking tack coat in accordance with Item 300, "Asphalts, Oils, and Emulsions."

Do not dilute emulsified asphalts at the terminal, in the field, or at any other location before use.

The Engineer will obtain at least 1 sample of the tack coat binder per project and test to verify compliance with Item 300. The Engineer will obtain the sample from the asphalt distributor immediately before use.

XXX.2. Construction

A. Placement Operations.

Non-Tracking Tack Coat. Clean the surface before placing the tack coat. Apply tack coat uniformly at a rate between 0.03 and 0.07 gal of residual asphalt per square yard of surface area, based on the surface and overlay characteristics. Another tack rate may be approved by the Engineer. Apply a thin uniform tack coat to all contact surfaces of curbs, structures, and joints. Prevent spattering of tack coat when placed adjacent to curbs, gutters, and structures.

Spray a 500-ft test strip to confirm tack uniformity with "double lap" or "triple lap" coverage. Clean and adjust spray equipment as necessary. Measure the track-free time in the field by waiting until the recommended curing time and driving over the strip with average-weight construction equipment. Repeat as necessary until there is no evidence of tracking or picking up on the equipment wheels. Construction may not proceed without approval from the Engineer.

During placement, construction and other traffic should be kept off the tack until the track-free time has been reached as determined in the test strip. The Engineer may suspend operations if inadequate rate or tack uniformity becomes an issue.

XXX.3. Measurement. At the Engineer's request, bond strength testing between the new overlay and the existing surface may be requested. Field cores may be taken and tested in accordance with a shear bond strength test (Tex-X-XXX). The average shear bond strength of three cores should be 30 psi or greater, with no single test result below 20 psi.